INTRODUCTION. [1])

The principal aim of the investigation of line intensities in a stellar spectrum is to obtain some information about temperature, density and other physical characteristics of the stellar atmosphere. In general this is done by comparing the equivalent widths of lines originating from different atomic levels, with different excitation potentials and of lines from neutral atoms with those of ions. This method has also been followed here.

But the spectra with which we are occupied at present, afford extra difficulties as a consequence of the crowding of lines. In order to be able to carry out accurately the above method, we ought to have made accurate measures of the equivalent widths of pure stellar lines, whereas in practice all lines are severely blended. Secondly, it is impossible to accurately determine the position of the continuous background in these spectra. These circumstances force us to develop a more exhaustive method of reduction, which will make it possible to take into account the effects of blending and background fully.

Two different methods to tackle the problem are possible. By the first, we try to divide the measured intensity of a blend into separate contributions of the several stellar lines in its region. This is the method which at first sight presents itself as the simpler one and we have tried its application in several ways. But these attempts were not very successful. In fact, the difficulty is, that with this mode of attack each blend presents an independant problem. If the blend is too narrow to allow of an estimate of the relative contributions of the components, derived from the general appearance of the line profile, as is generally the case, we must try to obtain in another way some information about the relative or absolute intensities of the weak components of the blend and this discussion, which must be repeated for each new blend, yields results which are very uncertain. If we subtract the estimated intensities of the weak lines from the equivalent width of the entire blend, the remaining difference, which corresponds to the equivalent width of the chief component will be influenced by the errors in the estimated intensities of the weak contributors and these resulting errors are very difficult to determine. Moreover, when the above procedure has been completed, it is possible that the physical conditions of the stellar atmosphere, which are obtained from a discussion of the equivalent widths of the stellar lines after correction for blend, will differ very much from the original estimates. As a consequence, the original estimates of the intensities of the weak contributors of the blend will contain systematic errors, and in order to eliminate them, the whole calculation must be repeated. It is clear that this mode of attack is not very well adapted to the present problem.

The difficulties of the above method are very great in the case of δ Cephei and other stars where the coefficient of continuous absorption is smaller than in the sun. In these stars the ratio

---

[1]) The long delay after the publication of Part I in 1939 is chiefly due to war circumstances. Though the title of the first part with common authorship had to be preserved, it must be stated here that the discussion in the present part is entirely the work of G. B. VAN ALBADA, who made it the subject of his thesis, and is responsible for the conclusions. A. P.

s/k of the coefficient of selective diffusion to that of continuous absorption is larger than for the corresponding lines in the sun and as a consequence of this the Doppler profiles are to a larger extent saturated. This circumstance means, that the curve of growth for these stars is much more horizontal than in the case of the sun, and lines, which in the solar spectra have an intensity ratio 1 : 10 *e.g.*, yield a ratio 1 : 3 in the spectrum of δ Cephei. This means that the weak components in the blends in the spectrum of δ Cephei play a much more important part than would be concluded from a comparisom with the solar spectrum, and an error in their estimated intensities will have a correspondingly great influence on the remaining difference, *i.e.* on the calculated intensity of the chief component of the blend.

The second method is just the reverse of the first. In this method we start with some suppositions about the physical conditions in the atmosphere and from these we calculate theoretical intensities for all stellar lines, which are then combined into blends. Instead of a large number of unknowns in the reduction, — in the first method we had several unknown intensities for each blend — we now have a limited number of unknowns, i.e. the coefficient of continous absorption, the temperature of the atmosphere, the degree of ionization, the Doppler width (which depends on temperature and turbulence), the resonance width of the line (which comprises also the effect of broadening by collisions). So the number of unknowns is limited to only 5, to which we add one more to represent the uncertainty in the position of the continuous background.

Now we calculate the intensity of each blend as a function of the six parameters mentioned above. A first investigation of the spectrum yields provisional values for these parameters. The blend intensities for each other set of values are then found by differential correction. In this way we find the equivalent width of each blend expressed theoretically as a linear function of six parameters defining the physical state of the stellar atmosphere. If then we write down these equations for all blends under investigation, we may calculate more accurate values of these parameters by the method of least squares.

This second method is the one employed in this paper. It will be considered more in detail in the following paragraphs.

I. PRELIMINARY ANALYSIS.

Method of first analysis.

The present analysis of the spectrum of δ Cephei and other stars consists of two parts. In the first part we start with the crude material from which we deduct provisional values for the physical parameters of the atmosphere. In the second part a more rigorous method is followed by which we obtain differential corrections to the first estimates. Here we will outline the method followed in the first part of the analysis.

The material consists of the measured equivalent widths contained in part I of this publication. All numbers given there represent measures of blends. From the entire list we select some 25 %, where the blending is not very serious. A list of the selected lines is given in the second paragraph following.

For the moment, we consider these lines as being unblended. We now compare the measured intensities with those given by C. W. ALLEN [1]) for the solar spectrum. It is at once obvious, that we must treat the lines of ions and those of neutral atoms separately, the last group being systematically weaker than the first. If we do so, we obtain a general relation between the equivalent widths of ionic and atomic lines in the star and the corresponding lines in the solar spectrum. But the method does not yet give numerical values for the physical parameters of the stellar atmosphere.

In order to obtain same, we derive a theoretical relation between the equivalent width of a stellar line and the number of atoms active in producing it, i.e., we calculate the theoretical curve of growth. The form and position of this curve depends on three parameters. The curve is shifted horizontally if the atomic concentration or the coefficient of continuous absorption is changed. A vertical shift will be the result of a change in the Doppler width. And finally a change in the resonance width will alter the shape of the upper part of the curve.

We now calculate for each line the number of active atoms for the solar spectrum. The number of active atoms for the star will stand in a fixed ratio to the number of active atoms in the sun. So if in a vertical direction we plot the logarithm of the equivalent width in the star against the logarithm of the number of active atoms as derived for the sun, this horizontal scale may be transferred into that valid for the star by a shift in its own direction.

If secondly the Doppler width for the star is not the same as that for the sun, the theoretical curve of growth must also be shifted vertically. So in general each parallel shift of the curve of growth is allowed. In this way we determine the position in which this curve fits best to the observations. The upper part of the curve then determines a provisional value for the resonance width.

This procedure yields very rapidly provisional values for the number of active atoms (as compared with the corresponding number for the sun), for the Doppler- and resonance-widths.

[1]) C. W. ALLEN „Fraunhofer Intensity Tables", Memoirs of the Commonwealth Solar Observatory, Canberra, No. 5—6 (1934—1938).

The temperature has not yet been determined. In fact, the method can be applied only to spectra which differ not too much from the solar spectrum. Otherwise another comparison star than the sun has to be used.

Computation of the theoretical curve of growth.

The theoretical curve of growth has been derived already by several authors. That we here repeat this calculation in a somewhat different way has two reasons.

First of all, in the more precise analysis, which follows the first estimate, it is not sufficient for us only to know the shape of the curve of growth itself, but at the same time we must make use of its differential corrections. For this reason, we prefer a mathematical expression to a pure numerical determination. Secondly, the mathematical expression which has been derived by J. G. BAKER [1]), has been calculated by the aid of a formula for the line depth which does not correspond to a possible atmospheric model. The difference becomes serious for large values of s/k, when the residual intensity in any case must be proportional to $(k/s)^{\frac{1}{2}}$, whereas the formula used by BAKER yields proportionality to k/s itself. As a consequence, errors in the calculated equivalent widths may result, which in some cases amount to as much as 30 %.

Therefore we here derive a new formula, based upon the atmospheric model of MILNE—EDDINGTON.

We start with the formula for a pure Doppler profile. In the following, for s/k we simply write s. The line depth, which we denote by $R = 1 - r$ (r = residual intensity) is determined by the usual formula of the M.-E.-model. The exact form of the expression depends a little on the coefficient of limb darkening. Here we employ it in its simplest form, which will be a sufficient approximation. This limitation, however, can easily be avoided as we make our calculations only with the help of a series development. We write :

$$(1a) \qquad r = \sqrt{\frac{1}{1+s}}$$

$$(1b) \qquad R = {}^1/_2\, s - {}^3/_8\, s^2 + {}^5/_{16}\, s^3 - {}^{35}/_{128}\, s^4 + \ldots\ldots\ldots\ldots\ldots\ldots\ldots \quad (s \leqq 1)$$

$$(1c) \qquad R = 1 - s^{-1/2} + {}^1/_2\, s^{-3/2} - {}^3/_8\, s^{-5/2} + {}^5/_{16}\, s^{-7/2} - \ldots\ldots\ldots\ldots\ldots \quad (s \geqq 1)$$

The value of s/k at the line centre we denote by s_0. In the case $s_0 < 1$ the expression (1 b) can immediately be integrated, if we use for s the ordinary Doppler formula $s = s_0\, e^{-x^2/b^2}$. The result is :

$$(2) \qquad D = b\sqrt{\pi}\left\{ {}^1/_2\, s_0 - {}^3/_8\, s_0^2\, \frac{1}{\sqrt{2}} + {}^5/_{16}\, s_0^3\, \frac{1}{\sqrt{3}} - {}^{35}/_{128}\, s_0^4\, \frac{1}{\sqrt{4}} + \ldots\ldots\right\} \quad (s_0 \leqq 1)$$

The equivalent width can be calculated from this formula numerically.

When $s_0 > 1$ we divide the line profile into two parts, separated by the point where $s = 1$. Each part is then integrated separately. In doing so, we obtain integrals of the form :

$$s_0^{-(p-1/2)} \int_0^{x_1} e^{(p-1/2)\, x^2/b^2}\, dx = \frac{b}{\sqrt{p-1/2}} \cdot e^{-(p-1/2)\, x_1^2/b^2} \int_0^{\frac{x_1}{b}\sqrt{p-1/2}} e^{y^2}\, dy$$

[1]) Ap. J. **84**, 474 (1936).

$$s_0 \int_{x_1}^{\infty} e^{-px^2/b^2}\,dx = \frac{b}{\sqrt{p}}\, e^{px_1/b^2} \int_{\frac{x_1}{b}\sqrt{p}}^{\infty} e^{-y^2}\,dy$$

We now write:

$$(3a, b) \qquad e^{-u^2}\int_0^u e^{x^2}\,dx = \frac{1}{2u} + uF(u); \qquad e^{u^2}\int_u^{\infty} e^{-x^2}\,dx = \frac{1}{2u} + u\,G(u)$$

For large values of u we may calculate $F(u)$ and $G(u)$ with the help of the asymptotic series:

$$(4a, b) \qquad \begin{aligned} F(u) &= {}^1/_4u^4 + {}^3/_8u^6 + {}^{15}/_{16}u^8 + {}^{105}/_{32}u^{10} + \ldots\ldots\ldots \\ G(u) &= {}^1/_4u^4 - {}^3/_8u^6 + {}^{15}/_{16}u^8 - {}^{105}/_{32}u^{10} + \ldots\ldots\ldots \end{aligned}$$

The term $1/2u$ leads to the following expressions:

$$2\frac{b^2}{2x_1}\left\{-2 + \frac{2}{3}\cdot\frac{1}{2} - \frac{2}{5}\cdot\frac{3}{8} + \frac{2}{7}\cdot\frac{5}{16} - \ldots\ldots\ldots\right\} = \frac{-2b^2}{x_1}\ln(1+\sqrt{2}) \text{ and}$$

$$2\frac{b^2}{2x_1}\left\{\frac{1}{2} - \frac{1}{2}\cdot\frac{3}{8} + \frac{1}{3}\cdot\frac{5}{16} - \frac{1}{4}\cdot\frac{35}{128} + \ldots\ldots\ldots\right\} = 2\frac{b^2}{x_1}\ln\frac{1+\sqrt{2}}{2}$$

Adding to these expressions the terms with F and G and putting $x_1 = b\sqrt{\ln s_0}$ we obtain for the equivalent widths of the inner and outer parts of the line:

$$(5a, b) \qquad \begin{aligned} D_i &= 2b\sqrt{\ln s_0}\left\{1 - \frac{\ln(1+\sqrt{2})}{\ln s_0} - F\left(\sqrt{{}^1/_2\ln s_0}\right) + {}^1/_2\,F\left(\sqrt{{}^3/_2\ln s_0}\right) - \right. \\ &\qquad \left. - {}^3/_8\,F\left(\sqrt{{}^5/_2\ln s_0}\right) + \ldots\ldots\right\} \\ D_o &= 2b\sqrt{\ln s_0}\left\{\frac{\ln\frac{1+\sqrt{2}}{2}}{\ln s_0} + {}^1/_2\,G\left(\sqrt{\ln s_0}\right) - {}^3/_8\,G\left(\sqrt{2\ln s_0}\right) + {}^5/_{16}\,G\left(\sqrt{3\ln s_0}\right) - \ldots\right\} \end{aligned}$$

From these series of expressions, the total equivalent width D of the Doppler profile may be calculated. The functions F and G are calculated with the help of the tables of JAHNKE and EMDE [1] for not too large values of u. For larger arguments the expressions (4) are used.

The results of the calculations are given in Tables 1—3 of the present volume. Table 1 gives the values of $D/2b$ for $s_0 \leqq 1$. Table 2 gives values of the auxiliary functions F and G. Table 3, finally, gives values of $D/2b\sqrt{\ln s_0}$ for $s_0 \geqq 1$. This last table has 4 columns, which give resp. the value of $\ln s_0$, and the equivalent widths of inner part, outer parts and entire line expressed in terms of $2x_1 = 2b\sqrt{\ln s_0}$.

Table 1.

s_0	0.0	0.1	0.2	0.3	0.4	0.5	0.6	0.7	0.8	0.9	1.0
$D/2b$	0.000	.042	.080	.115	.148	.177	.205	.231	.255	.279	.300

[1] E. JAHNKE und F. EMDE „Funktionentafeln mit Formeln und Kurven" 3. Aufl. (Leipzig usw. 1938).

Table 2.

u^2	$F(u)$	$G(u)$	u^2	$F(u)$	$G(u)$	u^2	$F(u)$	$G(u)$
0.0	$-\infty$	$-\infty$	1.0	+ .038	— .121	3.0	+ .044	— .020
.1	—4.064	—2.972	1.2	+ .064	— .091	3.5	+ .033	— .014
.2	—1.623	—1.224	1.4	+ .075	— .071	4.0	+ .026	— .012
.3	—0.845	—0.709	1.6	+ .076	— .057	4.5	+ .020	— .010
.4	— .478	— .474	1.8	+ .074	— .047	5.0	+ .016	— .008
.5	— .275	— .344	2.0	+ .070	— .039	5.5	+ .012	— .007
.6	— .152	— .264	2.2	+ .065	— .034	6.0	+ .010	— .006
.7	— .073	— .209	2.4	+ .059	— .029	7	+ .007	— .004
.8	— .021	— .171	2.6	+ .054	— .025	8	+ .005	— .003
.9	+ .014	— .143	2.8	+ .048	— .022	9	+ .004	— .003
1.0	+ .038	— .121	3.0	+ .044	— .020	10	+ .003	— .002

Table 3.

$(x_1 = b\sqrt{\ln s_0})$

$\ln s_0$	$D_i/2x_1$	$D_o/2x_1$	$D/2x_1$	$\ln s_0$	$D_i/2x_1$	$D_o/2x_1$	$D/2x_1$
0.0	0.293	∞	∞	3.0	0.638	0.055	0.693
.1	.305	0.713	1.018	3.5	.679	.047	.726
.2	.317	.453	0.770	4.0	.714	.042	.756
.3	.329	.342	.671	4.5	.744	.038	.782
.4	.342	.279	.621	5.0	.770	.034	.804
.5	.354	.237	.591	6	.811	.029	.840
.6	.367	.206	.573	7	.842	.025	.867
.7	.379	.183	.562	8	.865	.022	.887
.8	.392	.165	.557	9	.883	.019	.902
.9	.405	.150	.555	10	.897	.018	.915
1.0	.418	.138	.556	15	.936	.012	.948
1.5	.480	.099	.579	20	.953	.009	.962
2.0	.538	.078	.616	25	.963	.007	.970
2.5	.592	.064	.656	30	.982	.004	.986
3.0	.638	.055	.693	100	.991	.002	.993
				∞	1.000	.000	1.000

The present results are exact as far as eq. (1) for the line depth is adopted. If, instead, we use the approximative formula $R = s/(1+s)$, as is done e.g. by UNSÖLD [1]), the calculated equivalent widths will be too large. Indeed, if we write down only the first two terms of eq. (5) and compare their combination with the series (69,14) as given by UNSÖLD, we find two different results for the equivalent width :

$$\text{Formula (5)}: \quad D = 2b\sqrt{\ln s_0}\left\{1 - \frac{\ln 2}{\ln s_0} - \ldots\ldots\ldots\right\}$$

$$\text{UNSÖLD}: \quad D = 2b\sqrt{\ln s_0}\left\{1 - \frac{0.4112}{(\ln s_0)^2} - \ldots\ldots\ldots\right\}$$

Numerical calculation with the complete formulae shows, that the difference between both results may amount to as much as 30 % of the equivalent width.

[1]) A. UNSÖLD „Physik der Sternatmosphären", Berlin (1938) p. 265 ff.

We now turn to the calculation of the equivalent width of a line with resonance wings. The calculation becomes very simple if these wings are so heavy, that we neglect the influence of the Doppler core upon the equivalent width. Putting $s = C/x^2$ as a sufficient approximation of the resonance profile, integration of (1) yields $2\sqrt{C}$ for the surface of the line profile.

But the general case is not as simple. If Doppler broadening and resonance are of about the same importance, the formula for the coefficient of selective scattering gets very complicated. [1]) But fortunately it is possible to obtain a sufficiently accurate result with the help of a simplified method of calculation. To this end we schematically divide the line profile into two regions, the central part being determined solely by Doppler broadening and the outer parts only by resonance effect. The joint is made at the point where the values of s, as calculated for the inner and the outer parts of the line profile, are equal.

So we adopt as an approximate formula for the coefficient of scattering :

(6*a*, *b*, *c*) $s = s_0\, e^{-x^2/b^2}$ $(|x| < w)$ and $s = C/x^2$ $(|x| > w)$; $s_w = s_0\, e^{-w^2/b^2} = C/w^2$

The values of s_0 and of C are connected by the formula :

(7 *a*, *b*) $C/b^2 = \frac{a}{\sqrt{\pi}}\, s_0$; $a = \gamma/b$

which follows immediately from the integration of formulae $s = s_0\, e^{-x^2/b^2}$ and $s = \frac{C}{x^2 + \gamma^2}$ over the entire range of wave lengths.

w/b and s_w/s_0 may be calculated as a function of log a. The results are given in table 4.

Table 4.

log a	$\bar{4}.50$	$\bar{4}.75$	$\bar{3}.00$	$\bar{3}.25$	$\bar{3}.50$	$\bar{3}.75$	$\bar{2}.00$	$\bar{2}.25$	$\bar{2}.50$
w/b	3.321	3.224	3.124	3.019	2.909	2.794	2.673	2.543	2.404
s_w/s_0	$\bar{5}.209$	$\bar{5}.485$	$\bar{5}.762$	$\bar{4}.042$	$\bar{4}.324$	$\bar{4}.609$	$\bar{4}.897$	$\bar{3}.191$	$\bar{3}.489$

In order to find out whether this simplified model yields sufficiently accurate results, we make a numerical calculation for a very unfavourable case. If we differentiate (1) with respect to log s, the derivative will become a maximum for $s = 2$. This then, is the value of s for which an error in log s will have the greatest possible influence on the calculated line depth. So our simplified model will be worst in the case when $s_w = 2$, for at the junction the error in the value of log s will be a maximum. If now we make two calculations of the line profile, one by means of the simplified formula and the other with the accurate one, we may calculate the error caused by the use of (6) for this most unfavourable case. If we take $s_w = 2$, log $a = \bar{2}.50$, the largest relevant value, it is found, that the equivalent width calculated by the approximate formula is 0.956 of the true value. Thus the error committed will be at most 0.02 in log A, which is too small, to be of any importance in the present calculations. Accordingly, the use of the simplified formula is entirely justified.

From Table 4 it is seen, that w/b is at least equal to 2.4. This means that the junction is situated in the outer part of the Doppler profile. If we strictly follow the scheme of eq. (6), we must omit the part of the Doppler profile beyond $x = w$. But as the surface of this outer part is negligible as compared with the total Doppler surface and also with regard to the surface of the resonance wings, it is not necessary to complicate the calculations in doing so. So we may, quite as well, start with the total surface of the Doppler profile as given in the last column of Table 3 and add to it

[1]) F. Hjerting Ap. J. **88**, 508 (1938).

the resonance wings extending beyond $x = w$. By this procedure, the error committed, when we adopted the scheme of eq. (6) will even be reduced a little.

If then we proceed in this way, we find for the total equivalent width of the absorption line (denoted by A):

(8) $$A = D + 2W = D + 2w\,(\sqrt{1 + s_w} - 1)$$

if the surface of the resonance wing is denoted by W.

With the help of this formula, we calculate the equivalent width of the line profile as a function of log a and of log s_0. The results are given in Table 5.

Table 5. The table gives log $A/2b$ as a funtion of log a and log s_0.

log s_0	$a = 0$	log a								
		$\bar{4}.50$	$\bar{4}.75$	$\bar{3}.00$	$\bar{3}.25$	$\bar{3}.50$	$\bar{3}.75$	$\bar{2}.00$	$\bar{2}.25$	$\bar{2}.50$
$\bar{1}.0$	$\bar{2}.62$	$\bar{2}.62$	$\bar{2}.62$	$\bar{2}.62$	$\bar{2}.62$	$\bar{2}.62$	$\bar{2}.62$	$\bar{2}.62$	$\bar{2}.62$	$\bar{2}.62$
$\bar{1}.2$	$\bar{2}.81$	$\bar{2}.81$	$\bar{2}.81$	$\bar{2}.81$	$\bar{2}.81$	$\bar{2}.81$	$\bar{2}.81$	$\bar{2}.81$	$\bar{2}.81$	$\bar{2}.81$
$\bar{1}.4$	$\bar{2}.99$	$\bar{2}.99$	$\bar{2}.99$	$\bar{2}.99$	$\bar{2}.99$	$\bar{2}.99$	$\bar{2}.99$	$\bar{2}.99$	$\bar{2}.99$	1.00
$\bar{1}.6$	$\bar{1}.17$	$\bar{1}.17$	$\bar{1}.17$	$\bar{1}.17$	$\bar{1}.17$	$\bar{1}.17$	$\bar{1}.17$	$\bar{1}.17$	$\bar{1}.17$	$\bar{1}.17$
$\bar{1}.8$	$\bar{1}.33$	$\bar{1}.33$	$\bar{1}.33$	$\bar{1}.33$	$\bar{1}.33$	$\bar{1}.33$	$\bar{1}.33$	$\bar{1}.33$	$\bar{1}.33$	$\bar{1}.33$
0.0	$\bar{1}.48$	$\bar{1}.48$	$\bar{1}.48$	$\bar{1}.48$	$\bar{1}.48$	$\bar{1}.48$	$\bar{1}.48$	$\bar{1}.48$	$\bar{1}.48$	$\bar{1}.48$
0.2	$\bar{1}.61$	$\bar{1}.61$	$\bar{1}.61$	$\bar{1}.61$	$\bar{1}.61$	$\bar{1}.61$	$\bar{1}.61$	$\bar{1}.61$	$\bar{1}.61$	$\bar{1}.62$
0.4	$\bar{1}.73$	$\bar{1}.73$	$\bar{1}.73$	$\bar{1}.73$	$\bar{1}.73$	$\bar{1}.73$	$\bar{1}.73$	$\bar{1}.73$	$\bar{1}.73$	$\bar{1}.73$
0.6	$\bar{1}.83$	$\bar{1}.83$	$\bar{1}.83$	$\bar{1}.83$	$\bar{1}.83$	$\bar{1}.83$	$\bar{1}.83$	$\bar{1}.83$	$\bar{1}.83$	$\bar{1}.84$
0.8	$\bar{1}.91$	$\bar{1}.91$	$\bar{1}.91$	$\bar{1}.91$	$\bar{1}.91$	$\bar{1}.91$	$\bar{1}.92$	$\bar{1}.92$	$\bar{1}.92$	$\bar{1}.93$
1.0	$\bar{1}.99$	$\bar{1}.99$	$\bar{1}.99$	$\bar{1}.99$	$\bar{1}.99$	$\bar{1}.99$	$\bar{1}.99$	$\bar{1}.99$	0.00	0.00
1.2	0.05	0.05	0.05	0.05	0.05	0.05	0.05	0.06	0.06	0.07
1.4	0.10	0.10	0.10	0.10	0.10	0.11	0.11	0.11	0.12	0.13
1.6	0.15	0.15	0.15	0.15	0.16	0.16	0.16	0.16	0.18	0.19
1.8	0.19	0.19	0.19	0.19	0.19	0.20	0.20	0.21	0.22	0.25
2.0	0.23	0.23	0.23	0.23	0.23	0.24	0.24	0.25	0.27	0.31
2.2	0.26	0.26	0.26	0.26	0.26	0.27	0.28	0.29	0.32	0.37
2.4	0.29	0.29	0.29	0.29	0.30	0.31	0.32	0.34	0.38	0.44
2.6	0.31	0.32	0.32	0.32	0.33	0.34	0.36	0.39	0.44	0.51
2.8	0.34	0.34	0.34	0.35	0.36	0.37	0.40	0.44	0.51	0.59
3.0	0.36	0.36	0.37	0.37	0.39	0.41	0.45	0.50	0.58	0.67
3.2	0.37	0.38	0.39	0.40	0.42	0.45	0.50	0.57	0.66	0.76
3.4	0.39	0.40	0.41	0.43	0.46	0.50	0.56	0.64	0.74	0.86
3.6	0.41	0.43	0.44	0.46	0.50	0.56	0.63	0.73	0.84	0.95
3.8	0.42	0.45	0.47	0.50	0.55	0.62	0.71	0.81	0.93	1.05
4.0	0.44	0.48	0.52	0.55	0.61	0.70	0.80	0.91	1.02	1.14
4.2	0.45	0.51	0.55	0.61	0.68	0.78	0.88	1.00	1.12	1.24
4.4	0.46	0.55	0.60	0.67	0.76	0.86	0.99	1.09	1.21	1.34
4.6	0.48	0.59	0.66	0.74	0.84	0.95	1.07	1.19	1.31	1.44
4.8	0.49	0.65	0.73	0.82	0.93	1.05	1.17	1.29	1.41	1.53
5.0	0.50	0.72	0.81	0.91	1.03	1.14	1.26	1.39	1.51	1.63
5.2	0.51	0.79	0.89	1.00	1.12	1.24	1.36	1.49	1.61	1.73
5.4	0.52	0.87	0.98	1.10	1.22	1.34	1.46	1.59	1.71	1.83
5.6	0.53	0.96	1.07	1.19	1.31	1.44	1.56	1.68	1.81	1.93
5.8	0.54	1.06	1.17	1.29	1.41	1.53	1.66	1.78	1.91	2.03

As a final test of the accuracy of our calculations, we make a comparison with the results obtained by B. STRÖMGREN [1]) from a numerical calculation with the exact formula for the coefficient of scattering. STRÖMGREN gives log A/b (in our notation) as a function of log ε_0. In order to make the results comparable, we must change log ε_0 by an amount $\frac{\log 4/3}{3} = 0.042$, as our choice of the coefficient of limb darkening differs a little from that made by STRÖMGREN. After applying a corresponding correction to his figures for log $A/2b$, we obtain the following results, which are to be compared with our table 5:

log ε_0	log $a = \overline{3}.00$	log $a = \overline{3}.50$	log $a = \overline{2}.00$	log $a = \overline{2}.50$
$\overline{1}.0$	$\overline{2}.63$	$\overline{2}.63$	$\overline{2}.63$	$\overline{2}.63$
0.0	$\overline{1}.48$	$\overline{1}.48$	$\overline{1}.48$	$\overline{1}.48$
1.0	$\overline{1}.99$	$\overline{1}.99$	$\overline{1}.99$	0.01
2.0	0.23	0.23	0.24	0.31
3.0	0.37	0.40	0.48	0.67
4.0	0.53	0.70	0.89	1.12
5.0	0.90	1.13	1.37	1.62
6.0	1.37	1.62	1.87	2.12

As we see, the correspondence is entirely sufficient.

Compilation of the material.

The plates, used in this investigation are described already in the first part of Publ. 6. They show the spectra of 4 different stars. From one star (δ Equ) we have only one spectrum, whereas for each of the three other stars (δ Cep, ϑ Cyg, π Cep) we have two. In these spectra equivalent widths of the lines are measured in the way indicated in the first part of this publication; the results were given at the end of part 1.

Here we will for a first orientation use the measures listed there without further comment. This being done, we then proceed to a second approximation, in which the accurate significance of the figures published is submitted to a more sincere criticism.

We will not make use, however, of all equivalent widths listed in the tables mentioned above. For many of these measures refer to blends consisting of a multitude of lines of comparable strength. These lines are omitted from the list, as is also the case with lines which are not accurately measured, as a consequence of their nearness to other very strong lines, or plate errors, etc. So from the tables of Publ. 6, I we select a number of comparatively pure lines, for which, in a first approximation, we may neglect the effects of blending.

A further correction is made to the tables of Publ. 6, I. In order to make a proper selection of the lines possible, we thoroughly compared the measured equivalent widths with the original intensity curves. In doing so, it appeared, that in some cases the lists of table 6 included two or even three different lines, which, at an accurate inspection of the original curves could not be guaranteed as separate. In such cases, the lines were recombined into one. The corresponding figures in the tables of these section are provided with one or two notes of exclamation.

For the rest, the present tables contain a full list of the lines used in the preliminary investigation with their equivalent widths expressed in milli-angströms. The table gives log A.

[1]) Festschrift für ELIS STRÖMGREN, Kopenhagen (1940), p. 248.

The equivalent width A has been taken from the tables of part 1. The values used are those corrected for resonance wings (col. 4 and 8 in the tables for δ Cephei, col. 5, 6, 11, 12, 16 in the other tables).

The tablas also give the identification of the line (apart for atomic lines, ion lines and molecule lines) and the equivalent width in the solar spectrum as measured by C. W. ALLEN. These solar equivalent widths, which we denote by A_{sun}, are reduced to log ε_0 for the sun, with the help of a curve of growth with parameters :

$$b = 22.3\, mA \qquad \log a = \overline{2}.30$$

which corresponds very nearly to the curve used by ALLEN. The curve, used by us is given in table 6 :

Table 6. Curve of growth used for the sun.

log ε_0	log A	log ε_0	log A	log ε_0	log A
$\overline{1}.0$	0.27	1.0	1.65	3.0	2.24
$\overline{1}.2$	0.46	1.2	1.71	3.2	2.33
$\overline{1}.4$	0.65	1.4	1.77	3.4	2.42
$\overline{1}.6$	0.82	1.6	1.83	3.6	2.51
$\overline{1}.8$	0.98	1.8	1.88	3.8	2.60
0.0	1.13	2.0	1.93	4.0	2.70
0.2	1.26	2.2	1.98	4.2	2.79
0.4	1.38	2.4	2.04	4.4	2.89
0.6	1.48	2.6	2.10	4.6	2.99
0.8	1.57	2.8	2.17	4.8	3.09

Strictly speaking, we should use different curves of growth for different wave lengths and different atoms, as the Doppler width varies somewhat according to wave length and atomic mass. But in practice, these variations are not very important. Our spectra cover only a limited range of wave lengths and many of the lines are crowded within a very small part of the spectral range. Further most of the lines are due to iron or to elements of nearly the same atomic weight. And the contribution of turbulence to the Doppler width will presumably have the same value for all elements. So the differences between the curves of growth which should be used in different cases can only be small. If we neglect them altogether in the calculation of log ε_0 for the sun and neglect then again in the calculation of the curve of growth for the stellar spectrum, in the relation between log A_{sun} and log A_{star} this influence will be almost completely eliminated. This is the reason, why we use only curve of growth, which makes the necessary calculations much less laborious.

In table 7, some lines are denoted simply as "blend" or "absent". We excluded a line as a blend, when the total equivalent width of all minor contributors as measured by ALLEN was equal to at least one half of the equivalent width of the chief component. As the point at which the blend has been cutted may be situated at somewhat different places in the diverse spectra, in some cases a line has been included in one spectrum and excluded in the other spectrum of the same star. This, of course, is an indication, that the influence of the minor contributors is not negligible, and it is appropriate that in this way the line has acquired half weight by the exclusion of one measure.

Lines denoted as „absent" may in some cases be present nevertheless, but they do not correspond with a top or even with a detectable curvature in the registrogram. In some cases,

this may be the result of an accidental crowding of silver grains, which hides the line or shifts its top over so large a distance, that the identification of the line becomes questionable. If such a shift of the line occurs, the line in general is not denoted as "absent", but by a note of interrogation. This very often occurs in the spectrum of δ Equulei, where the silver grain is very troublesome.

If, on the other hand, notes of interrogation are put behind a measured equivalent width, this means, that the measure is a little inaccurate. In most cases this is due to the fact, that the line is situated at the border of a much stronger line. But there may be other causes also, as the situation of a line in the region of the wings of the Balmer lines, irregular profile of the line, small plate errors, cutting of heavy resonance wings, or almost completely blank line centre.

Table 7. Equivalent widths of lines used of for provisional curves of growth.

	Identif.	A sun	log ε_0 sun	log A (star)							
				δ Cephei		ϑ Cygni		π Cephei		δ Equulei	
				10607	10617	10616	10619	10610	10618	10608	
4050.68	Fe	56	1.32	1.85		1.81					
55.55	Mn	133	2.67	2.35		2.31					
58.22	Co?—*Fe*	104	2.33	2.04		2.21					
59.39	Mn	42	0.93	1.76		1.76					
59.72	Fe	72	1.72	1.98		1.94					
4062.45	Fe	117	2.50	2.45		2.37					
65.39	Fe	72	1.72	1.93?		2.01					
67.99	Fe—Mn	133	2.67	2.43		2.39					
68.54	Co	30	0.60	1.64		1.62!					
70.28	Fe *Mn*	70	1.68	2.11		1.87					
4070.78	Fe	105	2.34	2.37		2.20					
71.75	Fe	720	4.33	2.63!		2.61					
72.51	Fe	70	1.68	2.20		1.96					
79.85	Fe	88	2.06	2.29		2.16					
80.88	Fe	58	1.38	1.72		1.89					
4081.27	Fe —	38	0.82	2.09		1.79					
82.44	*Ti* Sc *Fe*	66	1.58	1.68		1.75					
82.95	*Mn* V	105	2.34	2.36!		2.14					
84.50	Fe	116	2.48	2.38		2.23					
89.23	Fe	60	1.42	2.20!		1.94					
4091.56	Fe	58	1.38	2.01		2.27!!?					
4107.50	Ce—Fe—Zr	116	2.49	2.56?		2.28?					2.09
08.54	— Ca?	56	1.32	2.03?		2.05?	1.92?				2.04
09.06	Fe	69	1.65	2.15?		1.98?	2.16?				2.11
10.54	Co	90	2.10	2.27		1.89?	1.93?				2.11
4111.79	V	96	2.20	2.22		1.94?	1.99??				2.12!
12.32	Fe	57	1.35	1.89		1.92?	1.94?				1.93
14.45	Fe	93	2.15	2.37		2.18	2.21				1.99
20.22	Fe	89	2.08	2.34		1.94	2.09				1.81
21.33	Co	126	2.60	2.31		2.06	2.06				2.01

	Identif.	A sun	log s_0 sun	log A (star)							
				δ Cephei		ϑ Cygni		π Cephei		δ Equulei	
				10607	10617	10616	10619	10610	10618	10608	
4121.81	*Fe*—Cr	89	2.08	2.28!		2.06	2.10			1.59	
26.19	Fe	93	2.15	2.18	2.14	2.02	1.90			1.75	
26.86	Fe	28	0.53	bl		1.45	1.68			?	
28.10	V —	84	1.98	2.48?	2.43	2.03	2.02			?	
29.19	Ce—*Cr*—Fe	62	1.48	2.06	2.07	1.85	1.89			1.89	
4130.05	Fe	53	1.23	bl		1.68	1.88			1.64	
32.07	Fe	380	3.78	2.67?	2.43	2.37	2.49			2.49!	
32.91	Fe	110	2.41	bl	2.21	2.02	2.03			1.76	
34.69	Fe	150	2.82	2.33?	bl	2.21	2.20			bl	
35.76	— Os	15	0.07	1.38	1.81	1.68	1.68			1.34	
4136.53	Fe	67	1.60	1.96	2.06	1.86	1.84			1.87	
37.01	Fe	102	2.30	2.34	2.31	2.03	2.03			1.95	
37.98	Fe	16	0.10	bl	1.57?	1.61	1.58			1.46	
39.94	Fe	78	1.86	2.12	2.21	1.89	1.91			1.85!	
40.41	Fe	53	1.23	2.00	2.00	1.83	1.78			1.62	
4141.87	Fe	62	1.48	bl	2.15	1.63	1.88			1.72	
43.88	Fe	440	3.89	2.60	2.51?	2.42?	2.47			bl	
45.20	Fe	32	0.65	?	?	error	1.57			1.89	
47.68	Fe	120	2.53	bl	2.38	error	2.11			1.78	
50.26	Fe	78	1.86	2.10	2.08	?	?			1.64?	
4154.51	Fe	130	2.64	bl	bl	2.06	2.18			2.01	
54.82	Fe	129	2.63	bl	bl	2.11	2.08			1.82	
57.79	Fe	128	2.62	2.47	2.41	2.18	2.16			1.89!	
58.80	Fe	93	2.15	2.27?	2.07	2.06	2.11			1.98	
67.28	Mg	270	3.43	2.41	2.43	2.37	2.45			bl	
4168.62	Fe	47	1.08	1.93	2.03	1.85	1.76			1.88	
68.95	Fe	57	1.35	1.92	2.08	1.65?	1.83			1.58	
74.92	Fe	109	2.40	bl	bl	2.15	2.13	bl		bl	
75.64	Fe	123	2.57	2.47	2.43	2.21	2.22	2.28!!		2.19!	
76.58	Fe—Mn	110	2.41	2.47	2.32	2.19	2.21	2.30		2.18!	
4182.39	Fe	86	2.02	2.15	2.26	1.99	1.91	2.20		?	
87.05	Fe	255	3.38	2.52	2.47	2.22	2.23	error		2.34!	
99.11	Zr—Fe	203	3.15	2.55	2.54	2.34	2.32	2.39		1.97	
4202.04	Fe	380	3.78	2.76	2.75!	2.43	2.48	2.48!		2.53!	
02.76	Fe	57	1.35	bl	bl	1.81	1.90	bl		bl	
4203.57	Fe—Cr	62	1.48	1.70?	2.11	1.60	1.58	2.15		?	
05.55	Fe	75	1.80	2.45	2.44	2.06	2.09	2.27		1.97	
06.70	Fe	100	2.27	2.24	2.22	2.06	2.05	2.26		1.95	
07.14	Fe	85	2.00	2.36	2.46	2.10	2.08	1.97		1.87	
08.61	Fe	88	2.06	2.26	2.11?	2.05	2.06	2.11		bl	

	Identif.	A sun	log s_0 sun	log A (star)						
				δ Cephei		ϑ Cygni		π Cephei		δ Equulei
				10607	10617	10616	10619	10610	10618	10608
4212.64	— Cr	62	1.48	1.52	abs	1.78	1.72	2.04		1.94!
16.19	Fe	140	2.73	2.36	bl	2.08	2.09	bl		1.91
22.22	Fe	160	2.89	2.60	2.55	2.27	2.23	2.30		2.05
24.18	Fe	115	2.48	bl	bl	2.10	2.21	2.19		bl
24.52	*Fe* Cr	80	1.90	bl	bl	2.01?	1.77	2.16		bl
4225.46	Fe	110	2.41	2.54	2.54	bl	2.21	2.40		?
26.74	Ca	1230	4.80	2.82	2.74?	2.68	2.71	2.92!		2.85!
29.52	Fe	67	1.60	bl	bl	2.02	1.95	2.13		bl
31.96	Sc? —	37	0.80	1.80	2.01	1.79	1.79	1.78		bl
33.61	Fe	220	3.23	2.23?	2.38	2.22	2.29	2.29		2.27
4235.95	Fe	370	3.73	2.69	2.62	2.44	2.42	2.65		bl
38.03	*Fe* Sc	100	2.27	2.28	bl	bl	bl	2.16		?
38.82	Fe	124	2.58	2.47	2.52	2.26	2.20	2.35?		?
41.12	Fe —	42	0.93	1.86	2.17?	1.59	1.67	1.99		?
43.82	Fe —	47	1.08	?	?	1.86	1.72	1.94?		bl
4246.09	Fe	71	1.70	2.20	2.15	2.09	2.07	2.14		1.91
50.13	Fe	310	3.56	2.54	2.50	2.40	2.39	2.51		2.32!
50.80	Fe	350	3.68	2.54	2.43	2.39	2.34	2.59		2.34!
54.35	Cr	320	3.59	2.65!	2.62	2.34	2.39	2.60		2.40!
57.66	Mn	52	1.20	1.80?	1.70?	1.68	1.53?	2.00		1.48
4260.49	Fe	580	4.14	2.62	2.62	2.50	2.49	2.69		bl
63.14	*Ti* Cr	50	1.15	2.00	1.96	1.95	1.91	1.99?		?
64.22	Fe	73	1.75	bl	2.14	1.98	1.88	2.12		bl
64.74	Fe	57	1.35	1.95	bl	1.87	1.76	2.04!		bl
65.27	*Fe*—Ti	60	1.42	1.96	2.11	1.83	1.90	2.08		1.67
4265.93	Mn	57	1.35	2.01	2.11!	1.97	1.97	1.98		1.91
66.97	Fe	82	1.94	bl	bl	2.05	2.03	bl		bl
68.76	Fe	69	1.65	2.24	2.06	2.11	2.06	2.19		1.38?
71.17	Fe	300	3.53	2.50	2.41	2.22	2.28	2.44		bl
71.78	Fe	750	4.37	2.73	2.65	2.50	2.50	2.80!		bl
4274.81	Cr	300	3.53	2.60	2.54	2.33	2.32	2.55		2.32!
76.68	*Fe* Ti	56	1.32		bl	1.90	bl	2.07		1.56
82.41	Fe	162	2.91	2.59	2.47	2.20	2.18	2.44		1.92
83.62	Ca	153	2.84	2.45	2.41	2.17	2.17	2.28		2.31!
87.41	Ti	66	1.58	1.32?	1.68?	1.51	1.50?	1.78		1.73
4289.37	Ca	143	2.76	2.34?	2.31?	2.05	2.07	2.03?		bl
89.73	Cr	240	3.32	2.41?	2.39?	2.21	2.23	2.50		bl
91.48	Fe	95	2.18	2.34	2.26	1.91	1.98	2.16		2.12
4318.66	*Ca* Ti	132	2.66	2.57	2.47	2.22	2.33	2.32		2.23!
21.80	Fe	56	1.33	2.10	2.02!	1.81	2.16	2.12		?

	Identif.	A sun	log s_0 sun	log A (star)							
				δ Cephei		ϑ Cygni		π Cephei		δ Equulei	
				10607	10617	10616	10619	10610	10618	10608	
4325.78	Fe	675	4.27	2.70	2.65	2.49?	2.60?	2.73		2.59	
27.92	Fe	310	3.56	2.25	2.31?	1.92?	2.17?	2.21		?	
31.65	Ni	65	1.55	2.29?	2.23?	1.87?	2.13?	2.19?		2.06	
48.95	Fe	56	1.33	2.19!?	2.16?	1.94?	2.10?	2.05		bl	
57.52	— Cr	20	0.27	1.98	2.03	bl		1.85		1.95	
4365.91	Fe	44	1.00	1.91	2.20	error	1.78	1.78		bl	
75.95	Fe	152	2.83	2.52	2.39	2.23	2.16	2.45		bl	
76.78	*Fe*—Cr	54	1.27	1.99	2.03	?	?	1.94		bl	
79.24	V	117	2.50	2.23	2.11	2.06	1.95	2.30		1.81	
81.12	Cr	23	0.37	1.59?	1.82	?	?	1.95		bl	
4383.56	Fe	1070	4.68	2.77	2.67	2.61	2.60	2.83??		2.76	
88.42	Fe	97	2.22	2.29	2.29	2.09	2.14	bl		bl	
89.26	Fe	69	1.65	2.13	2.03	1.86	1.79	2.06		?	
4404.76	Fe	749	4.37	2.77	2.67	2.54	2.52	2.76		2.66	
06.65	V	79	1.88	2.03	2.08	1.72	1.79!	2.28		1.79	
4415.14	Fe	400	3.80	bl	2.46	2.45	2.34	bl		bl	
25.45	Ca	143	2.76	2.51	2.48	2.26	2.15	bl		2.22	
27.32	Fe	166	2.94	2.65	2.56	2.32	2.28	bl		2.35	
28.55	V—Fe	30	0.60	2.02	2.03	1.79	1.64	2.18		1.65!	
33.23	Fe	103	2.32	2.38	2.27	2.12	1.95	2.20		bl	
4435.69	Ca	138	2.72	2.43	2.35	2.12	2.10	2.27		?	
36.95	*Fe*—Ni	64	1.52	1.97	2.19	1.90	1.81	2.02		?	
38.35	Fe	48	1.10	2.07	2.15	1.97	1.98	2.16		?	
42.35	Fe	191	3.09	2.44	2.29	2.14	2.14	2.46		?	
45.48	Fe —	36	0.77	1.75!	1.72	1.81!	1.80!	2.11		1.69	
4447.73	Fe	174	3.00	2.51	2.52!	2.23	2.14	2.43		2.26	
49.15	Ti	65	1.55	bl		2.06	1.78	2.34?		2.03	
55.90	Ca	131	2.65	2.42	bl	2.12	2.11	2.19	2.10?	bl	
62.46	Ni	70	1.68	bl	1.96?	1.80	1.78	bl		?	
65.82	Ti	38	0.82	1.58	1.57?	bl		bl	1.93	abs	
4484.23	Fe	96	2.20	2.50	2.40	2.17	2.19	error	2.30!!	2.22!	
85.68	Fe	81	1.92	2.35	2.31	2.02	2.10	2.26?	2.18	2.14	
90.78	Fe	68	1.63	1.93?	1.88?	1.89	1.77	2.25	2.16	bl	
92.69	Fe	33	0.68	bl		1.61	1.63	bl		abs	
94.58	Fe	198	3.12	2.65	2.59	2.32	2.27	2.56	2.41	bl	
4500.29	Cr	29	0.57	2.01	2.16	1.66	1.76	2.15	2.10	1.86!	
04.84	Fe	41	0.90	2.10	2.26	1.83!	1.79!	2.18	2.16	2.07!!	
11.90	Cr	45	1.02	bl		1.93	1.79	2.15	2.11	abs	
12.75	Ti	64	1.52	2.22	2.15	1.94	1.84	2.27	2.16	?	
17.54	Fe	86	2.02	2.20	2.01??	1.96	1.81	2.35	2.13	bl	

	Identif.	A sun	log s_0 sun	log$A$ (star)						
				δ Cephei		ϑ Cygni		π Cephei		δ Equulei
				10607	10617	10616	10619	10610	10618	10608
4528.63	Fe	240	3.32	2.69!	2.68	2.38	2.37	2.68!	2.57!	2.42
34.79	Ti	97	2.22	2.11?	2.00	1.91	2.02	2.14	2.20	abs
45.96	Cr	83	1.96	2.20	2.17	1.97	2.03	2.05	2.00	bl
47.86	*Fe* Ti	82	1.94	2.28	2.18	2.08	2.03	2.03	2.03	1.90
50.78	Fe	79	1.88	2.16!	2.23!	2.03	2.01	2.07	1.99	2.13
4571.10	Mg	94	2.17	2.24	2.17	2.09	1.85	2.35	2.33	2.16!
78.56	Ca	78	1.86	2.35	2.33!	2.27!	2.21!!	2.43	2.33	2.29
87.14	Fe	52	1.20	1.79?	2.01	2.02	1.89	1.99	2.23	1.81
4602.01	Fe	74	1.78	1.89	1.96	1.93	1.76	2.04	2.03	2.04!
02.95	Fe	119	2.52	2.54	2.47	2.28	2.23	2.39	2.37	2.24
4606.23	Ni	39	0.85	2.12	2.23	2.03	1.79	2.19	2.18	abs
11.30	Fe	102	2.30	2.43	2.45	2.39!	2.26!	2.49	2.52	2.37
16.13	Cr	84	1.98	2.36	bl	2.10	1.91	bl		bl
17.28	Ti	62	1.48	bl	abs	2.11	1.93	2.04	2.13	1.86
25.05	Fe	86	2.02	2.40	2.29	2.22	2.05	2.29	2.27	2.18
4626.18	Cr	75	1.80	2.39	2.34	2.05	1.91	2.37	2.41	2.06
30.13	Fe	66	1.58	2.12	1.62?	2.17	1.94	2.19	2.16	2.12!
43.47	Fe	74	1.78	2.41	2.34	2.26	2.10	2.50!	2.53!	?
46.17	Cr	103	2.32	2.58	2.50	2.17	2.15	2.51	2.51	2.34
47.44	Fe	100	2.27	2.50	bl	bl	2.23	bl		bl
4648.66	Ni	83	1.96	2.53	2.51	2.26	bl	2.24	2.24	2.26
51.29	Cr	74	1.78	2.30	2.26	1.93	1.93	2.31	2.28	2.22!
52.17	Cr	104	2.33	2.35	2.27	2.18	2.14	2.21	2.24	?
64.80	— *Cr* Na?	46	1.05	2.15	2.14	1.86	1.72	2.20	2.18	2.05
69.18	Fe	72	1.72	2.40	2.31	2.08	2.13	2.39	2.37	2.14
4683.57	Fe	49	1.12	2.12	2.21	2.01	2.00	2.29?	2.19	?
86.22	Ni	61	1.45	2.20	2.15	2.03	1.83	error	2.19	bl
87.40	Fe	30	0.60	2.09	2.09!	2.00	2.10	error	2.21	1.91
90.15	— Fe	54	1.27	2.05	1.81	2.08	1.97	error	2.24	?
4703.00	Mg	336	3.64	2.71	2.60	2.51	2.54	2.64	2.57	2.52
4715.77	Ni	75	1.80	2.36	2.34	2.08	2.12	2.21	1.93?	2.08
18.42	Cr	66	1.58	2.21	2.15	1.91?	2.13	2.24	2.15	1.85
21.00	Fe	48	1.10	2.13	1.82	1.97	2.00	2.22	2.21	2.06!
22.16	Zn	75	1.80	2.32	2.18	1.86	2.03	1.86	2.03	1.97
24.41	Cr	22	0.33	2.26!	2.23!	1.96	1.96!	2.24!	2.30!	1.57
4726.15	Fe	15	0.07	1.45?	1.90?	1.99	1.97	2.00	2.02	1.98!!
28.55	Fe	83	1.96	bl		bl		2.31	2.35	2.07
33.60	Fe	86	2.02	2.41	2.24?	2.20	2.19	2.54	2.54	2.08
35.85	Fe	58	1.38	2.11	1.97	1.79	1.98	2.22	2.18	?
41.54	Fe	70	1.68	bl	2.32	2.14	2.00	2.11	bl	bl

	Identif.	A sun	log s_0 sun	log A (star)						
				δ Cephei		ϑ Cygni		π Cephei		δ Equulei
				10607	10617	10616	10619	10610	10618	10608
4742.80	Ti	26	0.47	1.98	2.16?	1.89	2.05	2.31!	2.32!?	1.99!
44.39	Fe	47	1.08	2.13	2.18	2.20!	2.22!	2.11!	2.33!?	2.24!
45.81	Fe	74	1.78	2.41	2.27	2.25	2.20!	2.47!	2.46!	1.99
54.04	Mn	135	2.69	2.58	2.54!!	2.37	2.35	2.52!	2.56!	2.36!
59.28	Ti	41	0.90	2.20	1.97	2.01	1.45??	2.31	2.28	1.99
4761.53	Mn	73	1.75	2.16	2.10	2.18!?	2.03!??	2.33	2.36	bl
66.42	Mn	89	2.08	2.47	2.20?	2.32	2.23	2.42	2.48	bl
72.82	Fe	97	2.22	2.27	2.18	2.17	1.96	2.31	2.30	2.14
81.73	Ti	10	1.87	2.04!	2.08	2.06	1.64	2.23	2.24	1.82
83.43	Mn	142	2.75	2.68	2.56	2.29	2.35	2.57	2.61	2.49
4802.89	Fe	57	1.35	2.31	2.26	2.18	2.11	2.37!	2.29!	2.16
07.00	Ni	59	1.40	2.37	2.24	2.03	2.05	bl		2.17!
10.54	Zn	65	1.55	2.51	2.33	2.27	2.16	2.43	2.32	2.30!
17.81	*Fe*—Ni	43	0.97	2.39!	2.18	1.98	1.94	2.41	2.17	2.11
31.18	Ni	68	1.63	2.33	2.34	2.36!!	2.29!!	2.39?	2.44	2.29!
4832.72	Ni—*Fe*	58	1.38	2.38	2.34	2.24	2.22	2.39?	2.31	2.17
34.52	Fe	26	0.47	abs-		2.16	2.10	2.42!?	2.30?	1.88
41.79	— Fe	24	0.40	1.68?	2.09	2.06?	2.13!?	2.11	2.03	1.85
44.02	*Fe*—Ti	42	0.93	2.11	2.16	1.98??	2.11?	2.21	2.24	?
45.66	Fe	38	0.82	2.29	2.40!	2.13??	2.05?	2.47	2.15	2.22!
4847.31	Ca	21	0.30	abs		abs		2.02??	2.20	1.96
4903.32	Fe	118	2.51	2.46	2.38	2.22	2.22	2.32		bl
04.42	*Ni* V	78	1.86	2.36	2.17	2.08	2.15	?		bl
20.52	Fe	425	3.86	2.77	2.72	2.49	2.40	2.80		2.47
30.31	Fe	63	1.50	2.23	2.20	?	?	2.41!		2.27
4932.07	V —	25	0.43	2.18	2.36	2.20!	1.51!?	1.80		2.01
42.49	Cr	77	1.84	2.31	2.46!	2.19		2.21		2.17
46.40	Fe	106	2.36	2.32	2.37			2.44		2.15
50.11	Fe	82	1.94	2.27	2.32			2.30		
62.58	Fe	52	1.20		2.29			2.27		
4966.10	Fe	116	2.49		2.45			2.25		
73.11	Ti—Fe	81	1.92		2.33			2.29		

Ion lines.

	Identif.	A sun	log s_0 sun	log A (star)							
				δ Cephei		ϑ Cygni		π Cephei		δ Equulei	
				10607	10617	10616	10619	10610	10618	10608	
4050.33	Zr^+	23	0.37	2.43		1.86					
77.73	Sr^+	340	3.65	2.88?		2.55					
86.72	La^+	37	0.80	2.40		1.84					
4123.24	La^+	37	0.80	bl		1.88	1.94			bl	
28.74	Fe^+	41	0.90	2.34	2.23	1.85	1.98			1.85	
4138.36	— Fe^+ ?	23	0.37	2.15	2.30	1.80	1.79			1.52	
78.86	Fe^+	76	1.82	2.66	2.61	2.21	2.23	2.03		abs	
83.46	V^+ —	45	1.02	2.28	2.35	1.91	1.81	?		?	
86.62	Ce^+ —	59	1.40	2.23	2.22	1.69?	1.83?	2.10?		?	
4208.99	Zr^+	43	0.97	2.33?	2.45	1.86	2.00	2.11		bl	
4233.17	Fe^+	115	2.48	2.69	2.63!	2.31	2.21	2.16		2.03	
46.84	Sc^+	160	2.89	2.66	2.64	2.43	2.36	2.41		?	
63.61	La^+ —	19	0.23	1.57?	1.99	1.63	bl	1.71		?	
90.23	Ti^+	117	2.50	2.63	bl	2.29	2.31	2.32		2.18	
4300.06	Ti^+	150	2.82	bl		2.35	2.34	2.39		bl	
4316.80	Ti^+	42	0.93	2.42	2.37	1.96	2.14	2.08		bl	
17.32	Zr^+ —	11	$\bar{1}$.90	1.92?	1.93	bl	1.69	1.81		bl	
22.51	La^+	8	$\bar{1}$.71	1.92	2.13	1.67	1.87	1.52		abs	
33.76	La^+	30	0.60	2.50?	2.41?	1.90?	2.25?	2.32		2.17	
54.62	Sc^+	47	1.07	2.48	2.44	2.08?	2.18?	2.29		bl	
4364.67	Ce^+—La^+	10	$\bar{1}$.83	2.14	2.04	1.78	2.00	1.64		1.66	
68.64	— Nd^+	17	0.15	1.73?	bl	error	1.62	1.88		abs	
94.07	Ti^+	74	1.78	2.49	2.43	2.15	2.09	2.29?		2.18	
95.04	Ti^+	148	2.80	bl	2.66	2.40	2.40	bl		bl	
99.78	Ti^+	122	2.56	2.61	2.56	2.26	2.24	2.29		?	
4400.40	Sc^+	87	2.04	bl		2.18	2.10	2.37		bl	
11.94	Ti^+	43	0.97	2.41	2.40	1.81	1.89	2.31		2.03	
15.56	Sc^+	101	2.28	bl	2.46	2.06	1.97	bl		bl	
16.83	Fe^+	76	1.82	2.56	2.52	2.26!	2.18!	2.14		2.25!	
17.72	Ti^+	100	2.27	2.64	2.53	2.20	2.18	2.39		?	
4418.34	Ti^+	63	1.50	2.34	2.44	2.09	1.92	2.20		?	
31.37	Sc^+	24	0.40	2.18	2.26	1.88	1.72	2.02		abs	
43.81	Ti^+	146	2.78	2.66	2.67	2.26	2.24	2.24		bl	
44.56	Ti^+	56	1.32	2.43	2.50	2.11	1.82	2.34		2.14!	
68.50	Ti^+	141	2.74	2.75	2.57	2.29	2.30	2.35	2.25	?	
4486.91	Ce^+	12	$\bar{1}$.95	2.21	2.32!!	?	?	2.16!?	2.19!	1.86!	
91.41	Fe^+	79	1.88	2.62	2.56	2.10	2.18	2.29	2.24	bl	
93.53	Ti^+	29	0.57	2.30	2.35	1.78	1.99	2.03	1.91	abs	
4501.28	Ti^+	142	2.75	2.77	2.73	2.38	2.34	2.43	2.28	2.33	
08.29	Fe^+	85	2.00	2.74	2.71	2.27	2.25	2.41	2.30	2.28!	

	Identif.	A sun	log s_0 sun	log A (star)						
				δ Cephei		ϑ Cygni		π Cephei		δ Equulei
				10607	10617	10616	10619	10610	10618	10608
4515.34	Fe^+	103	2.32	2.70	2.65	2.29	2.24	2.35	2.27	2.27
20.23	Fe^+	80	1.90	2.71	2.63	2.35	2.30	2.48?	2.41	2.27
44.02	Ti^+ —	33	0.68	2.46!	2.41	1.97	2.00!	2.15	2.19	?
45.14	Ti^+	43	0.97	2.45	2.37	2.01	1.93	bl	2.18	abs
54.04	Ba^+	173	3.00	2.81	2.71	2.38	2.36	2.58	2.58	2.39
4554.99	Cr^+	37	0.80	2.23?	2.31	2.06	1.96	1.97	2.15?	1.71?
58.65	Cr^+	78	1.86	2.75	2.68	2.34	2.25	2.42	2.35	2.32!
62.37	Ce^+	19	0.23	2.22	2.20	2.09	1.86	1.98	2.16?	1.77
63.77	Ti^+	128	2.62	2.84	2.72	2.36	2.35	2.45	2.47?	2.38
68.33	Ti^+	19	0.23	bl	2.46	2.05	1.41?	bl		bl
4571.98	Ti^+	146	2.78	2.87	2.79	2.44	2.42	2.49	2.55	2.35
76.34	Fe^+	57	1.35	2.66	2.59	2.21	2.19	2.21	2.19	2.04
82.84	Fe^+	49	1.12	2.53	2.40	2.20	2'03	2.30!?	2.31!	1.94?
83.84	Fe^+	105	2.34	2.86	2.82	2.48	2.38	2.46?	2.43	2.42
88.21	Cr^+	67	1.60	2.68	2.63	2.26!	2.23!	2.38!	2.26!	2.24
4589.96	Cr^+—Ti^+	79	1.88	2.69	2.61	2.27	2.23	2.25	2.16	2.29!
92.06	Cr^+	46	1.05	2.40	2.44	1.96?	1.46?	bl		bl
4609.27	Ti^+ —	10	$\bar{1}$.83	2.16	2.27	1.95	1.60?	2.05	1.97	2.12!
20.52	Fe^+	51	1.18	2.55	2.44	2.17	2.04	2.19!	2.03!	2.20
28.16	Ce^+	14	0.03	2.27	2.10	1.93	1.68!	1.86	2.03?	1.79
4634.08	Cr^+	49	1.12	2.61	2.48	2.21	2.06	2.34	2.18	2.21
70.42	Sc_+	61	1.45	2.66	2.65	2.28	2.22	2.33	2.31	2.14
4719.51	Ti^+	12	$\bar{1}$.95	2.41	2.29	2.08	1.97	2.08	1.97	bl
31.48	Fe^+	80	1.90	2.62	2.61	2.03	2.32	bl	2.35	2.20
73.97	Ce^+	9	$\bar{1}$.76	2.05	2.05	2.15	1.96	1.90	2.13!	1.69
4805.10	Ti^+	76	1.82	2.70	2.64	2.25	2.28!	2.25	2.22	2.37!
12.36	Cr^+	28	0.53	bl	2.37	2.11!	1.99!	2.15	bl	?
48.25	— Cr^+	58	1.38	2.74	bl	2.38?	2.32?	bl		bl
83.69	Y^+	53	1.22	2.56	2.48	2.32	2.27	2.20	2.38	2.17!
4923.93	Fe^+	159	2.88	2.90	2.79	2.42	2.41	2.71!		2.48!

Molecular lines. (π Cephei 10610).

	Identif.	A sun	log s_0 sun	log A star
4207.41	CN	53	1.23	1.97
10.97	CH	75	1.80	1.85?
18.73	CH	78	1.86	1.82
24.86	CH	80	1.90	1.82
48.95	CH	66	1.58	1.93
4255.25	CH	65	1.55	1.65?
67.39	CH	65	1.55	1.82
81.97	CH	71	1.70	1.52?
4313.63	CH	59	1.40	1.82
23.01	CH?	59	1.40	2.05
4378.26	CH	55	1.30	1.92

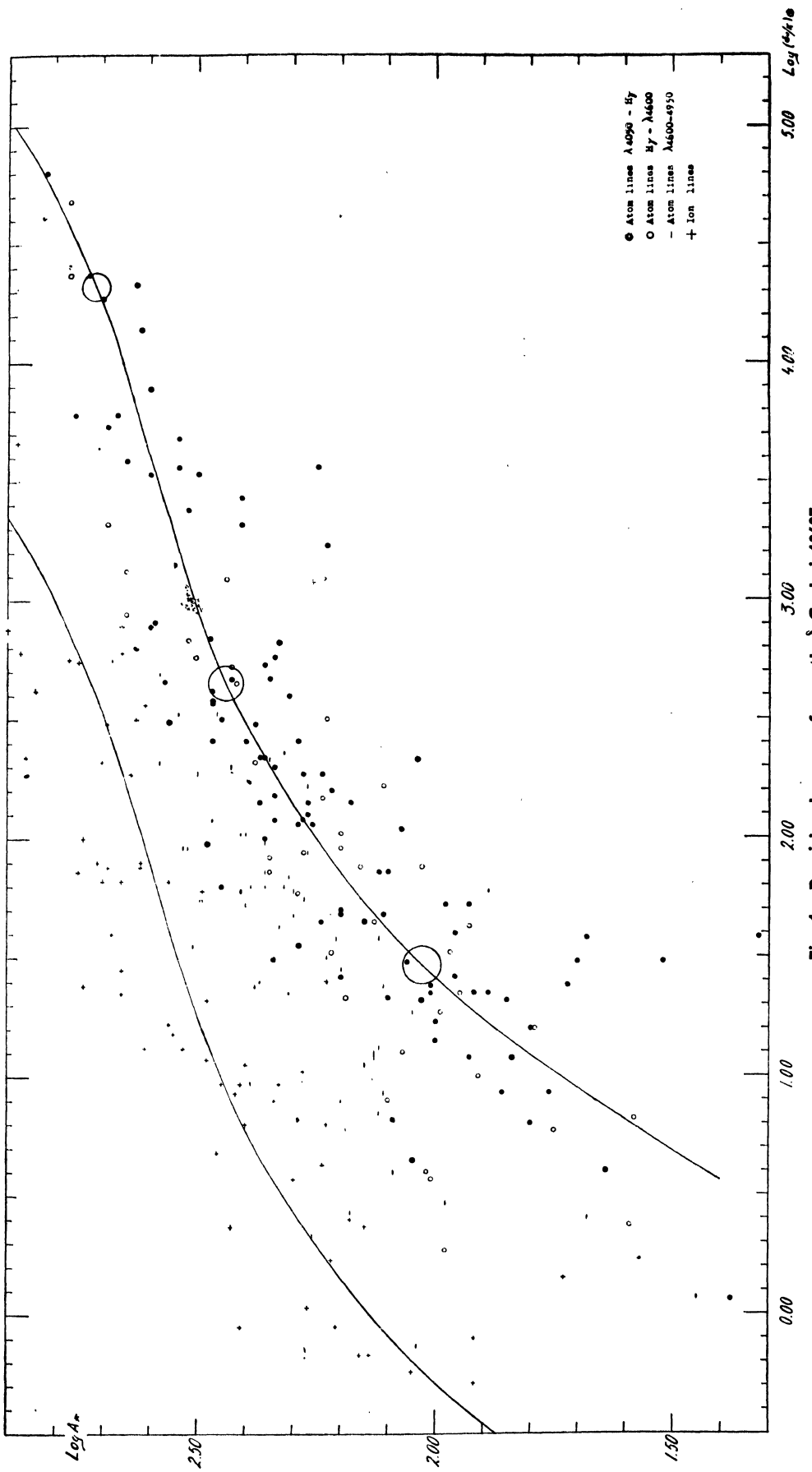

Fig. 1. Provisional curve of growth δ Cephei 10607.

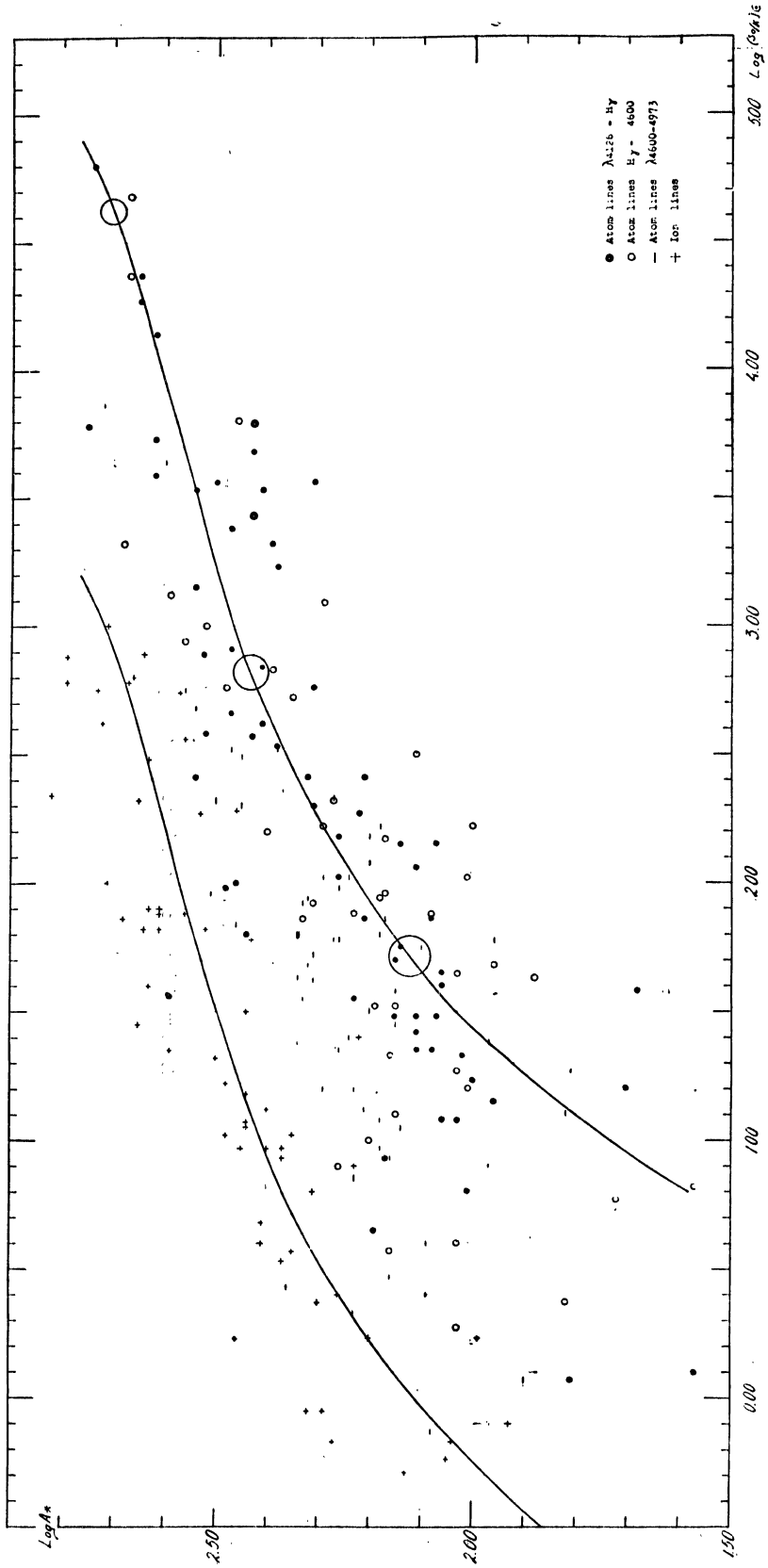

Fig. 2. Provisional curve of growth δ Cephei 10617.

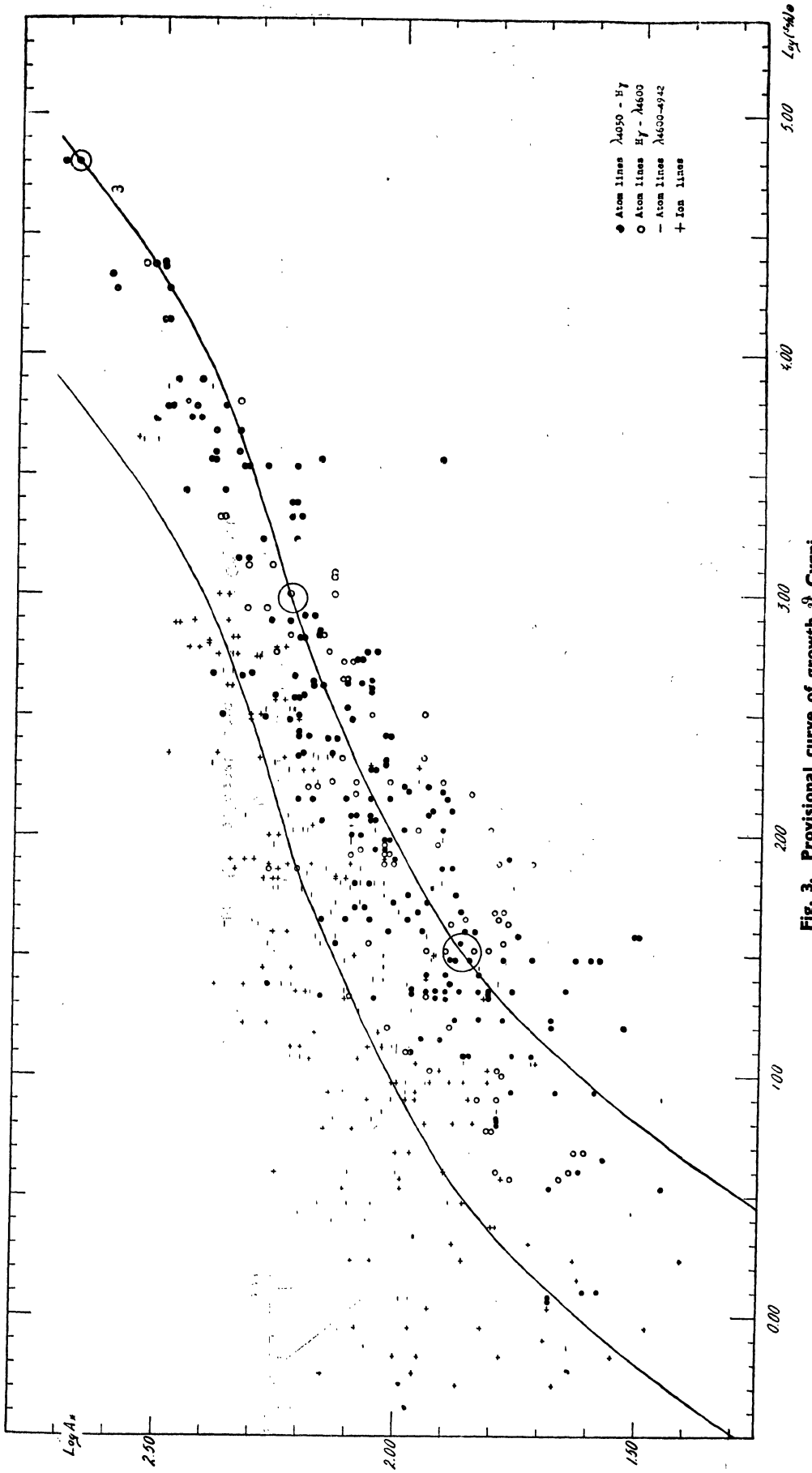

Fig. 3. Provisional curve of growth ϑ Cygni.

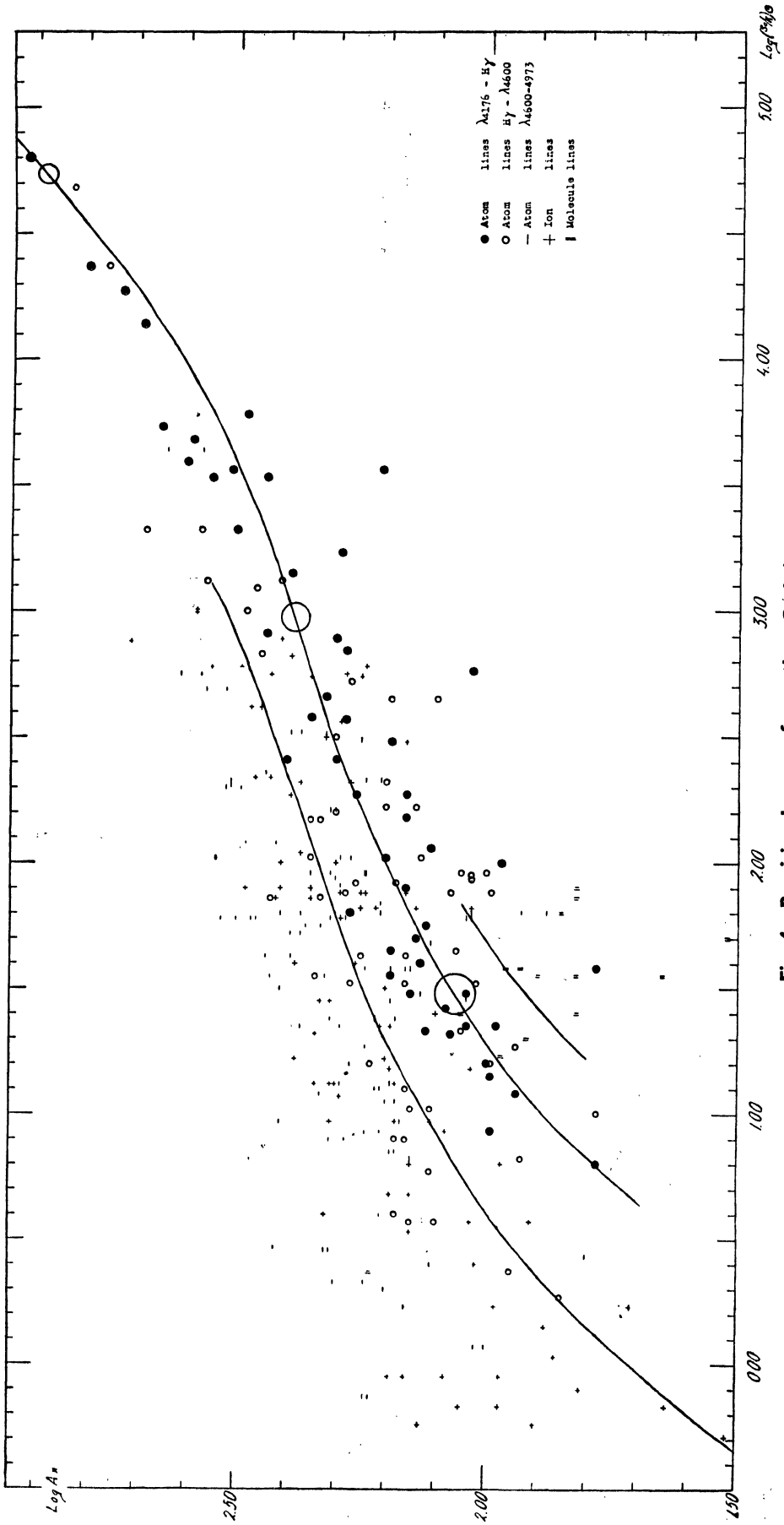

Fig. 4. Provisional curve of growth π Cephei.

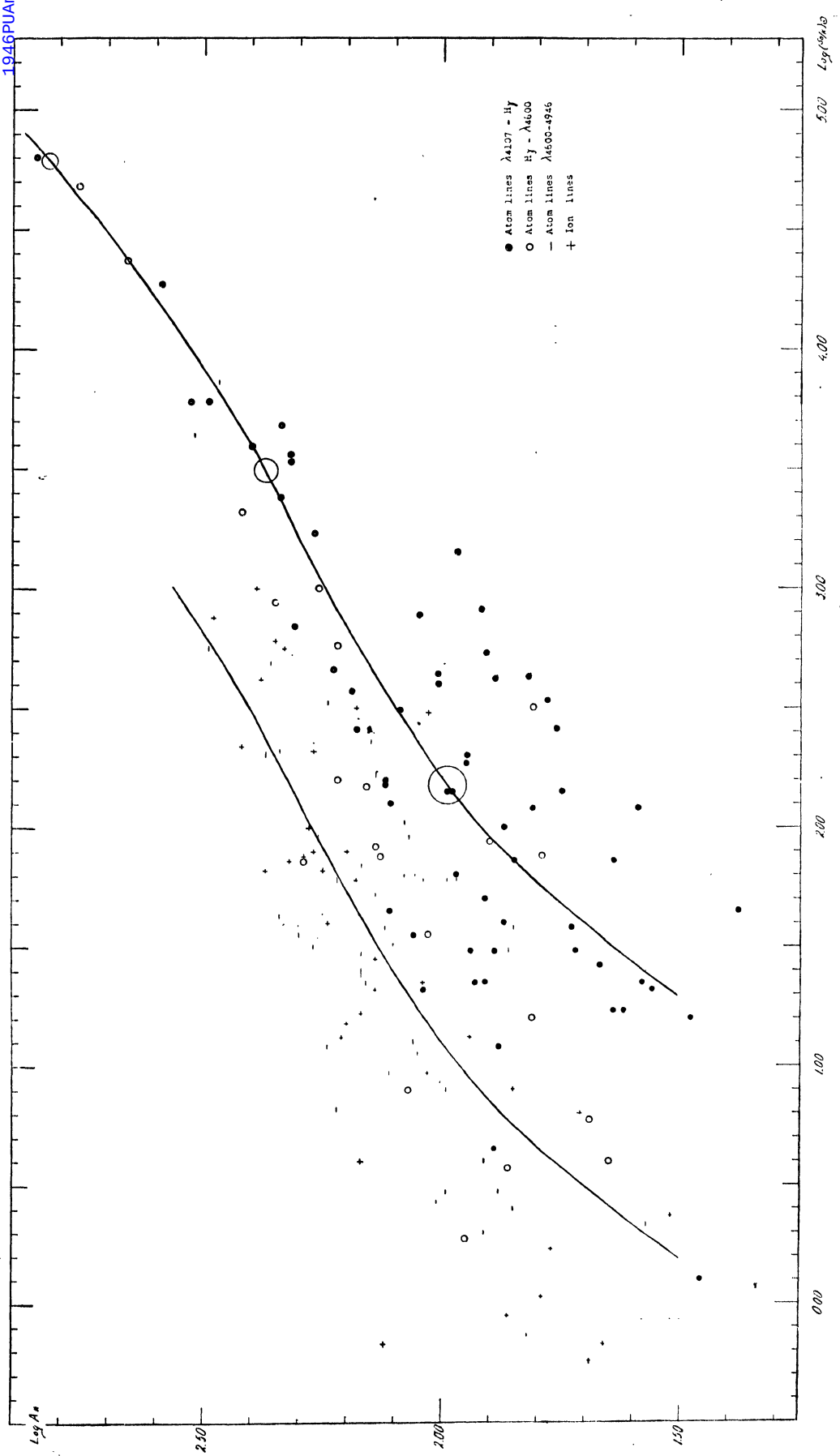

Fig. 5. Provisional curve of growth δ Equulei.

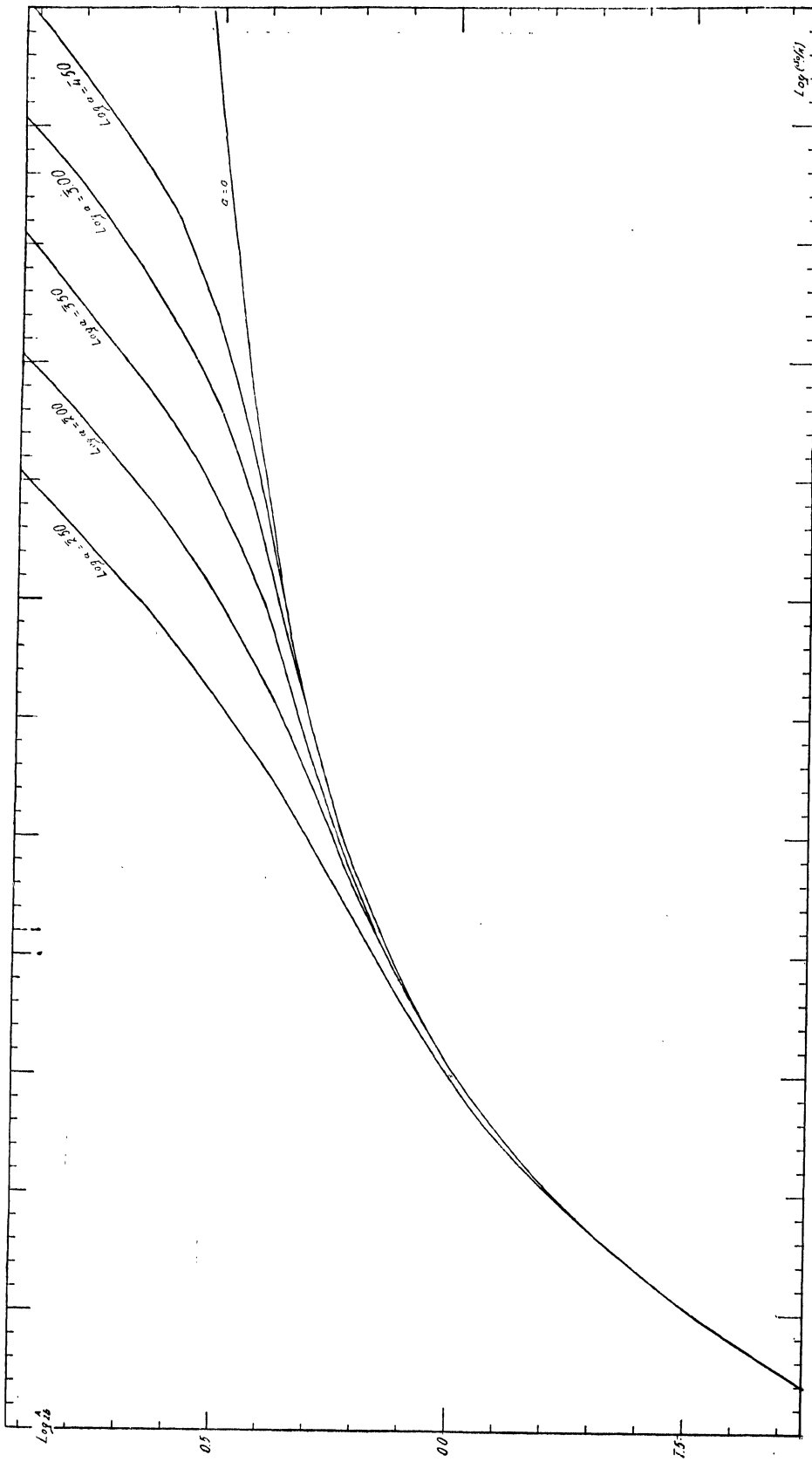

Fig. 6. Theoretical curves of growth.

The figures of table 7 are plotted in the diagrams of fig. 1—5. Fig. 6 reproduces the curves of growth given in table 5. It is to be noted, that the vertical scale in these diagrams is twice as large as the horizontal scale, so that the true curves are directed even more horizontally than is indicated by the figures.

Now in each diagram we mark three regions by small circles, through which the curve of growth has to pass. Then we move the whole set of theoretical curves of growth, drawn on a transparent sheet of paper, in such a way over the diagram, that its scales permanently remain parallel to the scales in the diagram and the theoretical curve always passes through the centre of the lowest region, denoted by a circle on the diagram. This movement is continued until the theoretical curve also passes through the second region denoted. The location of the scales is then fixed and we can read the values of the Doppler width for the stellar spectrum and the difference between the values of log s_0/k for corresponding lines in the sun and in the star. Finally the location of the highest circle indicates the value of log a, the ratio of resonance- to Doppler broadening.

The results obtained in this way can only be provisional of course, as the equivalent widths of the stellar lines have not yet been corrected for blending and background influences. So it would be premature to make an estimate of the accuracy of the results. They can only be considered as first approximations and they will have to undergo as yet a great number of systematic corrections.

The results, derived from the diagrams are collected in table 8.

Table 8. Provisional parameters of the curves of growth.

		δ Cep 10607	δ Cep 10617	ϑ Cygni	π Cephei	δ Equulei
log s_0/k $\left(\frac{\text{sun}}{\text{star}}\right)$	atomic lines	$\overline{1}.0$	$\overline{1}.0$	$\overline{1}.3$	$\overline{1}.6$	$\overline{2}.7$
	ion lines	0.7	0.7	0.3	0.3	$\overline{1}.6$
	molecules	—	—	—	$\overline{1}.2$	—
log $2b$ (Angström units)		$\overline{1}.27$	$\overline{1}.23$	$\overline{2}.92$	$\overline{1}.04$	$\overline{1}.04$
b (milli-Angström)		93	85	42	55	55
log a		$\overline{3}.25$	$\overline{3}.00$	$\overline{3}.50$	$\overline{3}.50$	$\overline{2}.25$
log γ		$\overline{4}.22$	$\overline{5}.93$	$\overline{4}.12$	$\overline{4}.24$	$\overline{4}.99$
γ/γ(cl)		2.8	1.4	2.2	3.0	16.6

II. METHOD OF THE SECOND ANALYSIS.

Computation of the blend intensity from the separate components.

Our second aim is to obtain a more accurate determination of the spectral parameters. In the introduction we already mentioned the method which we employed to this end. The second analysis starts with the construction of a theoretical spectrum and its differential corrections, derived from the provisional spectral parameters to which we allow slight variations. This theoretical spectrum is then compared with the observed one and from the results of this comparison we obtain the demanded differential corrections.

The first step in this procedure is to obtain the theoretical equivalent width of a blend which is composed of a number of lines of known strength. There are two reasons, why the equivalent width of the blend is different from the sum of the equivalent widths of the separate components. First of all, the blend never stands alone, but it is neighboured by other blends, and as all instrumentally broadened lines have gradual diminishing wings, adjacent blends always overlap to a certain extent. So it is never possible to make a "clear" cut, but in separating a blend from its neighbours, we always cut down the extreme wings, at the same time including in the equivalent width measured the wings of the adjacent line. The second reason is, that the overlapping of lines in a blend is not only due to the blurring by the instrument, but occurs also to some extent in the true profiles. In this case, it is no longer true, that the absorption caused by two combined profiles is equal to the sum of the contributions of the separate lines. The true equivalent width may be calculated only if we combine the values of s/k for the different lines and then calculate the line depth R directly by eq. (1).

We first consider the effect of geometrical cutting.

The observed profile of a line results from a combination of the true profile and the broadening by the instrumental curve. We may treat the instrumental curve as if it consists of a large number of very narrow lines. If now we give to each of these line elements a profile similar to the true profile of the line, the addition of the contributions of all these elements will yield the observed line profile.

So in this way each component of the blend is split into a large number of elementary lines, each of which has the same profile. For another component of the blend we may proceed in the same way, but the profiles of the elementary lines will now be similar to the true profile of this second component and so their shape will differ from that of the elements of the first series. Only in the case of resonance lines, which have all similar profiles, all line elements will have the same shape.

For very strong Doppler lines, the shape of the line tends to a rectangle. For weaker Doppler lines, the shape will be different from this figure. We must bear in mind, however, that the shape of the profile is of importance here only for the calculation of the cutting effect. As the Doppler widths are much smaller than the total width of the blend, only those Doppler profiles, which occur near the limits of the blend will be cut.

Now it is clear, from the fact that the limit of the blend is marked by a decrease in absorption, that the elementary lines which are situated near this limit, give only a small contribution to the total intensity. So it will be appropriate, to use for them a more approximate calculation. It will be shown that it is quite sufficient to treat also the weaker Doppler lines as having rectangular profiles.

The weakest Doppler lines, whose profiles are Gaussian curves, show the strongest deviations from a rectangular profile. For Doppler width b the fraction of the total surface between the limits $\pm c$ is given in Table 9.

Table 9.

c/b	Fraction of surface between limits $\pm c$.	c/b	Fraction of surface between limits $\pm c$.
0.0	0.000 (0.000)	1.0	0.843 (0.725)
0.2	.223 (.145)	1.2	.910 (.870)
0.4	.428 (.290)	1.4	.952 (1.000)
0.6	.604 (.435)	1.6	.976 —
0.8	.742 (.580)	1.8	.989 —

The second column of the table gives the calculated fractions for a Gaussian profile, the third column for a rectangular profile with half width $= 1.38\ b$. The difference between corresponding values never becomes greater than 1/6 of the equivalent width. As errors of this magnitude can be made only for the weakest lines, the shapes of stronger Doppler lines becoming more and more rectangular, the approximation by a rectangle will suffice for our purposes.

The widths of the rectangles we determined in a slightly arbitrary manner. In doing so, we took into account, that if a number of similar elementary lines is put side by side, in a way corresponding with the shape of the instrumental curve, the elements at the centre of the configuration will be the strongest, whereas the elements in the wings of the instrumental curve are weaker. So a cutting error in the centrally situated lines will effect the total equivalent width more than an error in the cutting effect of the side lines. This is the reason, why we adopted a comparatively large value for d, the half width of the rectangular profile. For in this case the error in the cutting of the centrally situated lines, which are cut near their edges is only very small and the greater cutting error for the side lines has no great influence, as these side lines themselves are very weak. As the errors committed in both cases have opposite signs, the total error in the integrated profile will be quite negligible.

It is clear, however, that such a result would not have been attained at, if we had neglected the true width of the Doppler profile altogether. Indeed, early calculations that were made on this basis, led to contradictory results.

Table 10. Effective half widths of Doppler lines.

$\log s_0$	$d/\frac{1}{2}D$	d/b	$\log s_0$	$d/\frac{1}{2}D$	d/b
$-\infty$	∞	1.38	2.4	1.08	2.10
0.0	4.74	1.38	2.8	1.06	2.28
0.4	2.62	1.40	3.2	1.04	2.45
0.8	1.80	1.48	3.6	1.02	2.62
1.2	1.42	1.60	4.0	1.02	2.78
1.6	1.24	1.76	4.4	1.00	2.93
2.0	1.14	1.93	4.8	1.00	3.09

The adopted values for d, the half width of the rectangle are given in Table 10. They are expressed in $\frac{1}{2}D$, the half equivalent width of the Doppler profile and in b, the Doppler width, as a unit.

Very simple is the formula for the cutting effect of the resonance wings. In accordance with our earlier approximations we suppose that these wings extend from the limit $x = w$ outwards. If then, such a wing is cut at $x = c > w$, the equivalent width of the remaining part will be equal to :

$$(9) \qquad W = \sqrt{C + w^2} - w - \sqrt{C + c^2} + c.$$

We now turn to the physical effect. For strong Doppler lines, which have almost rectangular profiles, the physical blending will occur only if the distance between the centres of the lines is less than half the sum total of the separate equivalent widths.

For other Doppler lines, we will estimate the effect of physical blending, adopting rectangular profiles with the effective widths of table 9. We consider two Doppler lines with equal equivalent width $= D$ and calculate the intensity of the blend when the centres of the lines are separated by a distance $= \Delta$. As the width of the adopted rectangles is equal to $2d$, their depth will be given by $R = D/2d$. The corresponding value of the coefficient of scattering may be calculated by (1) and is equal to s. In the overlapping part, with width $2d - \Delta$ the coefficient of scattering will equal $2s$.

Calculating again the depth of the combined profile in this central part and adding the undisturbed outer parts with depth R and total surface $2R\,\Delta$, we find for the total equivalent width of the blend (denoted by B) :

$$B = \frac{D\Delta}{d} + (2d - \Delta).\left\{1 - \frac{2d - D}{\sqrt{4d^2 + 4dD - D^2}}\right\} \quad (\Delta < 2d)$$

$$\text{or } \frac{B}{2D} = 1 - \left(1 - \frac{\Delta}{2d}\right).\left\{1 - \frac{d}{D} + \frac{2d/D - 1}{\sqrt{4 + 4D/d - D^2/d^2}}\right\} = 1 - \left(1 - \frac{\Delta}{2d}\right).f(D/d).$$

The values of f as a function of $D/2d$ are given below.

$D/2d$	0.0	0.1	0.2	0.3	0.4	0.5	0.6	0.7	0.8	0.9	1.0
f	0.00	0.13	0.21	0.28	0.34	0.38	0.41	0.44	0.46	0.48	0.50

The distance between two lines which are separated in the Rowland table is only seldom less than 100 mA. On the average, the 5737 lines in the region λ 4000—5000 are separated by a distance of 174 mA. As we shall see later, the value of b for the spectrum of δ Cephei is a little

Table 11. Correction for physical blending. Dopplerlines.

log s_0	$D/2b$	log $(1 - B/2D)$		
		$\Delta = b$	$\Delta = 2b$	$\Delta = 3b$
0.0	0.30	—0.07	—0.03	————
0.4	0.54	—0.10	—0.05	————
0.8	0.81	—0.13	—0.06	————
1.2	1.12	—0.15	—0.08	—0.01
1.6	1.41	—0.17	—0.10	—0.03
2.0	1.70	—0.19	—0.11	—0.05

smaller than this, probably about 60 or 65 mA. So the distance between the centres is generally of the order of $2b$ or $3b$ and is hardly ever less than b. For the other spectra the Doppler widths are distinctly smaller and so the lines will be more clearly separated.

If now we compare the values of $f(D/d)$ with those of table 10, we find $B/2D$ assuming $\Delta = b$, $\Delta = 2b$, resp. $\Delta = 3b$ as given in Table 11.

The first column of corrections yield the maximum values, which occur only in very unfavourable circumstances. The middle and last columns give the ordinary values. As we see, corrections become important only for lines with equivalent width larger than b, or 60 mA in the star. These lines correspond with solar lines of Rowland intensity 1 or 2 in the case of atomic lines, or intensity — 2 in the case of ion lines. For atomic lines of Rowland intensity 1 or smaller, no correction will be needed; for heavier lines only, if they are separated by a distance not surpassing 200 mA. As we shall see from an inspection of the Rowland table, corrections will be necessary only in a few cases and it is more practical to omit them, than to develop special calculating methods in order to include them.

A similar conclusion is found to apply if we consider lines with pure resonance profiles. If. e.g. two resonance lines of equivalent width A are separated by a distance $\Delta = A$, the correction for physical blending is found to be 0.053 in the logarithm. As the separations are usually larger than this limit, the correction will be of little significance.

Influence of instrumental broadening.

From the discussion in the preceeding paragraph it follows, that we may consider the stellar lines to consist of a rectangular Dopplerprofile (which we do not suppose to be completely black), in some cases accompanied by resonance wings; and that the contributions of the different components of the blend to the equivalent width may be added arithmetically. We now must consider the influence of the instrumental broadening, in order to know what part of the total absorption will be measured within the cutting limits of the blend.

The effect of the instrumental broadening will be different for Doppler- and resonance lines. A numerical calculation shows, that the natural width of the resonance profile is so much greater than the width of the artificially narrowed [1]) instrumental curve, that for the resonance wings the instrumental broadening may be neglected altogether. So we may restrict ourselves to the theoretically very simple case of the broadening of the rectangular Doppler profile.

The true profile of the Doppler line is supposed to be a rectangle of width $2d$ and surface D. Its depth will be equal to $D/2d$. The instrumental profile will be denoted by I_x, x being the spectral coordinate in the direction of wave length. The surface of the broadened profile of the Doppler line, between $x = 0$ and $x = c$ is given by:

$$S_c = (K_{d+c} - K_{d-c})\, D/2d, \text{ where} \tag{10}$$

$$K_c = \int_0^c J_y\, dy \qquad J_y = \int_0^y I_x\, dx. \tag{11}$$

When the instrumental curve is known, the function K may be tabulated and S may be calculated directly for each value of D, d and c. In order to facilitate the calculations, we may use a table, which immediately gives S/D as a function of d and c.

[1]) B.A.N. 301 (1937).

Differential corrections.

Now we are in a position, which allows us to calculate the intensity of a line or blend in the spectrum of the star, if its intensity in the sun and the different parameters of the curve of growth are known. At present we will try to investigate the differential corrections to the equivalent width, if the spectral parameters are changed.

We start with a pure Doppler line. The intensity of the entire line depends on the parameters s_0/k (which in this paragraph we shall denote simply by s) and b, the Doppler width.

From eq. (10) we derive by partial differentiation :

$$\frac{\partial \ln S}{\partial \ln b} = \frac{\partial \ln D}{\partial \ln b} + \frac{D}{2\,S\,d}\frac{\partial}{\partial \ln b}(K_{d+c} - K_{d-c}) - \frac{\partial \ln d}{\partial \ln b}$$

Now for constant values of s, D and d will both be proportional to b. So the first and third terms at the right hand side cancel and in the middle term we may replace the differentiation with respect to b by one with respect to d. Then the derivative of K becomes equal to Jd. We obtain

$$(12) \qquad \frac{\partial S}{\partial \ln b} = \frac{D}{2}(J_{d+c} - J_{d+c})$$

and in a similar way :

$$(13) \qquad \frac{\partial S}{\partial \ln d} = \frac{1}{2d}(K_{d+c} - K_{d-c})\,D\frac{\partial \ln D}{\partial \ln s} + \left\{\frac{J_{d+c} - J_{d-c}}{2} - \frac{K_{d+c} - K_{d-c}}{2d}\right\} D\frac{\partial \ln d}{\partial \ln s}$$

In the case of resonance wings, we may differentiate eq. (9) directly with respect to b, to s and to a if we take C from eq. (7) and w from (6). In these calculations, there appears the derivative of w with respect to a, which is found equal to :

$$\frac{\partial \ln w}{\partial \ln a} = -\tfrac{1}{2}\frac{b^2}{w^2 - b^2}, \text{ whereas } \frac{\partial \ln w}{\partial \ln b} = 1, \qquad \frac{\partial \ln w}{\partial \ln S} = 0$$

We combine all results, writing :

$$(14) \qquad \begin{aligned} &\frac{1}{2d}(K_{d+c} - K_{d-c}) = k \qquad && \tfrac{1}{2}(J_{d+c} - J_{d-c}) - k = j \\ &\sqrt{1 + w^2/C} - w/\sqrt{C} = f_w \qquad && \sqrt{1 + w^2/C} = g_w \quad g_w - f_w = h_w \end{aligned}$$

and obtain :

$$S = kD + (f_w - f_c).\ \sqrt{C}$$

$$\frac{\partial S}{\partial \ln b} = (k + j)\,D + (f_w - g_c).\ \sqrt{C}$$

$$(15) \qquad \frac{\partial S}{\partial \ln s} = k\frac{\partial D}{\partial \ln s} + j\,D\frac{\partial \ln d}{\partial \ln s} + \tfrac{1}{2}(g_w - g_c).\ \sqrt{C}$$

$$\frac{\partial S}{\partial \ln a} = \tfrac{1}{2}(g_w - g_c).\ \sqrt{C} + \tfrac{1}{2}\frac{b^2}{w^2 - b^2}h_w.\ \sqrt{C}$$

The resonance terms disappear, if the cutting distance c is smaller than w.

Combination of lines into one blend.

In combining a number of lines into one blend, we now simply add their respective contributions to the total equivalent width. In deriving differential corrections, however, we must take into account, that the intensities of the different lines may not be modified independently of one another, but that these corrections are determined by the variations of general spectral parameters. Of these parameters, we considered already 3, *viz* b, s and a.

We will suppose, that the parameters b and a, which refer resp. to the Doppler- and resonance widths, have the same values for all lines. This will be a sufficient approximation [1]). The parameter s, referring to the line strength, will obviously be different for different lines. But it is related to the line intensity in the solar spectrum and the difference between the value of s in the star and in the sun again is determined by general physical influences.

As our symbol s is only an abbreviation for s_0/k, the ratio of the selective diffusion at the centre of the line to continuous absorption, the value of s in the star depends first of all on the value of k. Further, the total number of active atoms is not given by s, but by the integral of s over the entire line profile and so is proportional to sb. As a consequence of this, if the atomic concentration in the star would be the same as in the sun, the parameter s would still differ and be proportional to $1/kb$.

Moreover we must take into account a possible difference in chemical composition between sun and star, a difference in degree of ionization and of excitation of the several atomic levels. If we take into account all these circumstances, we obtain :

$$(16)\qquad \Delta \log s = \Delta \log N - \Delta \log k - \Delta \log b + \Delta \log x - r\,\Delta \log \frac{x}{1-x} - E\,.\,\Delta\,\Theta$$

where N is the total number of atoms and ions, x is the degree of ionization, E the excitation potential, $\Theta = 5040/T$ and $r = 0$ for ions, $r = 1$ for neutral atoms. For all lines (atomic and ion lines) of one element the first four right hand terms have always the same value and so they may be combined into one constant, which we may denote by $\Delta_0 \log s$. Now we obtain the following formulae for the equivalent width B of the blend and its differential corrections :

$$B = \Sigma S \qquad \frac{\partial \log B}{\partial \log b} = \frac{1}{B}\sum \frac{\partial S}{\partial \ln b} \qquad \frac{\partial \log B}{\partial_0 \log s} = \frac{1}{B}\sum \frac{\partial S}{\partial \ln s}$$

$$(17)\qquad \frac{\partial \log B}{\partial \log a} = \frac{1}{B}\sum \frac{\partial S}{\partial \ln a} \qquad \frac{\partial \log B}{\partial \log \frac{x}{1-x}} = \frac{-1}{B}\sum r\,\frac{\partial S}{\partial \ln s}$$

$$\frac{\partial \log B}{\partial \Theta} = -\frac{1}{B}\sum E\,\frac{\partial S}{\partial \ln s}$$

Correction for continuous background.

The calculated blend intensities are not yet directly comparable to the measured equivalent widths. For the measurements in the spectrum are still influenced by possible errors in the continuous background adopted, which have not yet been taken into account.

If there was not such an error, the calculated equivalent width B would be comparable with the measured width A.

---

[1]) In fact, b depends a little on wave length and atomic weight But in a comparison between sun and star it enters only in the form $\Delta \log b$ and in this case this dependency is eliminated automatically.

We suppose, that the adopted continuous background is at a height h above the true background. (By "above" is meant : in the direction towards blank plate). If then c is the distance between the cutting points of the blend, we shall measure $B - ch$ instead of B as the surface of the line. This surface is to be compared with the measured surface $c - ch$ of a profile of width c with 100 % absorption. So for the equivalent width of the line we measure : $A = (B - ch)/(1 - h)$. Or reversely : $B = (1 - h)\, A + ch$.

For small values of h we may put :

$$\log B = \log A + 0.43 \frac{c - A}{A} h. \tag{18}$$

The background correction h will be a slowly varying function of the wave-length. We may introduce it as a new parameter in the representation of the spectrum, which has to be determined from the measured equivalent widths in just the same way as is the case with Doppler width, etc.

Differential correction of the curve of growth.

The parameters of the provisional curves of growth are given in Table 8. We now calculate, along the lines of the method which has been described in this chapter, theoretical values for the blend intensities and differential corrections to them. If then we compare these calculated values with the measured ones, to which a correction term for the background effect has been added, we obtain for each blend an equation, in which the parameters of the differential corrections and of background appear as unknowns. Combining a large number of these equations, we may calculate the differential corrections by the method of least squares.

The equation, which is obtained for one blend, has the form :

$$\log A = \log B + \frac{\partial \log B}{\partial \log b} \Delta \log b + \frac{\partial \log B}{\partial_0 \log s} \Delta_0 \log s + \frac{\partial \log B}{\partial \log a} \Delta \log a +$$

$$+ \frac{\partial \log B}{\partial \log \frac{x}{1-x}} \Delta \log \frac{x}{1-x} + \frac{\partial \log B}{\partial \Theta} \Delta \Theta - 0.43 \frac{c - A}{A} h + \varepsilon \tag{19}$$

Here ε is the accidental error in the measured equivalent width. Its average value will depend upon the intensity of the blend and its separation from its neighbours. Eventually, we ought to add still a term for the accidental error in log B, for this quantity has been derived from the measured equivalent widths in the sun. Originally we supposed, that the accidental error in log B would be negligible as compared with the errors in our own measures and we omitted this term in order to facilitate the calculations. Afterwards it appeared, that this supposition was not right. But it is not probable, that this circumstance will have a large influence upon the results, as the accidental errors in log B will depend on the intensity of the blend in somewhat the same way as the errors in log A. In this case, the results will not be changed.

We may write the equations (19) in a symbolic form :

$$a_{pi}\, x_p = t_i + \varepsilon_i. \tag{20}$$

Here the x_p are the 6 unknown parameters $\Delta \log b$ etc. and the a_{pi} are their coefficients. The index p may assume all values from 1 to 6 (more generally from 1 to m) and i varies from 1 to n, n indicating the total number of blends used in the investigation. The summation must be carried out over the index p, as is indicated by its double occurrence in one term. If we allow for different parts of the spectrum a somewhat different correction for background, the number of unknown

parameters (m) will be a little larger than 6. (In practice, we divided the spectrum into three regions, in each of which the background correction was determined independently, so m was equal to 8). The t_i represent the differences log A — log B.

We suppose that each equation has been multiplied by a weight factor, so that the probable squares of the accidental errors become equal. In this case, the x_p are to be determined in such a way, that $\Sigma\varepsilon_i^2$ becomes a minimum.

From this condition we find the normal equations :

(21) $b_{qp}\ x_p = u_q$, where $b_{qp} = a_{qi}\ a_{pi}$; $u_q = a_{qi}\ t_i$.

If the determinant of the b_{pq} is denoted by B and its minors by B_{pq}, the solution of eq. (21) is given by :

(22) $Bx_r = B_{rp}\ u_q$.

If the error in x_p is denoted by ξ_p, we have :

$$a_{pi}\ \xi_p = \varepsilon_i.$$

from which we derive :

$$B\,\xi_p = B_{pr}\ a_{ri}\ \varepsilon_i \text{ and } B^2\ \xi_p\ \xi_q = B_{pr}\ B_{qs}\ a_{ri}\ a_{sj}\ \varepsilon_i\ \varepsilon_j.$$

As the accidental errors in the different measures are independent, the probable value of $\varepsilon_i\ \varepsilon_j$ will be zero when $i \neq j$ and equal to $\overline{\varepsilon^2}$ when $i = j$. Inserting these values, we obtain :

(23) $B\ \overline{\xi_p\ \xi_q} = B_{pq}\ \overline{\varepsilon^2}$.

Here $\overline{\varepsilon^2}$ is found from :

(24) $(n—m)\ \overline{\varepsilon^2} = \Sigma\,(t_i - a_{pi}\ x_p)^2$

as may immediately be derived from $t_i - a_{pi}\ x_p = \varepsilon_i - a_{pi}\ \xi_p$.

So we may acquire the solutions of (20) with their probable errors. But the errors in the quantities x_p will not be independent of one another and it is necessary also to know their mutual relations. If then we impose to x_1 a variation y_1, we must change the other parameters x_p by an amount y_p. Between the y we have the relation $b_{pq}\ y_p = 0$ (where the summation over p has to be carried out for all values, from 1 to m and the index q is different from one), from which follows the solution :

(25) $$y_p = \frac{B_{1p}}{B_{11}}\ y_1.$$

With the help of this formula, we may also calculate the changes which will occur in the solution, if we adopt for one of the spectral parameters an (arbitrary) fixed value. It is not even necessary, that the changes in x_1 should be small, as (25) is immediately obtained from the linear equation (21).

III. THE INSTRUMENTAL CURVE.

Provisional determination of the instrumental profile.

In order to execute the calculations described in the preceeding chapter, we must know the form of the instrumental profile, i. e. we must know how the profile of an extremely narrow line is distorted by the instrument.

In part 1 of this investigation the problem of the determination of the instrumental profile has already been studied. There we started with an examination of the profiles of the emission lines from the comparison spectrum, the natural profiles of which are comparatively narrow. From the observed profiles of these lines, we deduced the shape of the instrumental curve.

In doing so, we met several difficulties, which have not been completely solved. One of these difficulties was, that lines of different intensity showed different profiles, the strong lines being somewhat narrower than the weak ones. This difference is the more surprising, since the true profile of the weak lines should be narrower than that of the heavy ones. So it seems, as if the shape of the instrumental profile depends on the line intensity.

In our preliminary investigations, the result of which is given in part I of this publication, we did not arrive at an explanation of this difference in shape. We only employed an empirical correction, by applying to the wave-length scale a multiplication factor dependent on line intensity, in order to reduce all profiles to the same width, corresponding to the profile of a line of moderate intensity. In this way the profile of lines of different intensities have been made comparable.

The second difficulty was, that accurate intensity measures can be obtained only from those parts of the profile, where the blackening of the photographic plate is neither too strong, nor too weak. So the central parts of the instrumental profile may be inferred only from lines of moderate intensity, whereas for the determination of the outer parts we are forced to use stronger lines. In connection with the systematic difference in width between strong and weak lines, this procedure, in which different parts of the instrumental profile have been determined from lines of different intensities, seems to be liable to very great uncertainties. But even when this use of the strong lines in the spectrum should be legitimate, the wings of the instrumental curve, which may extend far from the line centre in both directions, and may have a considerable surface notwithstanding their small intensity, cannot be determined by this method. For in any case the density of the silver deposit in the region of these wings will be much too low te be accurately measured.

A few figures will illustrate this difficulty more clearly. If we adopt as a unit the intensity of the radiation which reduces the transparency of the photographic plate to 50 %, then intensity 0.50 corresponds with a transparency of a little more than 90 %. Intensity 0.25 will reduce the transparency of the plate not further than to 98 %. So if the intensity falls to $\frac{1}{4}$ of the normal value or less, there will be no clearly distinguishable blackening of the plate. Wings of this intensity will be almost undetectable on the plate and nevertheless their total surface may be quite large.

Fortunately, in one of the comparison spectra which occur on the plates taken in 1929 at Victoria with the same instrument, a little drop of molten iron has caused a continuous background behind the emission profiles. On this plate the emission lines show clear wings, extending far from the line centre on both sides. The wings are clearly visible in this case, as in the region of moderate

photographic density an intensity change of 0.25 (from 1 to 0.75 or to 1.25) causes a difference in transparency of some 25 % (from 0.50 to 0.25 or to 0.75). So we were able to get some idea of shape, intensity and extension of the instrumental wings from the emission lines on this plate (cf. I Fig 4).

But is was not possible to use these 1929 profiles directly. Notwithstanding these plates having been taken with the same instrument as the 1924 plates, there appeared to be a great difference in the widths of the profiles, the 1929 profiles being much narrower. Their width is only about 60 % of that of the 1924 lines. So there seemed to be no other adequate use of the 1929 profiles than an indirect one. As a reasonable hypothesis, we assumed the outer part of the 1929 profile to differ from that of the 1924 plates only by a certain wave-length factor and so we made a combination of the 1929 instrumental wings and the central profile measured on the 1924 plates after applying a scale factor to the wings.

It is clear, that this method of determining the instrumental profile as a composition of different parts, derived from the profiles of lines of different intensities and even from plates taken in different years, is highly unsatisfactory. Indeed, it was shown by every measure, that the different profiles were not identical and we were forced to use a highly arbitrary method of reduction by wave-length scale factors, in order to enable the construction. So it is highly desirable, to have a method of control, to which the results obtained may be submitted.

This control yielded the third great difficulty. It was made by a comparison of the profiles determined in the stellar spectrum with those of the emission lines. As the crowding of lines in the stellar spectrum is very dense and the true profiles of the lines are unknown and possibly not very narrow, it is difficult or almost impossible to determine the shape of the instrumental curve from the profiles of the stellar lines. But if we assume the shape of these profiles to be similar to those of the comparison lines and allow only a difference in width, it becomes possible to determine also a scale of line widths for the stellar spectrum. This comparson was already made in the first part of this investigation and it appeared that, contrary to what had been expected, the profiles of the stellar lines were distinctly narrower than those determined in the comparison spectrum.

This result is the more surprising, as the true width of the stellar .lines is not negligible and their blending is serious. Both effects will increase the measured profile width. We might try to explain the difference in width from errors in the determination of the continuous background, which, if it is drawn too high, will hide the bases of the lines so that only their comparatively narrow tops remain visible. But it will be difficult to explain the very large difference in profile width from this effect alone.

The magnitude of the effect may be seen from Table 12. In this table we give the width of the line profile (expressed in μ on the plate) at a point where the intensity is 75 % of the central intensity. This figure was chosen in order to eliminate, as far as possible for lines in the stellar spectrum, the effect of blending, which would have been of much greater influence at a point with 0.50 of the central intensity.

The figures for the spectrum of π Cephei are omitted, because the lines in this spectrum are distinctly broader than in those of δ Cephei and ϑ Cygni. So it is possible, that a slight rotational broadening exists. The numbers given in Table 12 are all averages for a number of 6 to 23 lines. As a total, we used some 400 lines.

In our preliminary determination of equivalent widths, we made use of the knowledge of the instrumental profile only in order to obtain a partial separation between the different components of the blend. To this end we used the so called "contraction method".[1]) If $R(x)$ was the measured line

[1]) B.A.N. **301** (1937).

Table 12. Profile widths for lines in the stellar and comparison spectra.

δ Cephei 10607				ϑ Cygni 10616				δ Cephei 10617				ϑ Cygni 10619			
λ	Star	Comp.	Ratio	λ	Star	Comp.	Ratio	λ	Star	Comp.	Ratio	λ	Star	Comp.	Ratio
—	—	—	—	4056	20.4	28.0	0.73	—	—	—	—	—	—	—	—
4189	21.2	23.9	0.89	4170	22.3	29.4	0.76	4175	23.7	29.4	0.81	4174	23.1	27.7	0.83
—	—	—	—	4216	21.5	29.9	0.72	—	—	—	—	4228	20.9	28.6	0.73
4252	21.8	24.5	0.89	4264	20.7	30.7	0.67	4270	20.7	30.7	0.67	4278	21.5	29.6	0.72
4370	23.9	25.8	0.93	4347	18.8	32.1	0.58	4385	22.6	32.9	0.69	4372	22.0	31.8	0.69
4478	22.8	27.5	0.83	4444	21.5	34.3	0.63	—	—	—	—	4445	23.9	33.7	0.71
—	—	—	—	4518	21.2	36.2	0.59	4521	22.6	36.2	0.62	4520	25.3	36.2	0.70
4662	22.3	30.5	0.73	4625	22.6	38.6	0.58	4647	21.2	38.9	0.55	4604	25.8	38.6	0.67
—	—	—	—	—	—	—	—	—	—	—	—	4692	32.1	41.1	0.78
4880	29.9	34.5	0.87	4805	25.0	41.1	0.61	4809	29.4	41.1	0.72	4803	34.0	43.8	0.78

depth at the point x of the profile, we determined a reduced depth by the equation :

26) $R'(x) = 3\,R(x) - R(x-c) - R(x+c)$.

The effect of this reduction is, that the profiles are lowered at the points where they turn their hollow parts upward and raised in the other parts. So the profiles become narrower and steeper and the parts of a blend are more clearly separated. It is just the same effect, as if the true profile had been broadened not by the normal instrumental curve, but by a more narrow curve, as would be derived from the normal one by applying (26) to the instrumental curve itself.

If in (26) the distance c is chosen too large, the curve will be overcorrected and the contracted instrumental curve gets negative wings. If, on the other hand, c is chosen too small, the curve is undercorrected and the different lines will not be separated as clearly as would be possible. So it is necessary to choose an appropriate value for the contraction distance c, in accordance with the width and shape of the instrumental curve.

Whereas in the preliminary investigation we were fully aware of the difficulties which we encountered in the determination of the instrumental curve, we supposed, that it would be sufficient to know the true shape only approximately if we had no further aim than the determination of an appropriate value of c. So we adopted for the shape of the instrumental curve the results derived from the study of the iron emission lines and only reduced the wave-length scale of the curve in accordance with the figures of Table 12. In fact, as the best value of c we adopted 1.10 times the profile width as given in Table 12.

But in our present investigation a more accurate knowledge of the instrumental profile is necessary. So now we must study the problem of the determination of the instrumental curve in more detail than has been done in part I of this publication.

Possible causes of the discrepancies.

Theoretically, the instrumental curves for lines of different intensities and for emission and absorption lines ought to be identical. Differences can come into existence only, if the intensities registered in our diagram are not true intensities, *i.e.* if the intensity scale is distorted in some way.

This may occur in many ways. First of all the transmission of the photographic plate is not a linear function of the illumination of the plate, but this last quantity must be derived from the transmission by the aid of the so called transmission curve. Any error in the adopted transmission curve will change not only the intensity, but also the profile of the line.

Besides this general influence of an erroneous transmission curve, there may be local photographic effects resulting from the diffusion of light or developer in the photographic emulsion. If there was no such diffusion, the local transmission of the plate would depend only on the local illumination, but on account of the diffusion mentioned this will no longer be true. The diffusion of the developer causes the so called Eberhard effect. In the immediate neighbourhood of strongly exposed parts the developer will be exhausted sooner than in the neighbourhood of regions of less intense exposure. As a consequence of this, in the neighbourhood of strong emission lines the plate will be underdeveloped, while near blank spaces the reverse is true. In this way the Eberhard effect augments the photographic contrasts.

A third group of effects may occur at the registration of the plate with the Moll microphotometer. The slit of the thermocouple is not infinitely narrow and so we measure not the local transmission of the plate, but the average transmission over a certain region. As this transmission is not a linear function of the illumination, this effect also results into a distortion of the line profile. An effect of the same kind will be caused by the inertia of the instrument.

Finally it is possible, that all intensities are registered and measured without any appreciable error, but that they are not interpreted in the right way. This will be the case, if *e.g.* there is an undetected fog over the spectrum, or if we have made a wrong determination of the continuous background. We now will discuss these four types of effects separately.

Registration effects.

We will begin our discussion with the effects of registration, for which we can show easily that they did not contribute to the observed discrepancies.

First of all, the precautions taken when the registration was carried out, were sufficient to remove all doubt in this question. But even if there would have been no such precautions, it is easy to show, that these effects would influence the line profiles in just the reverse direction as was actually the case.

Over a considerable range in intensity, the transmission curve (which represents the connection between the transmission of the plate and the logarithm of the illumination), may be considered as a straight line. If in regions of moderate blackness we measure the average transmission of an entire region, this average transmission is related directly to the geometrical average of the intensities over the entire region.

If the illumination over the region is not constant, the (geometrical) average intensity measured will be smaller than the arithmetical average. If the latter had been measured, the profiles of emission and absorption lines would still have been similar. But as the geometrical average has now replaced the arithmetical, the intensities in the slopes of an emission profile will be measured too small, whereas in the horizontal parts of the profile there will be no perceptible error. As a consequence of this, the emission profile will be found too narrow. In an absorption line, the intensities at the slopes will be lowered too, which means an apparent increase of the absorption and a broadening of the profile. So as a consequence of this effect, the emission lines would appear narrower than the absorption lines. The reverse is true.

In a similar way, we may show that also the inertia of the instrument, if appreciable, would cause a relative broadening of the stellar lines. But as in the profiles of the emission lines of the comparison spectrum there is no trace of asymmetry, there is no necessity of discussing this possibility any further.

Local photographic effects.

The second group of effects which may be eliminated from our discussion are the local photographic effects. For the Eberhard effect this is immediately clear. As it results in a sharpening of the profiles in regions of great contrast, we would expect narrower profiles for the lines in the emission spectrum, where the photographic contrasts are great, than in the stellar spectrum, just contrary to what is actually observed. It seems, as if the precautions taken with the development of the plate have been sufficient to eliminate this effect to a large extent. [1])

More difficult is the consideration of the effect of light diffusion. Of course, its first result is a broadening of all lines, emission- as well as absorption lines and both in the same way. We must take into account the second order effects if the difference in behaviour between absorption and emission lines is to be studied.

As we are interested only in the distribution of light in the direction of the spectrum and in depth in the emulsion, the problem of diffusion and absorption of light in the photographic emulsion is essentially a two-dimensional problem. The co-ordinate in the direction of the spectrum will be denoted by x, the co-ordinate indicating the depth in the emulsion by z. We assume an infinite narrow pencil of incident light at the point (0,0) ; the fraction arriving at the point (x, z) is denoted by $p(x, z)$. It is clear, that the form of this function will depend also on the angle of incidence of the light on the plate, but since the same optics has been used when the emission spectrum was obtained as in the case of the illumination of the plate by starlight, we may suppose, that the function p will be the same in all cases under consideration. Clearly, the use of identical optical systems is a necessary condition to be fulfilled, if the profiles derived from the emission lines shall be of any value for a use in the reduction of the stellar spectrum.

If now we assume a constant illumination of the entire surface of the plate, the quantity of light getting at depth z in the emulsion will equal $\int p(x, z)\, dx = p(z)$. If on a continuous background C (which may be zero in the case of an emission line) stands an emission- or absorption line $\pm\, a\, Q(x)$, the intensity at the point (x, z) will be equal to :

$$(27) \qquad u(x, z) = C\, p(z) \pm a \int Q\,(x - y)\, p(y, z)\, dy.$$

If the photographic blackness at each point of the plate would be a linear function of the intensity, the registration of the plate would yield the integrated value of (27) over the entire depth of the emulsion, which we may write as :

$$(28) \qquad u(x) = Cp \pm a \int Q\,(x - y)\, p\,(y)\, dy$$

where $u(x) = \int u\,(x, z)\, dz$, etc.

In this case the measured profiles of all kinds of lines would still be identical.

But in fact the blackness of the plate is not a linear function of the intensity. This again, would do no wrong if the distribution of $u(x, z)$ with depth was equal to $u(x)\, p(z) / p$, for in this case it would be exactly the same as for an evenly illuminated plate. As the blackening marks from which the transmission curve has been deduced are ordinary continuous spectra, we would find precisely the right value for the illumination of the plate. So we must consider only the difference $u(x, z) - u(x)\, p(z) / p = v(x, z)$ and its influence on the integrated blackness of the plate.

The extra illumination $v(x, z)$ causes an extra blackening ∂s, where

$$(29) \qquad v\,(x, z) = \pm\, a \int Q\,(x - y) \left\{ p(y, z) - \frac{p(y)\, p(z)}{p} \right\} dy = \pm\, a \int Q\,(x - y)\, q\,(y, z)\, dy$$

[1]) The occurrence of negative wings near the strong absorption lines in the stellar spectrum at first seemed an indication of Eberhard effect. But it will be seen, that they find their explanation in a totally different way.

(30) $\delta s = s'\, v(x, z) + \frac{1}{2}\, s''\, v^2(x, z),$

which must be integrated over the entire depth of the photographic emulsion. The first and second derivatives of s are functions of the ,,normal'' illumination $u(x)\, p(z)/p$.

If we integrate (29) over all z, we obtain the extra blackening of the plate at x. This is to be compared with the extra blackening which would result from a change in the value of the integrated intensity $u(x)$, with an amount $w(x)$, when its distribution with depth still corresponds with the normal distribution for a continuous spectrum. In this case the extra illumination at the point (x, z) would be equal to $w(x)\, p(z)/p$ and instead of $v(x, z)$ we must insert this quantity in eq. (30).

If we choose $w(x)$ in the way, that both calculated values of s become equal, $w(x)$ will be the apparent extra intensity at x.

So $w(x)$ is determined by the relation :

$$(31)\quad \frac{w(x)}{p}\int s'\, p(z)\, dz + \tfrac{1}{2}\frac{w^2(x)}{p^2}\int s''\, p^2(z)\, dz = \int s'\, v(x, z)\, dz + \tfrac{1}{2}\int s''\, v^2\,(x,z)\, dz,$$

or to the same order of approximation :

$$(32)\quad w(x) = \frac{p\int s'\, v(x, z)\, dz}{\int s'\, p(z)\, dz} + \tfrac{1}{2}\frac{p\int s''\, v^2(x, z)\, dz}{\int s'\, p(z)\, dz} - \tfrac{1}{2}\frac{p^2\left\{\int s'\, v(x, z)\, dz\right\}}{\left\{\int s' p(z)\, dz\right\}^2}\quad \frac{\int s''\, p^2(z)\, dz}{p\int s'\, p(z)\, dz}$$

Here s' and s'' are determined by the "normal distribution of light" $u\,(x)\, p(z)/p$ and so may be considered as functions of x and z.

From (29) we see, that the first term in (32) is linear in λ and so it gives the same changes in shape for profiles of emission or absorption lines of every intensity. Differences in profile result from the quadratic terms. In order to make an easy calculation possible, we assume s to be proportional to the n^{th} power of the intensity. In this case we have between s'' and s' the relation :

$$(33)\quad s' = s''\, u(x)\, p(z)\, /\, (n - 1)\, p.$$

Inserting this in (32), the quadratic terms become :

$$\frac{(n - 1)\, p^2}{2\, u(x)}\left[\frac{\int s''\, v^2(x, z)\, dz}{\int s''\, p^2(z)\, dz} - \left\{\frac{\int s''\, v(x, z)\, p(z)\, dz}{\int s''\, p^2(z)\, dz}\right\}^2\right]$$

which may be written :

$$\frac{(n - 1)\, p^2}{2\, u(x)}\,\frac{\frac{1}{2}\iint s''\,(x, z)\, s''\,(x, t)\left(v(x, z)\, p(t) - v(x, t)\, p(z)\right)^2 dz\, dt}{\left\{\int s''\, p^2(z)\, dz\right\}^2}$$

The sign of this form depends on n. We have :

$$(34)\quad n - 1 = s''\, I/s'$$

if I is the intensity resulting in the blackness s. Our transmission curves [1]) do not give s directly; for the transmission of the plate is equal to e^{-s}. This function in the most important part of the transmission curve is a linear function of $\log I$. If we put :

$$(35)\quad e^{-s} = A - B \log I \qquad \text{we get:}$$

$$(36)\quad n - 1 = 0.43\; B\, e^s - I.$$

Now in the middle part of the transmission curve its slope B is about equal to 2. As in this case $e^{-s} = \frac{1}{2}$ we find $n - 1 = 0.72$ so that the second order term is positive.

[1]) We use the expression "transmission curve" instead of the customary "characteristic curve", in order to accentuate the difference between transmission and blackness.

The function $v(x, z)$ which occurs in the quadratic terms of (32) depends on the curvature of the line profile. This follows immediately from the definition of $v(x, z)$ and the symmetry of the diffusion function. So the quadratic terms will assume their largest values at the top of the line profile and become zero near the point of flexion. But since these quadratic terms are positive, it is clear, that their influence makes the line profile narrower.

In this way we should be able to explain, that the profiles of the strong emission lines are narrower than those of the weaker ones. But for absorption lines, the effect would be the reverse. Indeed, diffusion of light would in its second order effect make the profiles of absorption lines broader than those of emission lines. For the positive extra intensity at the centre of the line would now have the effect of filling up the depression so that the profile gets broader.

For this reason the effect of light diffusion fails equally well with respect to the explanation of the differences in profile as the effect of diffusion of developer. So now we will turn our attention from the local photographic effects to the other possibilities.

The determination of the transmission curve.

It is clear that, if the adopted transmission curve by which the measured transmission of the plate is transformed into light intensity would be wrong, this would have serious consequences for the shapes of the profiles.

Our transmission curves show the usual S-shaped form. Generally, we use only the central part of the curve, which may be considered approximatively as a straight line. The only serious error which may be expected is an error in the inclination of this line.

If the adopted inclination should be wrong, this would mean a change in the scale of $\log I$, *i.e.* the true values of I should be obtained from the measured values by applying a formula of the form $I_t = I_m^p$.

We will suppose, that the exponent p is larger than one. If it should be smaller, the effect would be just the reverse.

We suppose the true profile of the line is given by $C \pm a\,Q$ where C is the intensity of the continuous background, which in the case of emission lines may be equal to zero. The measured profile is then given by $(C \pm a\,Q)^{1/p}$. In the case of emission lines without a continuous background, this would mean that all profiles have the same form, i.e. $Q^{1/p}$ and differ only by an intensity factor, which now becomes $a^{1/p}$ instead of a. In the case of emission or absorption lines situated on a continuous background, the profiles of weak lines would be given by $\pm a\,Q/Cp$, and so these profiles would be similar to the true profile and show even the right intensity proportions. The only difference is, that all of them are weakened in the ratio $1/p$. But the measured profiles of strong emission lines would be broader, approximating the form $Q^{1/p}$, whereas absorption lines would become narrower. This is precisely what has been observed.

There seems to be no obvious reason, why the transmission curve as derived from the intensity marks on the plate shoold be incorrect. But there may be some doubt, whether this transmission curve may be applied directly to the comparison- or stellar spectra, which have been obtained in a somewhat different way. Even if the same optics have been used — as is probably the case — there remain the differences, that the time of exposure was much shorter for the lines in the emissionspectrum than for the comparison spectra from which the transmission curve has been obtained, whereas the time of exposure for the stellar spectrum is much longer. Moreover, as a consequence of the movement of the stellar image along the slit of the spectrograph, the latter has been obtained by intermittent illumination.

From the researches of KRON[1]) and others, it is known that the blackness of a photographic image is not a simple function of the total illumination $I\tau$, obtained from a light source I during a time τ, but that it depends also on the intensity of light itself. KRON has illuminated a photographic plate with light sources of different intensity, working during time intervals of different lengths and he determined for each degree of blackness the amount of illumination $I\tau$ which was necessary to produce it at different given values of the intensity I. So he obtained a set of "curves of constant blackness" (often indicated as "reciprocity curves"), each of them giving log $I\tau$ as a function of log I.

It appeared that these curves had the approximate form of hyperbolas, turning their branches upwards. This means that there is a certain value of I for which the illumination $I\tau$ which is necessary to produce the given degree of blackness attains a minimum. If then we illuminate with this intensity, the blackness produced is greater than with any other exposure, for which the product $I\tau$ remains constant.

This "optimum intensity" appeared to be independent of the time of illumination. It has a fixed value for each plate.

Further, if we plot the "curves of constant blackness" in the diagram (log I, log $I\tau$), it is seen, that all curves are parallel and shifted only in the direction of the log $I\tau$-axis. This means, that we must always travel along the same distance parallel to the $I\tau$-axis if we want to pass from one curve to another, independent of the value of I at which this is done. So starting from a given blackness, the multiplication of the time of exposure with a given factor always yields equal blacknesses again, independent of the intensity of the illumination.

We may put this result in an analytical form, writing :

$$\log I\tau = f(\log I) + g(t) \tag{37}$$

where t is the transmission of the plate.

We are interested in the shape of the transmission curve which gives t as a function of log I and constant τ. And we are especially interested in the relative slopes of the curves obtained for different values of τ, So we differentiate (37) with respect to log I, treating τ as a constant. We find :

$$1 = f'(\log I) + g'(t)\left(\frac{\partial t}{\partial \log I}\right)_\tau \quad \text{or,} \tag{38}$$

$$\left(\frac{\partial t}{\partial \log I}\right)_\tau = \frac{1 - f'(\log I)}{g'(t)}. \tag{39}$$

We may compare this expression with the slope of the "curve of constant blackness" given by (37). If we differentiate (37) with respect to log I, treating t as a constant, we obtain :

$$\left(\frac{\partial \log I\tau}{\partial \log I}\right)_t = f'(\log I). \tag{40}$$

So the slope of the curve of constant blackness is given by f' and the slope of the transmission curve by $(1 - f')/g'$.

If we compare different transmission curves, obtained for different values of τ, at equal values of t, the slopes of the curves are proportional to $1 - f'$, since g' in all cases has the same value.

Now for the comparison spectrum, which has been taken with a very intense light source, we are above the optimal intensity and f' is positive. This means, that the slope of the transmission

[1]) E. KRON, Publikationen des Astrophysikalischen Observatoriums zu Potsdam Nr. 67, Bd. **22**, 5. St. (1913).

curve must be slight. On the other hand, for a light source of little intensity, as is the case with the stellar spectrum, we are below the optimal intensity. f' is now negative and the transmission curve becomes steeper.

It is clear, to what kind of consequences this must lead. The slight slope of the transmission curve for the emission spectrum has the tendency to diminish the contrasts, *i.e.*, to broaden the lines. In the stellar spectrum the contrasts become sharper, but this does not influence the shape of the line profile except for the strongest lines ; in the weak lines the apparent depression only becomes somewhat greater but remains proportional to its true value.

Unfortunately, we have no accurate data about the magnitude of the effect. From the measures of KRON it seems probable, that $1 - f'$ should be about 1.17 for the stellar spectrum and 0.885 for the emission spectrum. The ratio of both values is equal to $1.17/0.885 = 1.32$. On the other hand, from measures on the 1929 plates it was found, that the transmission curve for the stellar spectrum would be steeper than that for the continuous spectra from which the transmission curve has been derived in the ratio 1/0.94. So we may suppose, that if the slope of the adopted transmission curve is equal to a, the slope of the true transmission curve of the stellar spectrum will be $1.06\ a$ and that for the comparison spectrum $0.806\ a$. From the measured intensities in the comparison spectrum, true intensities must be found by taking $I_t = I_m^{1.24}$, whereas for the stellar spectrum $I_t = Im^{0.94}$.

As we have seen, this transformation does not influence the shapes of the profiles for the stellar lines, but the true depth of the lines is only 0.94 times its measured value. This means, that all measured intensities and equivalent widths have to be reduced by a factor 0.94. For the strong stellar lines, with very deep depressions, this is no longer true, but the difference is not serious. The factor 0.94 corresponds with a correction 0.027 in log A and is of very little importance.

But the effect is of very great importance if we consider the shapes of the profiles of the comparison lines. The measured instrumental profile has been given at the top of p. 11 of the first part of this publication. If we apply an exponent 1.24 to all intensities given there, the profile becomes much narrower as is indicated in Table 13 :

Table 13. Measured and true instrumental curve. $I_t = I_m^{1.24}$.

Distance from centre	I_m	I_t	Distance from centre	I_m	I_t
0	1.000	1.000	20	0.578	0.507
4 μ	0.966	0.957	24	.489	.411
8	.889	.863	32	.350	.272
12	.791	.748	40	.271	.198
16	.688	.630			

If we measure the width of the "true" profile at the point where $I = 0.75$, we see, that it is 23.9 μ instead of 27.2 for the apparent profile. So the profile width has been reduced in the ratio 0.88. If we compare this value with the figures of Table 12, we see, that the profile widths of the stellar lines still differ from that of the true instrumental profile by a factor between 0.62 and 1.06. So there still remains a large unexplained difference.

Dependence of profile width on wave-length.

The figures of Table 12 show a strong dependence of the width ratio on wave length. It is tempting to explain this dependence as a result of the effect described above. The measures of KRON

are made with integrated light, so it is not possible to draw any inference from his results. But at the Kodak laboratory, J. H. WEBB [1]) has performed a similar research using monochromatic light of different wave lengths. According to his measures, the slope f' of the curve of constant blackness is independent of the wave length if the time of exposure remains unchanged. We may put this result in an analytical form, writing :

(41) $\log I\tau w = f(\log Iw) + g(s)$

where w is some function of the wave length. It is clear, that for a given wave length the slope of the curve of constant blackness will now as before be given by f', whereas the slope of the transmission curve also assumes the old value $(1-f')/g'$. So the wave length is of no influence on the slope of the transmission curve.

These results of WEBB, however, conflict with our own measures. In the first part of our investigation, we found a strong dependence of the slope of the transmission curve on wave length, as is shown in Table 14, which gives the slopes of the curves at the point of 50 % transmission.

Table 14. Slopes of transmission curves.

λ	10607	10608	10610	10616	10617	10618	10619	mean
4100	1.7	1.8	1.8	1.9	1.8	—	1.9	1.82
4200	1.9	1.9	1.9	2.1	2.0	2.0	2.0	1.97
4300	2.1	2.2	2.1	2.4	2.2	2.4	2.2	2.23
4400	2.3	2.4	2.4	2.6	2.3	2.5	2.4	2.41
4500	2.4	2.5	2.5	2.7	2.5	2.7	2.5	2.54
4600	2.3	2.5	2.5	2.6	2.5	2.6	2.4	2.49
4700	2.2	2.5	2.5	2.5	2.5	2.5	2.3	2.43
4800	2.2	2.4	2.4	2.3	2.4	2.5	2.1	2.33
4900	2.1	2.2	2.2	2.2	2.3	2.4	2.0	2.20

In his thesis on the "photographic sum-rule" A. VAN KREVELD [2]) mentioned the same fact that, in some cases, the transmission curves for different wave lengths were not parallel. He confirmed the rule found by WEBB, that for equal time of exposure and equal blackness the slope of the curve of constant blackness was independent of wave length. In Chapter VIII of his thesis, he determined the Schwarzschild exponent p, which in our notation would be denoted by $-\left(\frac{\partial \log I}{\partial \log \tau}\right)_t$ or $1/(1-f')$ as follows from eq. (37). This ratio was found to be independent of wave length. But it is precisely this quantity, which determines the slope of the curve of constant blackness (40) and stands in a narrow relation to the slope of the transmission curve (39).

VAN KREVELD, however, mentions two circumstances, which may disturb the parallelism of the transmission curves. One of them is a sensibilization of the plate, which has not occurred in our case. The other is a consequence of the unequal absorption of light of different wave lenght in the photographic emulsion.

In general, we may expect that the absorption of light in the emulsion diminishes with increasing wave lenght. Violet light will work chiefly on the upper layers of the emulsion, whereas the green rays penetrate much deeper. So violet light will cause a heavy blackening near the surface

[1]) J. H. WEBB, Journal of the Optical Society **23**, 316 (1933).

[2]) A. VAN KREVELD, De fotografische somwet en haar geldigheidsgebied, Thesis, Utrecht (1932).

of the emulsion, whereas green light causes a smaller blackening, extending over a much deeper layer. It is clear, that if the intensity of light is increased, the plate will soon become saturated in the case of violet light, wich does not work on the deeper layers of the emulsion. For green light, this saturation will occur only at much greater blackness. As a consequence, the transmission curve for light of long wave-length will be steeper than for violet light. From table 14 it is seen, that this effect may afford a partial explanation for the differences in slope between the transmission curves.

We will try to discuss this effect quantitatively. We suppose, that the beam of intensity I_0, which strikes the surface of the photographic emulsion, is reduced to I_z at depth z, so that

$$\log I_z = \log I_0 - kz, \tag{42}$$

where k is supposed to be a function of the wave length decreasing with increasing wave length. The calculations given below would undergo no change if kz was replaced by an arbitrary function of kz.

We suppose further, that the elementary blackening curves for all wave-lengths are parallel, so that if in an elementary layer of the plate the intensities I_v and I_g of violet and green light cause equal blackness, the intensities $c.\ I_v$ and $c.\ I_g$ will cause equal blackness too. In this case it is possible to define intensities of light of different wave length which cause equal blackness simply as equal intensities. The supposition made here, corresponds with the results obtained by VAN KREVELD, for plates where only the uppermost layer of the emulsion has been developed.

The blackness s at each particular depth in the emulsion will be a function of the local intensity I_z. The total blackness S of the plate is found by integrating s over the whole depth of the emulsion. The transmission t is equal to ϵ^{-S}.

We now take into account the different absorption of the several wave lengths. We ask, how the slope of the transmission curve depends on the value of k. It will be seen, that it is somewhat easier, not to discuss the slope of this curve directly, but to use the slope of the curve which defines the integrated blackness S as a function of $\log I_0$. This slope is given by

$$\frac{\partial S}{\partial \log I_0} = \int \frac{\partial s}{\partial x}\, dz,$$

where $\log I_z$, the argument of the local blackness s, has been denoted by the letter x.

If we change the wave-length of the incident beam of light, we must change its intensity too (on the scale adopted above) in order to retain the same value of the *integrated* blackness. The necessary change in $\log I_0$ is obtained from :

$$\delta S = \int s'dz.\ \delta \log I_0 - \int zs'dz.\ \delta k = 0. \tag{43}$$

where the derivative of s with respect to x has been denoted by s'.

In the same way, we obtain for the change in the slope of the S-curve :

$$\delta S' = \int s''dz.\ \delta \log I_0 - \int zs''dz.\ \delta k. \tag{44}$$

Combining (43) and (44) we find :

$$\left(\frac{\partial S'}{\partial k}\right)_{S = cons.} = \frac{\int s''dz}{\int s'dz}.\ \int zs'dz - \int zs''dz. \tag{45}$$

We divide this equation by $S' = \int s'\, dz$. Then it may be written as :

$$\left(\frac{\partial \ln S'}{\partial k}\right)_{S = cons.} = -\frac{\partial}{\partial \log I_0}\frac{\int zs'\, dz}{\int s'\, dz}. \tag{46}$$

Till so far, the calculation could be made in just the same way, if in (42) instead of kz there

would have been an arbitrary function of z and λ. But now we assume the specialized form of (42). In order to calculate $\int zs'\,dz$ we integrate $\int s\,dz$ by parts. Then we find:

$$S = \int s\,dz = s_1 + k\int zs'\,dz.$$

if the depth of the emulsion is put equal to one. Inserting this in (46), we find:

$$(47)\qquad \left(\frac{\partial \ln S'}{\partial k}\right)_{S=\,cons.} = -\frac{1}{k}\frac{\partial}{\partial \log I_0}\frac{S-s_1}{S'}.$$

It is easily seen, that there is one special case in which the right hand side of this equation is equal to zero, *i.e.*, when the relation between s and I assumes the form $s = c\,I^n$. In this case we have:

$$s = c\,I^n = c\,I_0{}^n\,10^{-nkz} \qquad s_1 = c\,I_0{}^n\,10^{-nk}$$

$$S = \int s\,dz = \frac{c\,I_0{}^n}{2.30\,nk}\,(1 - 10^{-nk})$$

$$S' = \frac{\partial S}{\partial \log I_0} = \frac{c\,I_0{}^n}{k}\quad (1 - 10^{-nk})$$

In this case $(S - s_1)/S'$ is independent of I_0 and then it follows from (47), that there can be no dependence of the inclination of the transmission curve on wave-length. But the inspection of the form of the transmission curve measured shows, that this conditon is not fulfilled in our case. So it is to be asked, what will be the consequences of a deviation from this ideal form.

There are two cases, in which this problem is very easy to solve. The first case occurs, when the absorption in the plate is so strong, that the blackness at the deapest level of the emulsion can be neglected. Then in our formula we have to take into account the integrated blackness only, which is directly connected with the measured transmission. Putting $t = e^{-S}$ and neglecting s_1, (47) assumes the form:

$$(48)\qquad \left(\frac{\partial \log t'}{\partial \log k}\right)_{t=\,cons.} = -\frac{\partial}{\partial \log I_0}\quad \frac{0.434^2}{\dfrac{\partial}{\partial \log I_0}\log(-\log t)}$$

We will apply this formula to a numerical example. To this end we use the transmission curve as measured for the spectrum δ Cephei 10617. As is seen from eq. (48) it is of no importance whether we use the curve valid either for the violet or for the green end of the spectrum, since the differentiation with respect to log I_0 occurs once in the denominator and once in the numerator, so that a change of scale in log I_0 has no influence on the result.

In the table below, we give t, $-\log t$ and $\log(-\log t)$ as a function of log I_0. The following columns give the first derivative of this quantity, its reciprocal, and finally the derivative of this last quantity. So the last column gives $-5.30\,\dfrac{\partial \log t'}{\partial \log k}$.

Notwithstanding the great inaccuracy of the final results, they are distinctly positive for the most important part of the transmission curve. In the region log $I_0 = -0.20$ to $+0.20$, corresponding to a transmission between 0.84 and 0.20, we find an average value of 1.24. This corresponds to a value of -0.23 for $\partial \log t'/\partial \log k$. As this value is negative, the slope of the transmission curve will increase with decreasing k or increasing wave length, as is actually observed, at least for wave-lengths below $\lambda = 4500$.

In order to get the observed change in the slope of the transmission curve from 1.82 to 2.54

log I_0	t	$-\log t$	$\log(-\log t)$	1st deriv.	recipr.	derivative	smoothed
— 0.60	0.987	0.0057	0.76 — 3				
— 0.50	0.982	0.0079	0.90 — 3	1.4	0.71		
— 0.40	0.968	0.0141	0.149 — 2	2.5	0.40	— 3.1	
— 0.30	0.933	0.0301	0.479 — 2	3.30	0.303	— 1.0	
— 0.20	0.843	0.0742	0.870 — 2	3.91	0.256	— 0.47	— 0.64
— 0.10	0.679	0.1681	0.226 — 1	3.56	0.281	+ 0.25	+ 0.14
0.00	0.500	0.3010	0.479 — 1	2.53	0.395	+ 1.14	+ 0.70
+ 0.10	0.323	0.491	0.691 — 1	2.12	0.472	+ 0.77	+ 1.24
+ 0.20	0.200	0.699	0.844 — 1	1.53	0.654	+ 1.82	+ 1.40
+ 0.30	0.124	0.907	0.958 — 1	1.14	0.877	+ 2.23	+ 1.65
+ 0.40	0.071	1.149	0.060	1.02	0.980	+ 1.03	+ 2.50
+ 0.50	0.041	1.387	0.142	0.82	1.22	+ 2.4	
+ 0.60	0.026	1.585	0.200	0.58	1.72	+ 5.0	

or in a ratio 1.40, k must change in a ratio 4.3 : 1. This indeed, is a very large variation. If, *e.g.* we suppose, that the smallest value of k corresponds to 50 % absorption (if k is smaller, it will not be possible to neglect s_1), the smallest value of k will be 0.30 and the largest 1.29, corresponding to an absorption of 95 %.

We now consider the other limiting case, when k is very small. In this case, we may use a series development for s. As $\log I_z = \log I_0 - kz$ we may write :

$$(49) \qquad s = s_0 - s'_0\, ks + \tfrac{1}{2}\, s''_0\, k^2 z^2 - \ldots\ldots$$

From this formula we may integrate S and after some calculations we obtain :

$$S - s_1 = \tfrac{1}{2}\, S'k - {}^1/_{12}\, S''k^2 + {}^1/_{720}\, S^{IV} k^4 - \ldots\ldots \text{ and}$$

$$(50) \qquad \frac{\partial \log S'}{\partial k^2} = +{}^1/_{24} \frac{\partial^2}{(\partial \log I_0)^2} \log S' - \ldots\ldots$$

It now follows, that the change in the slope will be proportional to the square of the inclination of the transmission curve.

We again make a numerical calculation. This is given in the table below. In order to calculate S', we start from $-\log t$, which is equal to 0.434 S; the constant difference which will occur in $\log S'$, if we proceed in this way, will be of no influence on the result.

log I_0	$-\log t$	0.434 S'	$\log S' - 0.36$	1st deriv.	2nd deriv.	smoothed
— 0.60	0.0057					
— 0.50	0.0079	0.022	0.34 — 2			
— 0.40	0.0141	0.062	0.79 — 2	4.5		
— 0.30	0.0301	0.160	0.204 — 1	4.1	— 4	
— 0.20	0.0742	0.441	0.644 — 1	4.40	+ 3	
— 0.10	0.1681	0.939	0.973 — 1	3.29	— 11.1	— 5.2
0.00	0.3010	1.329	0.124	1.51	— 17.8	— 6.7
+ 0.10	0.491	1.90	0.279	1.55	+ 4.0	— 8.1
+ 0.20	0.699	2.08	0.318	0.39	— 11.6	— 5.5
+ 0.30	0.907	2.08	0.318	0.00	— 3.9	— 2.4
+ 0.40	1.149	2.42	0.384	0.68	+ 6.8	— 4.7
+ 0.50	1.387	2.38	0.377	— 0.07	— 7.5	
+ 0.60	1.585	1.98	0.297	— 0.80	— 7.3	

Here the results obtained in the last column are even more irregular than in the first calculation, which is easy to understand, as now we have differentiated three times. But there is no doubt, that the figure in the last column is negative and we may estimate its average value as about — 6. So now we have $\partial \log t'/\partial k^2 = -\frac{1}{4}$. A change in log t' of 0.14 now would correspond to a change of 0.56 in k^2. If, again, the smallest value of k would be 0.30, the largest value would be 0.80. So we see, that this calculation yields a smaller necessary variation in k than the first. Indeed, this necessary variation will be even smaller than is calculated here, as we started from the transmission curve valid for the violet, which has the smallest inclination.

Of course, none of the above calculations is accurate. But they put limits to the necessary variation of k. A more accurate calculation would be possible in principle, but it will not be of much use if no very accurate data are at our disposal.

Till so far, we partly succeeded in explaining the increase of the inclination of the transmission curve between the violet end of the spectrum and $\lambda = 4500$. But for still larger wave lengths, the slope of the curve again diminishes. Perhaps this decrease is related to the nearness of the limit of sensitivity of the plate as we approach the long wave length limit. For VAN KREVELD has shown, that the slope of the transmission curve increases in wave length regions where the plate has been sensitized and where, as a consequence of this, the number of sensitive grains is augmented. If we suppose that near the limit of sensitivity of the plate the reverse will occur, the decrease of inclination of the transmission curve near the green end of the spectrum is explained. Indeed it is clear, that in this case the plate will be saturared sooner, so that the gradation must diminish.

It will be of importance to deduce from our present theory what will occur with the transmission curves valid for the stellar and for the comparison spectrum.

In the preceeding paragraph we concluded, that as a consequence of the illumination effect the transmission curve for the iron comparison spectrum would be much flatter than for the density marks. In the case of large k this will be of no influence on the change of log t' with wave length. But if on the contrary we use our calculations for small k, the wave-length effect will diminish in proportion to the square of the inclination of the curve.

Of course, there will not only be a change in the slope of the curve, but also a change in its form. Since the illumination effect is a result not of the different time of exposure but of its different intensity, it is clear that the transmission curve for the iron spectrum will differ from the curve for the density marks especially in the parts of high transmission. For in the dense parts the illumination has already been so intense that the slope of the curve approaches its limiting value, corresponding to the asymptotic region of the curve of constant blackness. Now if we look at the form of the transmission curve which has been derived for the density marks, it is seen, that the proportion S'/S, which would be constant if the curve had the form $S = c\, I^n$, diminishes with increasing I. If then we proceed to the curves valid for the iron comparison spectrum, the value of S' in this new curve will not differ very much from the old value in the dense regions, but it will be distinctly less in the region of high transmission. This means, that the shape of the curve now approaches more and more the ideal form represented by $S = c\, I^n$. So as a consequence of this effect, the wave-length effect will be smaller for the transmission curve for the iron comparison spectrum than for the curve which was derived from the density marks, even if we accept the calculation with large k.

From the measures of KRON we found that the slope of the transmission curves for the iron spectrum would be about 1.24 times smaller than the inclination of the adopted curve. Now it becomes clear that this figure may be valid for the elementary layers of the emulsion and that it will be a fair approximation in the violet region of the spectrum. But as we approach the longer wave lengths, the slope of the transmission curve for the density marks will rapidly increase, whereas the slope

of the curve for the iron spectrum changes much less. From the above it follows, that it will be difficult to predict these differences quantitatively, but we may get a fair approximation if we assume the inverse square law for the change in the slope. This hypothesis is supported by the results of a comparison with the 1929 plates; for the latter plates the slope of the transmission curve was half as much as for the plates which are here under consideration, and the wave-length effect turned out to be $\frac{1}{4}$. It will be applied in the calculation of the estimated theoretical slopes in Table 15. For the curve which applies to the stellar spectrum, the considerations must be reversed, of course.

Table 15. Estimated theoretical slopes of transmission curves.

λ	Density marks			All curves $\frac{\Delta \log}{\text{slope}^2}$	Comparison spectrum			Stellar spectrum		
	Slope	log	slope ^{2}		Slope	log	slope ^{2}	Slope	log	slope ^{2}
4100	1.82	0.260	3.3		1.47	0.167	2.2	1.94	0.288	3.8
4200	1.97	.294	3.9	+ 0.094	1.55	.190	2.4	2.12	.327	4.5
4300	2.23	.348	5.0	+ .121	1.67	.223	2.8	2.45	.389	6.0
4400	2.41	.382	5.8	+ .063	1.75	.242	3.1	2.69	.430	7.2
4500	2.54	.405	6.5	+ .037	1.79	.254	3.2	2.88	.459	8.3
4600	2.49	.396	6.2	— .014	1.78	.250	3.2	2.81	.448	7.9
4700	2.43	.386	5.9	— .017	1.76	.245	3.1	2.72	.435	7.4
4800	2.33	.367	5.4	— .034	1.72	.235	3.0	2.58	.411	6.7
4900	2 20	.342	4.8	— .049	1.66	.221	2.8	2.40	.380	5.8

The relatively small variation in the slope of the transmission curve for the comparison spectrum may throw some light on the variation of the relative profile widths of stellar and comparison lines with wave length. We already explained a factor 0.88 in the relative profile width as a consequence of the deviation by a factor 1.24 of the slope of the transmission curve for the comparison spectrum relative to that obtained from the density marks. Now it appears that this factor will depend on wave length in somewhat the same way as the difference in profile width itself. This will be shown in Table 16. In this table we collected the figures from Table 12, averaging over the four different spectra mentioned there. The observed variation in relative profile width (star : comparison) is compared with the variation in the relative slope of the transmission curve (density markings : comparison spectrum) and the variation in profile width which may be calculated from the slope ratio. The last column, finally, gives the remaining differences.

Table 16. Observed and calculated variation of relative profile width with wave length.

λ	Number of lines	Relative profile width	Relative slope transmission curve	Calculated rel. profile width	Obs : Calc
4143	63	0.79	1.25	0.88	0.90
4252	91	.71	1.31	.86	.83
4369	52	.69	1.37	.83	.83
4483	95	.66	1.41	.82	.80
4637	54	.65	1.39	.82	.79
4815	44	.71	1.35	.84	.85

We see that in this way the observed variation is only half explained. But the value 1.24 for the slope ratios with which we started at the violet limit of the spectrum, may indeed be too great, as the slope of the transmission curve at this wave length did not yet reach its limiting value

for the elementary layer. So it seems probable that at least great part of the observed variation can be explained in this way.

If this is true, the procedure by which we derived the true instrumental curve from the apparent one, is justified. Only the exponent 1.24 which has been used to this end before, will be too small. Perhaps 1.40 will be a better approximation. Table 17 gives the form of the instrumental profile after the application of this transformation.

Table 17. Corrected instrumental profile $(I_t = I_m^{1.40})$.

Distance from line centre	I_m	I_t	Distance from line centre	I_m	I_t
0	1.000	1.000	20	0.578	0.465
4 μ	0.966	0.953	24	.489	.367
8	.889	.848	32	.350	.230
12	.791	.719	40	.271	.161
16	.688	.593			

In this compuation we have assumed that only the slope of the transmission curve has been altered. But it is to be expected that also its shape will change. Fortunately, the form of the instrumental profile has been derived using only the central part of the transmission curve, so that errors from this source will not be large.

We remember, however, that the profile of the very strong emission lines was found to be narrower than that of the moderately blackened ones. This difference may be explained on the basis of the present theory. For we noted already, that the difference in slope between the transmission curve for the emission spectrum and the standard curve would be larger in the region of weak blackness than in the strongly blackened region. This means that whereas the moderately blackened emission lines are measured too broad, this effect diminishes for the very strong lines. So the profile of these latter lines will more approach the true one.

As to the stellar spectrum, we see from Table 15 that the slope ratio here will also show a change with wave length, decreasing first from a value 1.82 : 1.94 = 0.94 to 0.88 and then increasing again to 0.92. This change in slope will influence the profile only in the case of very strong lines, but in every case it will change the equivalent width. In order to obtain the true equivalent width from the measured one, we should multiply by the factors given here. This means a negative correction in log A, varying between the limits 0.027 — 0.056 — 0.036. We shall not apply this correction, since it is of little importance compared with the uncertainties in the measurements themselves.

Consequences of fog or wrong background.

A further agency that may cause a deviation of the apparent profiles of the emission lines from the true ones, may be a slight fog over the iron spectrum. As a consequence of the absence of a continuous background, such a fog would only be detected if it was caused by a rather strong illumination. A continuous fog of intensity 0.25 would cause a blackening of the plate of only 2 %. Nevertheless, if it is superposed upon the ordinary profile of the emission line, it will change the true intensities 1.00 and 0.75 to 1.25 and 1.00 and so diminish the intensity ratio from 1.33 to 1.25 or with a factor 0.94. So the presence of fog would make the apparent profiles of the emission lines of the comparison spectrum larger than the true ones.

It is clear, however, that this effect would be eliminated automatically if it occurs in the same

way at the place of the intensity marks from which the transmission curves have been deduced. Now a thorough inspection of microphotometer tracings showed that a possible extra fog over the emission spectrum is certainly smaller than $\frac{1}{2}$ %. So we may assume that its influence on the apparent profile is of little significance.

On the other hand we might try to explain the difference in profile width between the emission lines of the comparison spectrum and the stellar lines by supposing that the latter were measured too narrow. This would be the case, if the adopted continuous background was too high. For in this case the point where the apparent depression was 75 % of the central one, would be situated too near to the line centre.

If, however, we try to explain in this way the remaining difference in profile width between stellar and emission line, after the influence of the illumination effect has been eliminated (0.83 on the average), it is found, that a background correction of 20 % on the average would be required. This is an improbably high value. And whereas in the following we shall see that such a high correction is indicated in some cases also by another calculation, the dates are not uniform and for ϑ Cygni *e.g.*, they fail to indicate such a correction. So it does not seem adequate to assume that the remaining differences in profile width will be caused by background influences.

Conclusion.

The main problem relating to the determination of the instrumental curve was the difference in width between stellar lines and lines from the emission spectrum, the latter being much broader. There was a distinct variation of this effect with wave length also. Finally it appeared that the profiles of emission lines of different strength were not identical, but that the strongest lines were narrower than the others.

In the preceding we succeeded in giving at least a qualitative explanation of these facts. It appeared that they were caused by differences in slope and in shape of the transmission curves valid for different wave lengths and different illuminations. As a result of our investigations we arrived at the following conclusions.

1) The transmission curve for the iron comparison spectrum will be less inclined than the curve derived from the density marks. This produces the greater apparent width of the emission lines.

2) The differences in slope increase from the violet to $\lambda = 4500$ and then decrease a little towards the red end of the spectrum. This effect causes the variation of profile width with wave length.

3) The transmission curve for the iron spectrum will differ also in shape from the standard curve. The flattening of the curve will be strong in the regions of high transmission and less in the regions of great blackness. This causes the difference in profile between strong and weak emission lines, the stronger lines being the narrower ones.

4) The transmission curve for the stellar spectrum will be steeper than the adopted curve. This will cause no change in profile for the stellar lines (with the exception of the strongest lines only, which become a little flattened at the top), but the apparent equivalent width is increased a little. It is supposed, however, that this effect will not be of great importance.

5) The difference in steepness between the transmission curve for the stellar spectrum and the standard curve will also depend on wave-length. This variation, however, which is expected to be small, will be neglected in our further discussion.

6) The wave-length variation in the slope of the transmission curve varies approximately

as the square of the inclination of the curve. So it can be diminished by using plates of low gradation. As the photographic effects change not only the slope, but also the shape of the transmission curve, it is very doubtful, whether the accuracy of intensity measures on a photographic plate is increased by a contrastful development. The decrease of the accidental error in the intensity measure, which is a consequence of the greater steepness of the transmission curve, is paid by an increase of the systematic errors due to photographic effects.

7) In the preceeding we did not succeed in a complete quantitative treatment. But there is a strong coincidence between the predicted and the observed effects, and the estimated amounts of the effects are comparable with the observed ones. The remaining differences suggest rather an underestimate of the quantitative result than the effect of other agencies.

8) Other possible effects which have been studied theoretically, appear to work in the opposite direction or to be quantitatively insufficient. It is possible, of course, that some of them give minor contributions to the observed differences.

9) If the above theory is right, the differences in width between the apparent profiles of stellar and emission lines will also correspond to a difference in shape .The relation between the profiles will be approximately in accordance with the formula $I_t = I_m^p$ where I_t corresponds to the profile of the stellar lines, I_m to the emission lines and p may be as large as 1.40 or even larger.

The adopted instrumental curve.

The above theory of the instrumental curve has been developed at the same time that the equivalent widths of the stellar lines were discussed and the spectral parameters calculated. Part of this investigation was made during the winter 1944—1945, when it was impossible to procure the necessary litterature or to perform the necessary testing measures. So we were obliged to apply partially empirical corrections to the instrumental curve. In applying these corrections, we also used as a guide the profile, measured on one of the 1929-plates, that had already been used for the wings. When we tried to use these profiles for the central parts, it was found, that they were much narrower than those derived from the 1924 plates. Now, however, that we have explained the great width of the emission lines on the 1924 plates as a consequence of photographic effects, it appears that the profile measured on the 1929 plate on a continuous background will be much more reliable than the profiles obtained from the 1924 plates.

For we have shown, that the photographic effects will not change the shape of the profiles of not too strong lines, situated on a continuous background. So the profile of an emission line on a continuous background will also be directly applicable to the stellar spectrum, regardless of the question, whether the transmission curves have different slopes.

The instrumental curve, which was finally adopted for the stellar spectrum is given in Table 18. It agrees approximately with the shape of the 1924 curve as well as with the observed width of the stellar lines. Its form corresponds approximately to the formula $I_t = I_m^{2.20}$.

This exponent seems to be rather large, if it must be explained on the basis of the discussed effects alone. It is possible, however, that the true exponant is smaller and that the remaining difference is due to fog over the iron spectrum. Although the error which would be caused by fog would introduce a somewhat different mathematical expression for the true line profile, the numerical differences are not large. Indeed, in computing the profile of table 18 we used an exponential formula with exponent 1.32 and then further reduced the width of the profile by subtracting a supposed fog of 0.35. As this operation has almost the same result as the direct application of an exponent 2.20,

it appears that every arbitrary combination of fog with the effect of slope of the transmission curve, would give almost the same results.

Only when we assume a large background correction, the adopted instrumental profile may be wrong. For in this case it would be narrower than the true profiles of the stellar lines.

Table 18. Final instrumental curve.

Distance to centre	Intensity	Contracted curve	Distance to centre	Intensity	Contracted curve
0	1.00	0.168	50	0.026	— 0.006
5 μ	0.90	.137	55	.019	— . .002
10	.71	.089	60	.015	— .001
15	.54	.045	65	.011	— .001
20	.30	— .011	70	.008	—
25	.20	— .024	75	.006	—
30	.15	— .020	80	.005	—
35	.08	— .022	85	.004	—
40	.05	— .012	90	.003	—
45	.038	— .007	95	.002	—
			100	.001	—

The contracted profile has been obtained by applying eq. (26). For the distance c we choose 20, as the width of the profile is now only $^2/_3$ of its original value. The same value of this parameter has been taken in the reduction of the stellar spectra. The contracted profile has been normalized so as to make its surface equal to unity for a unit distance of $2\frac{1}{2}$ μ.

The contracted instrumental curve has negative wings. This feature was also shown in our registered spectra. This may be an indication that the adopted instrumental curve is not far from the true one. The occurrence of negative wings could have been avoided by chosing a somewhat larger value for the contraction distance. The presence of negative wings is not a fundamental limitation to the validity of the method, for these wings can be included as exactly as positive wings would be.

IV. THE CONSTRUCTION OF THE THEORETICAL SPECTRUM.

Auxiliary Tables.

We now start with the calculation of theoretical equivalent widths. As a base we have the provisional curves of growth, whose parameters are given in table 8 and the instrumental curve of table 18. The solar equivalent widths of the components of a blend have been taken from the tables of C. W. ALLEN. The intensities of the very weak lines have been estimated from the Rowland figures. Then with the help of the curve of growth for the sun and the corresponding curves for the star we compute the stellar equivalent width of each component. The total intensity of each line is then distributed according to the instrumental curve, and the part within the limits at which the blend is cut has been calculated by formulae 9, 10, 11.

Table 19 gives, as function of the solar equivalent width $A_\odot$, the equivalent width in the star A_* and the line parameters D (surface of the Doppler core), d (effective width of the Doppler core), $\sqrt{C}$ (surface of half resonance profile) and the differential terms.

The spectrum of δ Equulei has been excluded from the discussion, because the measurements are too inaccurate.

Table 20 gives the values of k and j which are used in the calculation of the equivalent width of the cut Doppler profiles. These quantities are given as functions of d and c, the effective width of the Doppler profile, which may be taken from Table 19 and the cutting distance. Both distances are expressed in a "normal distance" n as a unit, which varies according to the varying width of the instrumental profile (see Table 20c).

Table 20. Cutting functions.

Table 20a. The cutting function k (eq. (14)).

c \ d	0	3	6	9	12	15
0	0.00	0.00	0.00	0.00	0.00	0.00
1	.16	.14	.11	.08	.05	.04
2	.31	.28	.22	.15	.10	.07
3	.44	.40	.32	.22	.16	.11
4	.54	.50	.40	.30	.21	.15
5	.62	.58	.48	.36	.26	.19
6	.67	.63	.54	.42	.31	.23
9	.69	.67	.63	.55	.45	.35
12	.62	.62	.62	.59	.54	.46
15	.56	.56	.57	.58	.57	.53
20	.51	.51	.52	.53	.55	.55
25	.50	.50	.50	.51	.51	.52
30	.50	.50	.50	.50	.50	.51

Table 19. Comparison of solar and stellar equivalent widths.

Atomlines							Ionlines						
$A_\odot$	A_*	D	d	$\sqrt{C}$	$D\frac{\partial \ln D}{\partial \ln s}$	$D\frac{\partial \ln d}{\partial \ln s}$	$A_\odot$	A_*	D	d	$\sqrt{C}$	$D\frac{\partial \ln D}{\partial \ln s}$	$D\frac{\partial \ln d}{\partial \ln s}$
19*a*. δ Cephei 10607. $\log 2b = 2.27$ $\log a = \overline{3}.25$							$\log s_0/k$ (star — sun) $= \begin{matrix}\overline{1}.00 \text{ (atoms)} \\ 0.70 \text{ (ions)}\end{matrix}$						
0	0	0	128	0	0	0	0	0	0	128	0	0	0
10	5	5	128	1	5	0	5	71	71	128	4	45	1
20	14	14	128	1	13	0	10	116	116	131	5	58	6
30	27	27	128	2	22	0	15	148	148	137	7	62	10
40	46	46	128	3	34	0	20	177	177	142	9	64	15
60	102	102	130	5	55	4	30	222	222	152	13	63	21
80	167	167	140	8	64	13	40	261	260	163	18	60	25
100	218	218	151	13	63	20	50	298	295	174	25	57	29
150	292	290	171	24	58	28	60	331	327	183	34	53	31
200	333	329	184	35	53	31	80	395	383	203	59	47	33
250	364	357	192	45	51	32	100	447	419	218	89	43	33
300	388	376	199	55	47	32	150	566	470	239	170	39	33
400	422	404	214	74	45	33	200	681	497	253	245	36	32
500	452	422	219	93	42	33	250	797	513	262	316	34	32
750	524	456	232	141	40	33	300	926	528	264	389	34	31
1000	598	480	245	191	38	33	350	1049	539	270	457	33	31
1250	673	496	252	240	37	33	400	1177	549	275	525	32	31
19*b*. δ Cephei 10617. $\log 2b = 2.23$ $\log a = \overline{3}.00$							$\log s_0/k$ (star — sun) $= \begin{matrix}\overline{1}.00 \text{ (atoms)} \\ 0.70 \text{ (ions)}\end{matrix}$						
0	0	0	117	0	0	0	0	0	0	117	0	0	0
10	5	5	117	1	5	0	5	65	65	117	2	41	1
20	13	13	117	1	12	0	10	106	106	120	4	53	5
30	25	25	117	1	21	0	15	135	135	125	5	58	9
40	42	42	117	2	31	0	20	162	162	130	6	58	14
60	94	94	119	3	51	4	30	203	203	139	9	58	19
80	152	152	128	6	58	12	40	238	238	149	13	55	23
100	199	199	138	9	58	18	50	271	269	156	17	52	26
150	268	266	156	16	53	26	60	301	299	167	23	48	28
200	303	301	169	23	48	29	80	356	350	186	41	43	30
250	330	326	175	31	46	30	100	397	383	199	62	39	30
300	349	343	182	38	43	30	150	479	429	218	118	36	30
400	379	369	196	51	41	30	200	554	454	232	170	33	30
500	402	386	201	65	39	30	250	629	469	239	219	31	29
750	452	417	212	98	37	30	300	709	483	242	269	31	29
1000	501	439	224	132	35	30	350	787	493	247	316	30	29
1250	549	453	231	166	34	30	400	870	502	251	363	30	29

19c. ϑ Cygni. $\log 2b = 1.92$ $\log a = \overline{3}.50$ $\log s_0/k$ (star — sun) $= \begin{matrix}\overline{1}.30 \text{ (atoms)} \\ 0.30 \text{ (ions)}\end{matrix}$

Atomlines							Ionlines						
$A\odot$	A_*	D	d	$\sqrt{C}$	$D\frac{\partial \ln D}{\partial \ln s}$	$D\frac{\partial \ln d}{\partial \ln s}$	$A\odot$	A_*	D	d	$\sqrt{C}$	$D\frac{\partial \ln D}{\partial \ln s}$	$D\frac{\partial \ln d}{\partial \ln s}$
0	0	0	57	0	0	0	0	0	0	57	0	0	0
10	5	5	57	1	5	0	5	17	17	57	1	13	0
20	12	12	57	1	10	0	10	31	31	57	2	20	1
30	21	21	57	2	15	0	15	43	43	58	3	23	2
40	33	33	57	2	21	1	20	54	54	59	3	26	3
60	63	63	61	4	28	4	30	74	74	63	5	28	6
80	93	93	66	7	29	8	40	91	91	66	7	28	8
100	116	116	73	11	27	11	50	109	109	70	9	27	11
150	149	146	82	21	24	14	60	126	124	75	13	26	12
200	169	163	88	30	22	15	80	154	150	82	22	23	14
250	183	174	92	38	21	15	100	177	169	90	34	21	15
300	198	182	96	47	20	15	150	223	194	100	65	19	15
400	219	193	100	63	19	15	200	263	207	106	93	18	15
500	241	201	103	79	18	15	250	304	216	110	120	17	15
750	302	215	110	120	17	15	300	346	222	113	148	16	14
1000	371	225	115	162	16	14	350	393	227	116	174	16	14
1250	445	232	118	204	15	14	400	438	232	116	200	15	14

19d. π Cephei. $2b = 2.04$ $\log a = \overline{3}.50$ $\log s_0/k$ (star — sun) $= \begin{matrix}0.30 \text{ (ions)} \\ \overline{1}.60 \text{ (atoms)} \\ \overline{1}.20 \text{ (molecules)}\end{matrix}$

0	0	0	76	0	0	0	0	0	0	76	0	0	0
10	12	12	76	1	10	0	5	22	22	76	2	17	0
20	27	27	76	2	20	0	10	41	41	76	3	27	1
30	45	45	76	3	28	1	15	57	57	76	3	31	2
40	65	65	78	4	34	3	20	72	72	78	4	35	4
60	109	109	85	8	38	9	30	99	99	83	7	38	8
80	147	147	95	13	35	14	40	121	121	87	9	38	11
100	178	176	102	20	33	17	50	144	144	93	12	36	14
150	223	214	115	38	29	19	60	167	165	99	17	35	16
200	252	234	124	55	27	19	80	205	199	109	30	31	19
250	278	248	128	71	26	19	100	236	224	119	45	28	19
300	301	257	134	87	25	20	150	300	257	133	85	25	20
400	348	272	139	117	23	20	200	358	274	140	123	23	20
500	399	283	144	148	23	20	250	416	286	146	158	22	19
750	533	301	153	224	21	19	300	478	294	150	195	21	19
1000	676	312	156	302	20	19	350	539	301	154	229	21	19
1250	827	321	160	380	19	19	400	601	307	154	263	20	19
					Molecule lines:		0	0		76		0	0
							25	18		76		14	0
							50	55		77		31	2
							75	107		84		38	8
							100	145		94		36	14

Table 20*b*. The cutting function *j*. (eq. (14)).

c \ *d*	0	3	6	9	12	15
0	0.00	0.00	0.00	0.00	0.00	0.00
3	.00	— .06	— .19	— .25	— .22	— .16
6	.00	— .07	— .23	— .36	— .38	— .32
9	.00	— .03	— .13	— .28	— .41	— .37
12	.00	.00	— .02	— .12	— .29	— .42
15	.00	+ .01	+ .02	.00	— .10	— .28
18	.00	.00	+ .02	+ .04	+ .02	— .09
21	.00	.00	+ .01	+ .04	+ .06	+ .04
24	.00	.00	+ .01	+ .02	+ .04	+ .06
27	.00	.00	.00	+ .01	+ .02	+ .05
30	.00	.00	.00	.00	+ .01	+ .02

Table 20*c*. Normal distances in mA.

Plate numbers λ	10607/10	10616/17/18	10619
4100	21	20	20
4200	24	23	24
4300	29	27	28
4400	34	32	34
4500	40	37	41
4600	47	44	49
4700	54	51	59
4800	63	61	72
4900	73	71	86

In Table 20 we clearly see the influence of the negative wings of the contracted instrumental profile. The quantity k determines the fraction of the surface of the Doppler profile situated between the limits 0 and c. It is clear that this fraction can become greater than $\frac{1}{2}$ only in the case of negative wings.

Compilation of the material.

Table 21 gives a list of all lines used in the second investigation. It is an extract from the lines given in Table 7, from which have been omitted all lines which, according to the identification in the revised Rowland Table, are not of single origin. (This does not mean of course the omission of blends, for which the different components appear separated in the solar spectrum).

The remaining lines are tabulated below, for ϑ Cephei, δ Cygni and π Cephei simultaneously. The first column gives in the odd rows the wave length of the line, in the even rows the excitation potential. The other columns are taken in groups of three. The first and second column of each group give the wave length at which the blend has been cut. The third column gives the logarithm of the measured equivalent width in the star. Notes of exclamation and of interrogation have the same meaning as in Table 7. In each group of columns the odd and even rows apply to different spectra of the same star, as has been indicated in the headings.

The tabulated equivalent widths differ somewhat from those given in Table 7 because now we used the values which are not corrected for the influence of resonance wings.

Table 21. Measured equivalent widths of cut blends.

Table 21*a*. Lines of *Fe I*.

λ	δ Cephei 10607 10617			ϑ Cygni 10616 10619			π Cephei 10610 10618		
Exc. Pot.	λ_1	λ_2	log B	λ_1	λ_2	log B	λ_1	λ_2	log B
4059.72	9.60	9.86	1.98	9.57	9.88	1.94	—	—	—
3.53	—	—	—	—	—	—	—	—	—
4062.45	2.19	2.76	2.40	2.25	2.63	2.26	—	—	—
2.833	—	—	—	—	—	—	—	—	—
4065.39	5.34	5.67	1.94?	5.19	5.60	2.02	—	—	—
3.415	—	—	—	—	—	—	—	—	—
4070.78	0.48	1.18	2.34	0.63	0.96	2.15	—	—	—
3.227	—	—	—	—	—	—	—	—	—
4071.75	1.18	2.20!	2.59!	1.48	2.06	2.50	—	—	—
1.601	—	—	—	—	—	—	—	—	—
4072.51	2.29	2.80	2.21	2.16	2.74	2.05	—	—	—
3.415	—	—	—	—	—	—	—	—	—
4079.85	9.59	0.12	2.27	9.72	0.03	2.12	—	—	—
2.846	—	—	—	—	—	—	—	—	—
4080.88	0.65	0.96	1.76	0.55	1.00	1.89	—	—	—
3.278	—	—	—	—	—	—	—	—	—
4084.50	4.10	4.80	2.34	4.30	4.66	2.16	—	—	—
3.318	—	—	—	—	—	—	—	—	—
4089.23	8.88	9.58!	2.20!	9.03	9.43	1.94	—	—	—
2.936	—	—	—	—	—	—	—	—	—
4091.56	1.27	1.88	2.01	1.07!!	1.79	2.20!!?	—	—	—
2.819	—	—	—	—	—	—	—	—	—
4109.06	8.91	9.35	2.19?	8.86	9.23	1.95?	—	—	—
3.278	—	—	—	8.78	9.28	2.14?	—	—	—
4112.32	2.13	2.47	1.90	2.03	2.51	1.91?	—	—	—
3.382	—	—	—	2.07	2.51	1.93?	—	—	—
4114.45	4.18	4.80	2.30	4.07	4.74	2.17	—	—	—
2.819	—	—	—	4.13	4.75	2.19	—	—	—
4120.22	9.97	0.53	2.28	0.00	0.61	1.94	—	—	—
2.977	—	—	—	9.97	0.42	2.09	—	—	—
4126.19	6.03	6.42	2.15	6.04	6.46	2.02	—	—	—
3.318	5.98	6.38	2.11	6.04	6.34	1.90	—	—	—

Table 21*a*. (continued).

λ Exc. Pot.	δ Cephei 10607 10617 λ_1	λ_2	log B	ϑ Cygni 10616 10619 λ_1	λ_2	log B	π Cephei 10610 10618 λ_1	λ_2	log B
4126.86	6.42	7.03	1.93	6.71	7.02	1.45	—	—	—
2.833	6.38	6.90	1.97	6.74	7.16	1.68	—	—	—
(4130.05	9.39	0.25	2.44	9.85	0.22	1.68	—	—	—)
1.551)	9.46	0.09	2.26	9.87	0.46	1.89	—	—	—)
4132.07	1.68	2.50	2.61?	1.79	2.27	2.30	—	—	—
1.601	1.78	2.34	2.37	1.82	2.44	2.43	—	—	—
4132.91	2.50	3.17	2.43	2.71	3.25	2.03	—	—	—
1.601	2.78	3.20	2.15	2.74	3.07	2.05	—	—	—
4134.69	4.60	5.01	2.22	4.52	4.95	2.16	—	—	—
2.819	4.26	5.10	2.46	4.50	5.02	2.20	—	—	—
4136.53	6.23	6.76	2.02	6.32	6.67	1.86	—	—	—
3.354	6.11	6.76	2.09	6.32	6.80	1.84	—	—	—
4137.01	6.76	7.25	2.26	6.79	7.23	2.03	—	—	—
3.40	6.76	7.34	2.26	8.60	7.27	2.03	—	—	—
4137.98	7.25	8.04	2.35	7.86	8.22	1.61	—	—	—
2.820	7.94	8.14	1.63	7.80	8.11	1.58	—	—	—
4139.94	9.43	0.15	2.12	9.58	0.09	1.89	—	—	—
0.986	9.55	0.26	2.17	9.55	0.17	1.91	—	—	—
(4140.41	0.15	0.71	2.00	0.20	0.56	1.83	—	—	—)
3.402)	0.26	0.76	2.03	0.20	0.52	1.78	—	—	—)
4141.87	1.40	1.95	2.17	1.65	1.98	1.64	—	—	—
3.005	1.66	2.09	2.13	1.57	2.08	1.88	—	—	—
4143.88	3.61	4.27	2.50	3.75	4.25	2.32?	—	—	—
1.551	3.67	4.20	2.41?	3.69	4.39	2.37	—	—	—
4145.20	4.71	5.27	2.08	5.14	5.48	error	—	—	—
2.681	4.81	5.52	2.20	5.15	5.48	1.58	—	—	—
4147,68	7.24	7.91	2.42	7.47	7.96	error	—	—	—
1.478	7.40	8.00	2.34	7.46	7.94	2.11	—	—	—
4150.26	0.10	0.56	2.12	0.14	0.62	2.05	—	—	—
3.415	0.14	0.63	2.11	0.02	0.72	2.14	—	—	—
4154.51	4.18	4.58	2.25	4.22	4.59	2.06	—	—	—
2.819	4.16!	4.64	2.29!	4.32	4.69	2.15	—	—	—
4154.82	4.58	5.09	2.35	4.59	5.05	2.11	—	—	—
3.354	4.64	5.18	2.31	4.69	5.05	2.09	—	—	—

Table 21*a*. (continued).

λ Exc. Pot.	δ Cephei 10607 10617			ϑ Cygni 10616 10619			π Cephei 10610 10618		
	λ_1	λ_2	log B	λ_1	λ_2	log B	λ_1	λ_2	log B
4157.79	7.37	8.07	2.40	7.55	8.09	2.16	—	—	—
3.402	7.31	8.13	2.35	7.58	8.05	2.16	—	—	—
4158.80	8.45	8.92	2.24	8.58	9.07	2.06	—	—	—
3.415	8.56	8.97	2.12	8.50	9.04	2.11	—	—	—
4168.62	8.43	8.77	1.93	8.34	8.84	1.86	—	—	—
3.354	8.46	8.86	2.03	8.36	8.81	1.77	—	—	—
4168.95	8.77	9.17	1.92	8.84	9.21	1.66	—	—	—
3.402	8.86	9.40	2.08	8.81	9.20	1.84	—	—	—
4174.92	4.60	5.29	2.32	4.63	5.28	2.16	4.75	5.47!!	2.41!!
0.911	4.69	5.31	2.28	4.71	5.37	2.13	—	—	—
4175.64	5.29	6.15	2.45	5.36	5.96	2.18	5.47	6.30!!	2.30!!
2.833	5.31	6.19	2.41	5.37	5.97	2.22	—	—	—
4182.39	2.12	2.56	2.17	2.13	2.58	2.00	2.07	2.53	2.18
3.004	2.18	2.75	2.22	2.21	2.59	1.91	—	—	—
4187.05	6.79	7.27	2.42	6.83	7.33	2.19	6.86	7.52	2.41?
2.439	6.84	7.42	2.39	6.76	7.26	2.20	—	—	—
4202.04	1.43	2.60	2.70	1.42	2.25	2.37	1.45!	2.15	2.47!
1.478	1.66	2.58!	2.67!	1.45	2.34	2.42	—	—	—
4205.55	5.14	6.03	2.44	5.31	5.82	2.06	5.24	5.74	2.27
3.402	5.24	6.04	2.43	5.32	5.84	2.09	—	—	—
4206.70	6.37	6.90	2.27	6.41	6.96	2.06	6.55	6.91	2.26
0.051	6.40	6.96	2.30	6.44	6.94	2.05	—	—	—
4207.14	6.90	7.60	2.30	6.96	7.56	2.10	6.91	7.22	1.97
2.819	6.96	7.64	2.36	6.94	7.53	2.08	—	—	—
(4208.61	8.04	8.73	2.28	8.33	8.82	2.05	8.34	8.70	2.11)
3.382	8.12	8.68	2.16	8.23	8.77	2.07	—	—	—)
4216.19	5.88	6.55	2.43	6.00	6.53	2.10	6.01	6.74	2.39
0.000	5.91	6.60	2.38	5.85	6.47	2.11	—	—	—
4222.22	1.78	2.57	2.50	2.00	2.47	2.22	1.97	2.42	2.25
2.439	1.85	2.61	2.49	2.00	2.49	2.20	—	—	—
4224.18	3.77	4.83!	2.60!	3.97	4.39	2.10	3.99	4.35	2.19
3.354	3.80	4.98!	2.58!	3.93	4.47	2.21	—	—	—
4225.46	4.83	5.62	2.49	5.11	5.78	2.23	5.03	5.62	2.37
3.402	4.98	5.71	2.49	5.02	5.72	2.23	—	—	—

Table 21*a*. (continued).

λ	δ Cephei 10607 10617			ϑ Cygni 10616 10619			π Cephei 10610 10618		
Exc. Pot.	λ_1	λ_2	log B	λ_1	λ_2	log B	λ_1	λ_2	log B
4233.61	3.45	3.85	2.24	3.44	3.96	2.20	3.37	3.83	2.30
2.471	3.39	3.93	2.34	3.35	3.90	2.24	—	—	—
4235.95	5.41	6.30	2.61	5.67	6.39	2.38	5.55	6.50	2.61
2.415	5.52	6.21	2.53	5.60	6.22	2.35	—	—	—
4238.82	8.51	9.18	2.41	8.56	9.12	2.25	8.59	9.11	2.33?
3.382	8.42	9.17	2.45	8.49	9.11	2.20	—	—	—
4246.09	5.63	6.32	2.26	5.77	6.27	2.11	5.76	6.44	2.17
3.63	5.75	6.37	2.22	5.80	6.38	2.09	—	—	—
4250.13	9.53	0.37	2.48	9.90	0.42	2.32	9.80	0.42	2.44
2.458	9.79	0.51	2.44	9.88	0.36	2.30	—	—	—
4250.80	0.37	1.15	2.53	0.58	1.08	2.35	0.41	1.18	2.55
1.551	0.51	1.12	2.49	0.57	1.08	2.31	—	—	—
4260.49	0.33	1.12	2.50	0.22	0.99	2.44	0.28	1.09	2.59
2.389	0.27	1.06	2.52	0.18	0.88	2.44	—	—	—
4264.22	3.70!	4.56	2.29!	3.94	4.47	1.98	4.00	4.44	2.12
3.354	3.86	4.43	2.15	4.01	4.50	1.88	—	—	—
4264.74	4.56	5.07	1.95	4.53	5.04	1.87	4.44	5.01!	2.04!
3.943	4.43	5.09!	2.13!	4.50	4.97	1.76	—	—	—
4266.97	6.50	7.39	2.32	6.61	7.24	2.05	6.39	7.14	2.15
2.716	6.53	7.32	2.27	6.64	7.22	2.03	—	—	—
4268.76	8.30	9.00	2.25	8.46	9.18	2.11	8.42	9.06	2.20
3.29	8.37	8.90	2.08	8.38	8.99	2.06	—	—	—
4271.17	0.76	1.40	2.49	0.92	1.35	2.24	0.85	1.31	2.37
2.439	0.81	1.46	2.41	0.87	1.45	2.28	—	—	—
4271.78	1.40	2.45	2.65	1.42	2.11	2.42	1.31	2.59!	2.77!
1.478	1.46	2.17	2.55	1.45	2.18	2.41	—	—	—
4282.41	2.04	2.75	2.54	2.20	2.72	2.20	2.13	2.70	2.36
2.167	2.02	2.79	2.45	2.09	2.67	2.18	—	—	—
4325.78	5.42	6.43	2.66	5.43	6.10	2.45?	5.35	6.26	2.68
1.601	5.35	6.24	2.60	5.38	6.17	2.54?	—	—	—
4327.92	7.55	8.26	2.26	7.68	8.39	1.91?	7.60	8.31	2.22
3.29	7.41	8.53	2.28?	7.52	8.34	2.16?	—	—	—
4348.95	8.80	9.29	2.03?	8.56	9.14	1.91?	8.77	9.29	2.05
2.977	8.68	9.34	2.13?	8.56	9.42	2.06?	—	—	—
4365.91	5.66	6.10	1.91	5.53	6.14	error	5.70	6.15	1.78
2.977	5.52	6.35	2.20	5.63	6.48	2.05	—	—	—

Table 21*a*. (continued).

λ Exc. Pot.	δ Cephei 10607 10617 λ_1	λ_2	log B	ϑ Cygni 10616 10619 λ_1	λ_2	log B	π Cephei 10610 10618 λ_1	λ_2	log B
4375.95	5.46	6.33	2.47	5.45	6.22	2.23	5.60	6.47	2.41
0.000	5.59	6.31	2.37	5.48	6.16	2.16	—	—	—
4383.56	3.03	3.95	2.66	3.10	3.97	2.52	3.25	4.00	2.65
1.478	3.18	3.96	2.55	3.08	4.00	2.52	—	—	—
4388.42	8.21	8.86	2.30	8.13	8.71	2.09	8.25	9.09	2.32
3.587	8.17	8.87	2.30	8.09	8.72	2.14	—	—	—
4389.26	8.86	9.63	2.14	9.04	9.69	1.86	9.10	9.59	2.06
0.051	8.94	9.55	2.03	8.99	9.63	1.79	—	—	—
4404.76	4.19	5.32	2.69	4.31	5.06	2.46	4.31	5.40	2.71
1.551	4.32	5.49	2.61	4.31	5.17	2.46	—	—	—
4415.14	4.13	5.96	2.86	4.54	5.38	2.43	4.47	6.02	2.74
1.601	4.72	5.30	2.44	4.52	5.40	2.34	—	—	—
4427.32	6.79	7.73	2.61	6.89	7.87	2.32	6.75	8.11	2.57
0.051	6.65	7.66	2.53	6.86	7.59	2.28	—	—	—
4438.35	7.91	8.76	2.07	8.03	8.79	1.97	8.08	8.78	2.16
3.671	7.96	8.73	2.15	7.97	9.00	1.98	—	—	—
4442.35	2.04	2.70	2.40	2.00	2.67	2.14	2.00	2.82	2.40
2.188	2.07	2.67	2.32	2.00	2.79	2.14	—	—	—
4447.73	7.31	8.22	2.45	7.35	8.12	2.23	7.26	8.09	2.40
2.213	7.32	8.66!	2.48!	7.39	8.12	2.14	—	—	—
4484.23	3.36	4.56	2.50	3.64	4.61	2.17	4.09	4.73	2.12
3.587	3.64	4.55	2.40	3.70	4.63	2.19	3.65!	5.00!	2.30!!
4485.68	5.31	6.12	2.35	5.22	6.17	2.02	5.32	6.39	2.26?
3.671	5.12	6.16	2.31	5.30	6.14	2.10	5.29	6.38	2.18
(4490.78	0.34	0.93	2.01	0.37	1.06	1.89	0.35	1.06	2.25)
3.926	0.47	1.00	1.96	0.46	1.05	1.77	0.44	1.18	2.16)
4492.69	2.09	3.14	2.08	2.46	2.89	1.61	2.05	2.95	2.14
3.967	1.94	2.92	2.06	2.52	2.98	1.63	2.30	3.07	2.00
4494.58	3.93	5.14	2.62	3.91	4.94	2.32	4.20	5.23	2.52
2.188	3.92	4.92	2.54	3.96	4.90	2.27	4.31	5.22	2.41
4504.84	4.43	5.24	2.12	4.71	5.64!	1.83!	4.42	5.50	2.18
3.252	4.22	5.27	2.27	4.62	5.59!	1.79!	4.44	5.33	2.16
4528.63	7.85!	9.07	2.64!	8.12	8.99	2.38	7.70!	9.17	2.64!
2.167	7.76	9.04	2.62	8.15	9.02	2.37	7.80!	9.05	2.55!

Table 21*a*. (continued).

λ	δ Cephei 10607 10617			ϑ Cygni 10616 10619			π Cephei 10610 10618		
Exc. Pot.	λ_1	λ_2	log B	λ_1	λ_2	log B	λ_1	λ_2	log B
4587.14	6.76	7.40	1.88	6.44	7.48	2.02	6.80	7.45	1.99
3.56	6.68	7.56	2.09	6.77	7.49	1.89	6.80	7.56	2.23
4602.01	1.79	2.32	1.91	1.65	2.40	1.93	1.64	2.44	2.04
1.601	1.82	2.49	1.98	1.52	2.26	1.76	1.62	2.48	2.04
4602.95	2.42	3.42	2.51	2.50	3.47	2.28	2.41	3.53	2.39
1.478	2.49	3.70	2.45	2.44	3.54	2.23	2.66	3.59	2.37
4625.05	4.46	5.55	2.40	4.69	5.50	2.22	4.49	5.51	2.29
3.227	4.56	5.55	2.29	4.72	5.53	2.05	4.52	5.62	2.27
4630.13	9.86	0.67	2.20	9.69	0.88	2.17	9.88	0.93	2.19
2.269	9.94	0.30	1.75	9.70	0.81	1.94	9.94	0.74	2.16
4643.47	2.93	4.03	2.41	3.00	4.35	2.26	2.65!	4.10	2.50!
3.638	3.00	4.18	2.34	2.90	4.08	2.10	2.68!	4.44	2.53!
4647.44	6.89	7.90	2.50	6.81	8.29	2.30	6.93	8.51!	2.60!
2.936	7.00	7.95	2.36	6.81	7.96	2.23	7.06	8.36!	2.49!
4669.18	8.64	9.80	2.41	8.77	9.64	2.08	8.74	9.89	2.39
3.638	8.79	9.84	2.33	8.65	9.76	2.13	9.02	0.03	2.37
4683.57	3.12	4.24	2.12	3.13	4.12	2.01	3.14	4.23	2.29
2.819	3.33	4.59	2.21	2.77	4.42	2.00	3.26	4.30	2.19
4687.40	6.82	7.74	2.09	6.71	7.82	2.00	error	error	error
2.819	6.92	8.16!	2.09!	6.93	8.18	2.10	6.99	8.08	2.21
4726.15	6.00	6.56	1.45	5.37	6.56	1.99	5.49	6.49	2.00
2.985	6.00	7.01	1.90	5.33	6.50	1.97	5.76	6.73	2.02
4728.55	7.91	8.82	2.34	7.93	9.48	2.28	7.99	9.01	2.31
3.638	7.99	9.34	2.31	8.11	9.37	2.12	8.20	9.25	2.35
4733.60	3.07	4.05	2.42	2.97	4.64	2.20	3.11	5.23	2.54
1.478	3.26	4.20	2.24	2.80	4.22	2.19	3.09	5.00	2.54
4735.85	5.39	6.10	2.11	5.16	6.08	1.79	5.23	6.45	2.22
4.06	5.30	6.31	1.97	5.08	6.10	1.98	5.23	6.20	2.18
4741.54	0.88!	2.19	2.30!	1.14	2.04	2.14	1.20	2.04	2.11
2.819	1.10	2.60	2.32	1.37	2.15	2.00	0.93	1.62	2.12
(4772.82	2.44	3.53	2.27	2.32	3.48	2.17	2.28	3.47	2.31)
1.551	2.56	3.56	2.18	2.47	3.48	1.96	2.20	3.50	2.30)
4834.52	4.40	5.25	1.60	3.82	5.16	2.16	3.30!	5.33	2.42!?
2.414	4.46	5.44	1.93	3.73	5.12	2.10	3.14	4.66	2.30

Table 21*a*. (continued).

λ	δ Cephei 10607 10617			ϑ Cygni 10616 10619			π Cephei 10610 10618		
Exc. Pot.	λ_1	λ_2	log B	λ_1	λ_2	log *B*	λ_1	λ_2	log *B*
4903.32	2.55	3.89	2.46	2.83	4.07	2.22	3.00	4.18	2.32
2.870	2.57	3.93	2.38	2.68	3.86	2.22	—	—	—
4920.52	9.77	1.35	2.72	9.69	1.33	2.49	9.82	1.84	2.75
2.820	9.72	1.26	2.66	9.78	1.30	2.40	—	—	—
4930.31	9.81	1.35	2.24	9.45	0.45	2.03	9.84	1.72!	2.41!
3.943	9.94	0.98	2.20	9.40	0.78	1.92	—	—	—
4946.40	5.88	6.92	2.32	—	—	—	5.65	6.98	2.44
3.354	5.87	6.95	2.37	—	—	—	—	—	—
4950.11	9.19	0.38	2.27	—	—	—	9.65	0.88	2.31
3.402	9.42	0.72	2.32	—	—	—	—	—	—
4962.58	—	—	—	—	—	—	1.55	2.94	2.28
4.160	1.69	2.92	2.30	—	—	—	—	—	—
4966.10	—	—	—	—	—	—	5.64	6.71	2.25
3.318	5.46	7.07	2.45	—	—	—	—	—	—

Table 21*b*. Lines of Fe^+.

4128.74	8.47	9.02	2.30	8.58	8.92	1.85	—	—	—
2.572	8.53	9.04	2.20	8.27	9.00	1.98	—	—	—
4178.86	8.26	9.05	2.58	8.52	9.11	2.18	8.77	9.20	2.05
2.572	8.52	9.12	2.48	8.54	9.11	2.19	—	—	—
4233.17	2.57	3.45	2.65	2.91	3.44	2.32	3.00	3.37	2.16
2.572	2.54!	3.39	2.59!	2.86	3.35	2.23	—	—	—
4416.83	6.23	7.27	2.56	6.13!	7.18	2.26!	6.59	7.13	2.15
2.766	6.21	7.16	2.49	6.14!	7.07	2.18!	—	—	—
4491.41	0.93	1.96	2.57	1.06	1.69	2.10	1.06	2.00	2.30
2.843	1.00	1.84	2.50	1.05	1.87	2.18	1.27	2.12	2.24
4508.29	7.68	8.93	2.66	7.88	8.63	2.27	7.76	9.08	2.35
2.843	7.60	8.72	2.61	7.75	8.83	2.25	7.61	8.71	2.30
4515.34	4.75	6.02	2.64	5.00	5.77	2.29	4.87	5.87	2.35
2.832	4.83	6.01	2.59	5.00	6.00	2.24	4.94	5.91	2.27
4520.23	9.53	0.78	2.67	9.44	0.54	2.35	9.56	0.94	2.48?
2.795	9.48	0.86	2.60	9.42	0.75	2.30	9.18	0.98	2.41
4576.34	5.63	6.84	2.59	6.04	6.91	2.21	6.02	6.83	2.14
2.832	5.77	6.90	2.52	5.74	6.87	2.19	6.06	6.92	2.19

Table 21*b*. (continued).

λ Exc. Pot.	δ Cephei 10607 10617 λ_1	λ_2	log B	ϑ Cygni 10616 10619 λ_1	λ_2	log B	π Cephei 10610 10618 λ_1	λ_2	log B
4582.84	2.09	3.19	2.55	2.04	3.20	2.20	2.22!	3.30	2.30!
2.832	2.13	3.09	2.45	2.45	3.33	2.03	1.90!	3.22	2.31!
4583.84	3.19	4.52	2.79	3.20	4.58	2.48	3.30	4.39	2.46?
2.795	3.09	4.47	2.76	3.33	4.39	2.38	3.22	4.35	2.43
4620.52	9.92	0.97	2.51	0.10	1.20	2.17	9.96	1.39!	2.21!
2.816	0.08	1.19	2.44	9.72	0.96	2.04	0.35	1.42!	2.03!
4731.48	0.88	2.07	2.60	1.21	1.90	2.03	0.65	2.31	2.59
2.879	0.79	2.50	2.58	0.89	2.22	2.32	0.56	1.74	2.35
4923.93	2.73	5.10	2.85	3.27	4.54	2.42	3.08!	5.21	2.71!
2.879	3.20	4.96	2.75	2.81	4.58	2.41	—	—	—
Table 21*c*. Lines of *Ti I*.									
4287.41	7.29	7.50	1.46	7.26	7.63	1.51	7.27	7.59	1.79
0.832	7.14	7.50	1.77	7.19	7.50	1.49	—	—	—
4449.15	8.59	9.63	2.37	8.82	9.80	2.06	8.64	9.88	2.35
1.879	8.67	9.59	2.30	8.92	9.54	1.78	—	—	—
4465.82	5.61	6.07	1.66	5.03	6.06	1.84	5.79	7.32	error
1.732	5.73	6.12	1.62	5.23	6.20	1.80	5.50	6.06	1.93
4512.75	2.29	3.27	2.23	2.35	3.23	1.94	2.20	3.15	2.27
0.832	2.25	3.00	2.16	2.39	3.19	1.84	2.34	3.23	2.16
4534.79	4.61	5.18	2.18	4.51	5.05	1.91	4.49	5.18	2.14
0.832	4.58	5.20	2.10	4.52	5.39	2.02	4.49	5.31	2.20
4617.28	6.47	7.87	2.03	6.93	7.94	2.11	6.95	7.82	2.04
1.741	5.88	8.20!	2.64!	6.87	8.05	1.93	7.02	7.87	2.13
4742.80	2.19	3.16	1.98	2.22	3.56	1.89	2.04	3.48!	2.31!
2.227	2.60	3.78	2.16	2.41	3.61	2.05	2.18!	3.63	2.32!?
4759.28	8.62	9.90	2.20	8.84	9.56	2.01	8.50	0.29	2.31
2.246	8.47	9.72	1.97	9.05	9.52	1.45?	8.83	0.36	2.28
4781.73	1.00!	2.49	2.09!	0.96	2.37	2.06	0.69	2.36	2.23
0.845	1.02	2.53	2.09	1.04	2.02	1.64	0.76	2.43	2.26
Table 21*d*. Lines of Ti^+.									
4290.23	0.07	0.72	2.54	9.99	0.51	2.29	9.99	0.58	2.35
1.160	9.94	0.64	2.56	9.99	0.51	2.31	—	—	—
4300.06	9.68	0.82	2.77	9.69	0.39	2.35	9.81	0.30	2.39
1.175	9.57	0.76!	2.70!	9.76	0.46	2.34	—	—	—

Table 21*d*. (continued).

λ Exc. Pot.	δ Cephei 10607 10617			ϑ Cygni 10616 10619			π Cephei 10610 10618		
	λ_1	λ_2	log B	λ_1	λ_2	log B	λ_1	λ_2	log B
4316.80	6.45	7.21	2.43	6.30	7.03	1.96	6.51	7.10	2.07
2.039	6.37	7.19	2.38	6.51	7.16	2.14	—	—	—
4394.07	3.54	4.41	2.50	3.74	4.34	2.15	3.67	4.30	2.29
1.216	3.64	4.40	2.44	3.55	4.37	2.09	—	—	—
4395.04	4.57	5.50	2.66	4.77	5.50	2.40	4.36	5.82	2.70
1.079	4.64	5.47	2.60	4.74	5.48	2.40	—	—	—
4399.78	9.34	0.11	2.54	9.10	9.93	2.26	9.41	0.07	2.29
1.232	9.22	0.06	2.52	9.20	0.21	2.24	—	—	—
4411.94	1.53	2.49	2.42	1.77	2.31	1.81	1.63	2.51	2.31
1.219	1.61	2.64	2.42	1.74	2.31	1.89	—	—	—
4417.72	7.27	8.11	2.57	7.30	8.04	2.20	7.13	8.08	2.39
1.160	7.26	8.10	2.50	7.32	8.07	2.18	—	—	—
4418,34	8.11	8.75	2.39	8.04	8.69	2.09	8.08	8.75	2.20
1.232	8.10	8.71	2.40	8.05	8.72	1.92	—	—	—
4443.81	3.44	4.20	2.56	3.44	4.11	2.26	3.50	4.06	2.24
1.075	3.38	4.23	2.56	3.52	4.15	2.24	—	—	—
4444.56	4.20	4.98	2.48	4.31	5.06	2.11	4.06	5.00	2.35
1.111	4.23	5.18	2.50	4.25	4.87	1.82	—	—	—
4468.50	7.86	8.88	2.65	8.03	8.78	2.29	8.09	8.85	2.35
1.126	8.07	8.87	2.47	8.12	8.92	2.30	8.17	8.92	2.25
4493.53	3.14	3.93	2.32	3.11	3.81	1.78	2.95	3.74	2.05
1.075	2.92	3.92	2.35	3.20	3.96	1.99	3.34	3.78	1.91
4501.28	0.77	1.89	2.69	0.88	1.67	2.38	0.78	1.64	2.43
1.111	0.82	2.14	2.65	0.82	1.73	2.34	0.80	1.58	2.28
4545.14	4.82	5.64	2.45	4.85	5.59	2.01	4.94	5.66	2.22
1.126	4.88	5.53	2.38	4.86	5.53	1.93	5.02	5.68	2.16
4563.77	2.98	4.36	2.74	3.44	4.29	2.36	2.81	4.21	2.44
1.216	3.00	4.35	2.66	3.25	4.24	2.35	3.17	4.36	2.47?
4568.33	7.81	8.99	2.48	7.92	8.63	2.05	7.96	9.21	2.35?
1.219	7.78	8.75	2.40	8.07	8.44	1.41	8.00	9.10	2.31
4571.98	1.37	2.67	2.80	1.39	2.33	2.44	1.54	2.54	2.49
1.565	1.37	2.67	2.71	1.39	2.58	2.42	1.42	2.63	2.52
4719.51	9.11	0.56	2.41	8.81	0.21	2.08	9.32	0.29	2.06
1.238	9.09	0.16	2.29	9.03	0.33	1.97	9.14	0.30	2.18
4805.10	4.21	5.96	2.68	4.56	5.37	2.25	3.73	6.00	2.55
2.052	4.30	6.52	2.64	4.25	6.16!	2.28!	4.02	5.92	2.55

Table 21e. Lines of *Cr I*.

λ	δ Cephei 10607 10617			ϑ Cygni 10616 10619			π Cephei 10610 10618		
Exc. Pot.	λ_1	λ_2	log B	λ_1	λ_2	log B	λ_1	λ_2	log B
4254.35	3.63!	4.73	2.58!	4.08	4.62	2.28	4.00	4.64	2.49
0.000	3.75	4.78	2.54	4.02	4.62	2.31	—	—	—
4274.81	4.26	5.22	2.55	4.55	5.16	2.32	4.29	5.11	2.51
0.000	4.48	5.26	2.47	4.49	5.09	2.32	—	—	—
4289.73	9.47	0.07	2.50	9.52	0.00	2.21	9.47	9.99	2.44
0.000	9.52	9.94	2.32	9.52	9.99	2.23	—	—	—
4381.12	0.93	1.30	1.60	1.09	1.79	1.79	0.99	1.51	1.97
2.697	0.94	1.47	1.83	0.90	1.93	1.93	—	—	—
4500.29	0.06	0.77	2.12	0.15	0.58	1.66	9.81	0.78	2.15
3.061	9.92	0.82	2.27	0.05	0.82	1.76	9.88	0.80	2.10
4511.90	1.33	2.29	2.20	1.53	2.35	1.93	1.40	2.37	2.15
3.074	1.34	2.25	2.18	1.71	2.39	1.79	1.57	2.34	2.11
4545.96	5.64	6.32	2.20	5.59	6.22	1.97	5.66	6.37	2.05
0.937	5.53	6.38	2.18	5.53	6.49	2.03	5.68	6.32	2.00
4616.13	5.82	6.47	2.36	5.77	6.40	2.10	5.58	6.91	2.38
0.979	5.88	7.30	2.56	5.87	6.49	1.91	5.54	7.02	2.46
4626.18	5.55	7.00	2.40	5.50	6.40	2.05	5.51	6.92	2.37
0.964	5.55	6.99	2.35	5.76	6.56	1.91	5.62	7.18	2.41
4646.17	5.44	6.89	2.58	5.84	6.67	2.17	5.76	6.93	2.51
1.026	5.48	7.00	2.50	5.54	6.63	2.15	5.83	7.07	2.51
4651.29	0.76	1.77	2.30	0.84	1.73	1.93	0.47	1.90	2.31
0.979	0.85	1.82	2.26	0.93	1.70	1.93	0.87	1.80	2.28
4652.17	1.77	2.65	2.35	1.73	2.87	2.18	1.79	2.77	2.21
0.999	1.82	2.82	2.27	1.70	2.90	2.14	1.80	2.79	2.24
4718.42	8.05	8.97	2.21	7.96	8.59	1.91	8.05	9.32	2.24
3.181	8.00	8.98	2.15	7.78	9.03	2.13	8.02	9.14	2.15
4724.41	3.98	5.46!	2.26!	4.08	5.15	1.96	3.97	5.26!	2.40!
3.074	3.76!	5.46	2.23!	3.79!	5.33	1.96!	3.92	5.70!	2.30!
4942.49	1.48	3.10	2.31	1.95	3.13	2.19	1.83	3.09	2.21
0.937	1.42!	3.41	2.46!	—	—	—	—	—	—

Table 21f. Lines of *Cr*$^+$.

4554.99	4.57	5.28	2.33	4.49	5.44	2.07	4.66	5.29	2.01
4.054	4.56	5.43	2.37	4.68	5.34	1.96	4.71	5.58	2.18

Table 21*f*. (continued).

λ Exc. Pot.	δ Cephei 10607 10617 λ_1	λ_2	log B	ϑ Cygni 10616 10619 λ_1	λ_2	log B	π Cephei 10610 10618 λ_1	λ_2	log B
4558.65	7.90	9.27	2.70	8.06	8.98	2.34	7.67	9.33	2.43
4.056	7.98	9.13	2.62	8.14	9.03	2.25	7.83	9.49	2.35
4588.21	7.57	8.73	2.63	7.48!	8.65	2.26!	7.45!	8.86	2.38!
4.054	7.60	8.86	2.60	7.49!	8.79	2.23!	7.56!	8.74	2.26!
4592.06	1.56	2.24	2.39	1.74	2.26	1.96	1.79	3.07	2.50
4.057	1.67	2.44	2.45	1.88	2.25	1.46	1.84	3.17	2.49
4634.08	3.39	4.66	2.58	3.41	4.48	2.21	3.57	4.59	2.34
4.055	3.51	4.75	2.48	3.59	4.51	2.06	3.52	4.43	2.18
4812.36	1.35	3.31	2.53	1.84	3.00!	2.11!	1.75	2.84	2.15
3.848	1.49	2.86	2.37	1.63!	3.02	1.99!	2.18	3.55	2.35

Table 21*g*. Lines of *Ca I*.

4226.74	6.09	7.10	2.72	6.26	7.08	2.59	6.13!	7.00	2.82!
0.000	6.13	7.05	2.63	6.20	6.98	2.59	—	—	—
4283.02	2.75	3.37	2.41	2.76	3.27	2.17	2.70	3.40	2.29
1.878	2.79	3.54	2.37	2.78	3.23	2.17	—	—	—
4289.37	9.16	9.47	2.29	9.14	9.52	2.05	9.18	9.47	2.08
1.871	9.06	9.52	2.28	9.16	9.52	2.07	—	—	—
4425.45	5.02	5.86	2.45	5.15	5.85	2.26	5.05	6.32	2.56
1.871	4.96	5.78	2.40	5.02	5.82	2.15	—	—	—
4435.69	5.37	6.06	2.39	5.40	6.02	2.12	5.43	6.04	2.27
1.878	5.38	5.98	2.32	5.40	6.07	2.10	—	—	—
4455.90	5.45	6.23	2.44	5.59	6.22	2.12	5.64	6.14	2.19
1.891	5.65	6.38	2.36	5.51	6.25	2.11	5.66	6.19	2.10?
4578.56	8.06	9.00	2.36	7.89!	8.98	2.27!	7.86	9.52	2.43
2.510	8.12	9.22!	2.23!	7.98!	9.46!	2.21!!	8.32	9.38	2.33

Table 21*h*. Lines of *Mn I*.

4055.55	5.34	5.84	2.28	5.37	5.73	2.21	—	—	—
2.133	—	—	—	—	—	—	—	—	—
4059.39	9.27	9.60	1.76	9.26	9.52	1.76	—	—	—
3.060	—	—	—	—	—	—	—	—	—
4257.66	7.24	7.79	1.82	7.38	7.86	1.68	7.09	7.82	2.01
2.940	7.45	7.82	1.71	7.34	7.67	1.53?	—	—	—
4265.93	5.54	6.34	2.01	5.59	6.25	1.97	5.63	6.30	2.08
2.928	5.75	6.51!	2.11!	5.65	6.45	1.97	—	—	—

Table 21*h*. (continued).

λ	δ Cephei 10607 10617			ϑ Cygni 10616 10619			π Cephei 10610 10618		
Exc. Pot.	λ_1	λ_2	log B	λ_1	λ_2	log B	λ_1	λ_2	log B
4754.04	3.31	5.11	2.57	3.50	5.08	2.37	3.54	5.32!	2.52!
2.272	2.88!	5.16!	2.54!!	3.19	4.95	2.35	3.02	5.49!	2.56!
4761.53	0.76	1.77	2.16	0.63!	1.87	2.18!	0.61	1.91	2.33
2.940	1.00	1.96	2.10	1.22	1.60	1.61??	0.36	2.16	2.36
4766.42	6.14	7.16	2.47	5.87	7.08	2.32	6.24	7.37	2.42
2.907	5.92	6.46	2.03?	6.09	7.31	2.23	6.14	7.52	2.48
4783.43	2.84	4.44	2.64	2.37	3.92	2.29	2.36	4.65	2.57
2.288	2.53	4.72	2.56	2.02	4.52	2.35	2.50	4.71	2.59
Table 21*i*. Lines of *Ni I*.									
4331.65	1.10	2.14	2.29?	1.38	1.85	1.87?	1.26	2.00	2.19?
1.669	1.28	2.12	2.23?	1.13	1.94	2.13??	—	—	—
4462.46	0.63	2.77	2.31	2.27	2.83	1.80	2.06	2.85	2.45?
3.450	2.30	2.82	1.97	2.31	2.77	1.78	1.78	2.91	2.47?
4606.23	5.90	6.78	2.12	6.03	7.07	2.03	5.87	6.57	2.19
3.582	5.97	7.14	2.23	5.93	6.74	1.79	5.98	6.73	2.18
4648.66	7.90	9.36	2.53	8.29	9.45	2.26	8.51	9.26	2.24
3.405	7.95	9.38	2.51	7.96	9.20	2.24	8.36	9.22	2.24
4686.22	5.75	6.82	2.20	5.79	6.71	2.03	error	error	error
3.582	5.96	6.92	2.15	5.88	6.73	1.83	5.86	6.95	2.19
4715.77	5.23	6.27	2.36	5.30	6.15	2.08	5.28	6.28	2.22
3.528	5.16	6.57	2.34	5.09	6.47	2.12	5.63	6.18	1.94
4807.00	6.20	7.47	2.38	6.45	7.20	2.03	6.87	8.45	2.50
3.663	6.52	7.58	2.24	6.15	7.41	2.05	6.59	7.98	2.36
4831.18	0.47	1.74	2.33	0.13!	2.17!	2.36!!	0.73	2.16	2.39?
3.590	0.17	1.96	2.34	9.98!	2.12!	2.29!!	0.34	1.97	2.44
Table 21*j*. Lines of other neutral atoms.									
Co I 4068.54	8.44	8.76	1.72	8.26!	8.75	1.75!	—	—	—
1.947	—	—	—	—	—	—	—	—	—
4110.54	0.32	0.80	2.21	0.30	0.62	1.89?	—	—	—
1.044	—	—	—	0.33	0.72	1.93?	—	—	—
4121.33	1.08	1.57	2.25	1.07	1.48	2.06	—	—	—
0.919	—	—	—	1.06	1.51	2.06	—	—	—
V I 4111.79	1.62	2.13	2.18	1.65	2.03	1.94?	—	—	—
0.299	—	—	—	1.55	2.07	1.99??	—	—	—

Table 21*j*. (continued).

	λ Exc. Pot.	δ Cephei 10607 10617 λ_1	λ_2	log *B*	ϑ Cygni 10616 10619 λ_1	λ_2	log *B*	π Cephei 10610 10618 λ_1	λ_2	log *B*
V I	4379.24	8.76	9.48	2.24	8.53	9.45	2.06	8.78	9.62	2.30
	0.299	8.54	9.59	2.11	8.93	9.58	1.95	—	—	—
	4406.65	6.11	6.90	2.05	6.51	7.17	1.78	6.30	7.01	2.29
	0.299	6.16	6.87	2.09	6.10	7.10!	1.79!	—	—	—
Mg I	4571.10	0.58	1.37	2.32	0.42	1.39	2.09	0.65	1.54	2.35
	0.000	0.16	1.37	2.27	0.48	1.39	1.85	0.54	1.42	2.35
Zn I	4722.16	1.74	2.75	2.32	1.71	2.71	1.86	1.73	2.93	2.30
	4.012	1.47	2.76	2.18	1.57	2.61	2.03	1.85	2.62	2.00
	4810.54	9.62	1.35	2.50	9.98	1.51	2.27	9.89	1.75	2.43
	4.060	9.90	1.37	2.33	9.73	1.19	2.16	9.89	1.25	2.32

Table 21*k*. Lines of Sc^+.

4246.84	6.32	7.12	2.56	6.49	7.07	2.34	6.44	7.08	2.34
0.314	6.46	7.16	2.52	6.64	7.08	2.28	—	—	—
4354.62	3.96	4.81	2.48	4.08	4.62	2.08?	4.18	4.92	2.29
0.603	4.16	4.86	2.43	4.10	4.90	2.18?	—	—	—
4400.40	0.10	0.93	2.57	0.08	0.78	2.18	0.10	0.79	2.37
0.603	0.06	0.88	2.52	0.26	0.77	2.10	—	—	—
4415.56	4.13	5.96	2.86	5.38	5.95	2.08	4.47	6.02	2.74
0.593	5.30	6.00	2.41	5.40	5.84	1.97	—	—	—
4431.37	1.03	1.73	2.19	1.14	1.78	1.88	1.16	1.78	2.02
0.603	0.98	1.74	2.26	1.13	1.74	1.72	—	—	—
4670.42	9.80	0.93	2.65	9.64	1.16	2.28	9.89	0.94	2.33
1.351	9.80	1.13	2.62	9.76	0.92	2.22	0.14	1.28	2.31

Table 21*l*. Lines of other ions.

Zr^+ 4050.33	0.04	0.62	2.34	0.24	0.53	1.87	—	—	—
0.710	—	—	—	—	—	—	—	—	—
4208.99	8.73	9.26	2.27	8.82	9.24	1.86	8.70	9.14	2.11
0.710	8.68	9.40	2.40	8.77	9.25	2.00	—	—	—
Sr^+ 4077.73	7.16	8.20	2.80?	7.39	8.02	2.46	—	—	—
0.000	—	—	—	—	—	—	—	—	—
La^+ 4086.72	6.40	6.99	2.34	6.49	6.77	1.84	—	—	—
0.000	—	—	—	—	—	—	—	—	—
4123.24	2.99	3.52	2.28	3.01	3.41	1.88	—	—	—
0.320	—	—	—	3.06	3.50	1.94	—	—	—

Table 21*l*. (continued).

	λ	δ Cephei 10607 10617			ϑ Cygni 10616 10619			π Cephei 10610 10618		
	Exc. Pot.	λ_1	λ_2	log B	λ_1	λ_2	log B	λ_1	λ_2	log B
Ia+	4322.51	2.23	2.76	1.94	2.05	2.75	1.67	2.33	2.75	1.53
	0.172	2.10	2.88	2.14	2.18	2.73	1.88	—	—	—
	4333.76	3.40	4.44	2.50?	3.49	4.33	1.90?	3.47	4.42	2.32
	0.172	3.41	4.56	2.41?	3.45	4.58	2.25?	—	—	—
Cc+	4486.91	6.45	7.37	2.21	6.88	7.34	1.48?	6.39	7.40!	2.16!?
	0.89	6.16!	7.77!	2.32!!	6.84	7.52	1.82?	6.53	7.63!	2.19!
	4562.37	1.84	2.92	2.32	1.88	2.91	2.09	2.01	2.90	1.98
	;.000	2.04	3.00	2.25	1.76	2.78	1.86	2.05	3.06	2.16
	4628.16	7.58	8.46	2.30	8.00	8.92	1.54	7.99	8.76	1.86
	0.04	7.67	8.80	2.15	7.79	8.70!	1.68!	8.08	8.97	2.03?
	4773.97	3.53	4.53	2.05	3.48	4.92	2.15	3.47	4.23	1.90
	0.44	3.56	4.77	2.05	3.48	5.00	1.89	3.50	4.57!	2.13!
Ba+	4554.04	3.38	4.57	2.72	3.66	4.49	2.37	3.72	4.66	2.53
	0.000	3.24	4.56	2.65	3.49	4.43	2.36	3.73	4.71	2.51
Y+	4883.69	2.73	4.32	2.54	2.35	4.29	2.32	3.24	4.39	2.20
	1.079	2.80	4.30	2.48	2.75	4.43	2.27	2.66	4.44	2.38

Accuracy of measured equivalent widths.

The measured equivalent widths are not all of the same accuracy. The lines are situated very differently in the spectrum ; some are distinctly separated from their neighbours, whereas in other cases adjacent lines merge almost completely into one. When measures of equivalent widths are made, not all of them can be used with the same weight. It is difficult, however, to estimate the weights of the lines individually and so we will use a more statistical method.

The accurary of a measurement will chiefly depend on two circumstances : 1. the intensity of the line and 2. its more or less distinct separation from its neighbours. Both factors, however, are interrelated. Strong lines will generally be clearly distinguishable among the surrounding weaker absorptions, and even when their limits are not quite sharp, we cannot expect great errors from this source. On the other hand, the weak lines are influenced in a much greater degree by the indefiniteness of their limits. Part of the consequences of this effect will be eliminated in the discussion, as we take into account the cutting of the blend. So in determining the mean error of a measurement of equivalent width, we must eliminate the influence of cutting.

So it seems, as if the most important parameter determining the accuracy of the measure will be the intensity of the line. Only in a few special cases, as e.g. in the case of two very close and strong lines, it will be necessary to assume a somewhat smaller accuracy.

In order to determine the accuracy of the measures, lines were taken which were almost exactly cut in the same way in the two spectra of ϑ Cygni or of π Cephei, so that we might assume that the cutting error was eliminated. From the differences between the results of the two spectra of each star — taken 10616 — 10619 and 10610 — 10618 — we obtained their

mean error. In Table 22 the first column gives the range of equivalent width for each intensity group. The next columns contain 1) the square of the average systematic difference between two corresponding results, 2) the average square accidental difference and 3) the number of lines used.

Table 22. Average square difference between corresponding measures of equivalent widths.

Table 22*a*. ϑ Cygni.

B in *mA*	4113—4200	4200—4323	4355—4600	4600—4840	4883—4937
0— 39.5	+ 7 166 35	0 149 38	++ 44 203 46	2 515 18	++ 350 250 3
40— 59.5	1 339 23	++ 50 398 24	0 526 45	++ 92 783 31	— — —
60— 79.5	3 482 18	14 582 23	++ 289 669 34	++ 299 584 32	++ 2530 3746 6
80— 99.5	10 351 9	0 401 17	++ 335 457 25	++ 467 1008 24	++ 256 377 6
100—149.5	— — 56 239 24	3 289 34	++ 30 490 38	++ 320 793 39	++ 812 1737 10
150—199.5	— — 35 168 16	8 307 16	++ 149 455 26	++ 970 1131 24	++ 1170 1983 6
200—299.5	41 375 9	23 536 15	++ 196 716 25	++ 894 1337 8	++ 2144 1854 6
300—	— — —	— 692 1044 3	+ 169 259 3	+ 484 882 2	+ 8281 — 1

Table 22*b*. π Cephei

B in *mA*	4456—4600	4600—4850	4872—4900
0— 39.5	++ 77 148 5	100 965 7	— — —
40— 59.5	10 1117 6	— — 488 374 7	++ 625 2 2
60— 79.5	48 620 9	35 523 12	— — —
80— 99.5	94 962 7	— — 306 665 11	— — —
100—149.5	+ 36 509 24	— 106 1858 18	25 2888 2
150—199.5	++ 790 1891 19	12 1792 25	— — 3969 307 3
200—299.5	++ 1656 827 31	+ 114 2759 33	— 10000 — 1
300—	++ 1289 3369 8	25 1232 14	++ 807 1304 5

In general, the systematic difference will probably be real, when the figure in 1) exceeds the quotient of the values of 2) and 3). In such cases only the first figure is preceded by a + or —, indicating the sign of the difference; if it exceeds twice the quotient, so that there is a stronger indication of the reality of the systematic differences, it is preceded by + + resp. — —. They might be attributed to differences in the adopted background.

As to the accidental errors, we see that in the violet part of the spectrum of ϑ Cygni the average square first increases with increasing equivalent width, then, at about 80 mA, begins to decrease, and at about 200 mA begins to increase again. Since a regular increase with equivalent width would be a quite normal phenomenon, we divide (for ϑ Cygni) the average square accidental difference by the average equivalent width of the group; then, as indicated by the following table, the quotient shows a sudden decrease at a certain value (about 100) of the equivalent width.

B	0—40	40—60	60—80	80—100	100—150	150—200	200—300	300—∞
4113—4200	5.9	6.9	7.2	3.9	1.9	1.0	1.6	—
4200—4323	5.3	8.7	8.4	4.5	2.3	1.8	2.3	2.8
4355—4600	7.2	11.0	9.6	5.1	4.1	2.7	3.0	0.7
4600—4840	16.6	16.0	8.5	11.6	6.6	6.4	5.9	2.8
4883—4937	7.8	—	54.3	3.9	14.6	11.5	7.7	—

It seems probable, that the sudden decrease in the relative error is a consequence of the cutting effect. A slightly different cutting means the inclusion or exclusion of some very weak lines and consequently a slight change in the equivalent width. It seems, as if for lines of a definite strength the cutting becomes suddenly more regular. For lines in the violet region of the spectrum, this occurs at a strength between 80 and 200 mA.

In the long wave-length region the width of the instrumental profile is larger; if we denote the scale factor by s, the surface of lines with similar profile will be in the ratio $1/s^2$. In order to obtain the equivalent width, we must divide the surface measured in square millimeters by the dispersion d, which is less at greater wave-lengths than in the violet region. So the equivalent widths of similar profiles will be in the ratio $1 : s^2/d$. For the different wave-length regions, this ratio becomes subsequently : 1.0, 1.2, 2.0, 3.3, 5.5; so with an equivalent width of 80 mA correspond values of 80, 96, 160, 264 and 440 mA. We see that the effect is present here indeed for the larger values.

We may try to make the computed average square differences for the different wave-length regions comparable, by dividing each equivalent width by a factor s^2/d and the square differences by the square of this factor, *i.e.* by 1.0, 1.4, 4.0, 11, and 30. Table 23 gives in the second column the reduced square accidental *error* of *one* measure (half the square accidental difference of Table 22). The first colomn gives the reduced equivalent width, the third column gives the weight of the determination.

Table 23. Reduced average square accidental errors of one measure.

Table 23*a*. ϑ Cygni.

4113—4200			4200—4323			4355—4600			4600—4840			4883—4937		
28	83	34	23	52	37	19	45	89	19	33	101	20	30	26
49	170	22	38	138	23	39	73	57	43	42	61	44	31	5
67	241	17	58	202	22	60	61	37	69	61	7			
89	176	8	74	139	16	86	57	25	96	40	1			
124	120	23	103	100	33	118	90	24						
171	84	15	145	107	15	184	32	2						
237	188	8	193	186	14									
			309	362	2									

Table 23*b*. π Cephei.

4456—4600			4600—4850			4872—4900		
18	86	9	19	28	33	20	12	5
38	96	14	45	83	41	63	22	4
62	64	23	75	127	32			
86	236	18	108	57	13			
122	103	30						
182	421	7						

In order to get a practicable system for determining weights, we divide the spectrum of ϑ Cygni into two parts, separated by $H\gamma$. We then combine the values for the average square error in each part of the spectrum. Thus we obtain the following system :

Table 24. Determination of weight factors.

ϑ Cygni 4113—4323			ϑ Cygni 4355—4937			π Cephei 4456—4900		
25	67	0.14	19	38	0.14	19	37	0.14
43	154	.13	41	56	.08	38	82	.10
62	219	.10	61	61	.06	69	101	.06
79	151	.07	86	56	.04	95	169	.06
113	108	.04	123	85	.03	131	163	.04
158	96	.03						
217	202	.03						

1st col. Average equivalent width (reduced). 2d col. Average square error of one determination. 3d col. Average error in log B (= 0.43/B times square root of preceeding number).

In using these values, we must bear in mind, that the equivalent widths in the wave lenght region above 4340 have been reduced by an average factor of about 3. From table 24 we may directly deduce the weights of the different measures. The following system of weights was adopted:

Table 25. Adopted system of weights.

log B		Adopted Weight	Average Error
4000—4340	4340—5000		
< 1.60	< 1.70	1	.0.14
1.60—1.89	1.70—1.99	2	.13
1.90—1.99	2.00—2.19	3	.08
2.00—2.09	2.20—2.39	4	.05
2.10—2.19	2.40—2.59	5	.04
2.20—2.29	2.60—2.69	6	.03
$\geqq 2.30$	$\geqq 2.70$	7	.03

The adopted weights do not correspond exactly to the calculated errors, because in the original calculation the values have been combined in a somewhat different manner. However, the differences are not at all important in practice. Measures of weight 1 only rarely occur in our calculations. It is seen, that weight 1 corresponds approximately to a mean error 0.20 in log B. In the cases of doubtful measures (denoted by notes of interrogation) the weight has been multiplied by a factor $^2/_3$.

It is interesting, to compare these results with those obtained by C. W. ALLEN for the solar spectrum [1]). For the average of 4 measures ALLEN estimates the probable error as 8 %. The quadratic mean error in the logarithm of one measure is then equal to $0.86/0.67 \times 0.08 = 0.10$. So our measures can fully compete with those obtained by ALLEN for the solar spectrum with a 20 times greater dispersion. It is clear, that this unexpected result will be cihefly due to ALLEN's method of measuring central intensities only.

Derivation of theoretical equivalent widths.

In Chapter II, we have outlined the method for the calculation of theoretical equivalent widths. We now will illustrate it by the example of the line λ 4128.74 of Fe^+ in the spectrum

[1]) Memoir No. 5, part. 1, p. 18.

of δ Cephei 10607. We first give the entire calculation in the short form in which it has been made and then illustrate it by some remarks.

λ **4128.74** Fe^+; **8.47 — 9.02**; n = **22** *mA*.

λ	Identif.	$A_\odot$	*E.P.*	D D_s d_s	d	c_2 c_1	k j	kD jD	kD_s jd_s	id. × *E.P.*
4128.10	*V* —	84	0.27	178 64 15	6.5	42 17	—.05 —.02	—9 — 4	—3 0	—1 0
.74	Fe^+	41	2.57	264 60 25	7.5	13 —12	1.20 —.06	317 —16	72 —2	185 —4
9.19	*Ce—Cr Fe*	62	3.15	109 56 5	6.0	—7.7 —33	—.10 + .17	—11 +19	—6 +1	—18 +3
								297 — 1	63 —1	166 —1

B = 297. ∂_b = 296. ∂_s = 62. ∂_x = 70. ∂_Θ = — 165.
1.00. 0.21. 0.24. — 0.56.

Col. 1 and 2 need no explanation. Col. 3 gives the equivalent width as measured by ALLEN. Col. 4 gives the excitation potential. Col. 5 gives the values of D, $D\frac{\partial \ln D}{\partial \ln s}$ and $D\frac{\partial \ln d}{\partial \ln s}$, which have been taken from Table 19*a*. Col. 6 gives the value of d, also taken from Table 19*a*, but expressed in normal distances. For the line of Fe^+ e.g., we have d = 164 mA = 7.5 n. Col. 7 gives the distance of the line centre from the cutting point, also expressed in normal distances. For the line of Fe^+ the distance c_2 is equal to 9.02—8.74 = 0.28 A, corresponding with 13 n. Col. 8 then gives the values of k and j, from Tables 17 and 18. If again we take the line of F^+, we find that for d = 7.5. and for c_2 = 13 k = 0.60; for c_1 = — 12 we have k = — 0.60; the difference of both values is equal to 1.20. In a similar manner we calculated j. Col. 9 and 10 need no explanation, col. 11 contains the values of col. 10 multiplied by the exictation potential.

From eqs. (15) it follows that the equivalent width of the blend will be found by the summation of kD. The differential correction with respect to b we get, if we add jD and divide by D. The calculation of the differential corrections with respect to s and to Θ will be clear without further comment. The correction with respect to the ionization follows, when we take into account the lines of ionized atoms only.

In the example given here, it was not necessary to include the calculation of resonance wings. In practice, these wings were of importance only in a few of the very strongest lines. And even there, they were generally of little importance, as we must include in the calculation only those parts of the wings, which are situated within the cutting limits of the blend. This calculation afforded no arithmetical difficulty.

It appears that the arithmetical part of the computation is quite simple and can be made in a relatively short time. But much more difficult is the physical part. At first, there is the question which lines should be included. In this respect we put a general limit, including all lines, which would give a positive or negative contribution to the equivalent width of 5 mA or more. In many cases this criterion made the inclusion of very weak solar lines necessary, when these were situated favourably. The most common number of components to be treated was from 4 to 6, but in some cases it was as large as 9 or even larger, whereas, in other cases we could limit ourselves to 2 or even to the chief component alone.

A serious difficulty concerns the identification of the lines and their expected intensities. When the computations were made, the Revised Multiplet Table by CHARLOTTE E. MOORE[1]) was not yet at our disposal. In many cases the origin of a solar line or of an unknown contributor could

[1]) Contributions from the Princeton Observatory No. 20 (1945).

not even be guessed. In the case of the example given above, Miss MOORE gives many lines in the neighbourhood of the blend, which have not been included in our identifications, *viz.*: 4128.07 Ce^+, 8.14 Mn^+, 8.87 Mn^+, whereas the line 9.19 is partly due to Ce^+. Though in view of the great strength of ion lines in the spectrum of δ Cephei, it seems that the influence of some of these lines might be important, it is, of course, impossible to state something definite about their intensities without a thorough investigation of the different multiplets to which they belong. In many other cases the excitation potential of part of the lines were unknown, or the lines had not been measured by ALLEN. Then we had to make use of the intensities and the temperature classification as listed in the Revised Rowland Table.

In order to hold the uncertainties from these sources within reasonable limits, all results were rejected, where the contributions of the secondary lines to the intensity of a blend was larger than 0.10 in the logarithm. Nevertheless, there certainly will be cases, where the influence of an unknown contributor (chiefly when it is an ion line) makes the result of the calculation highly uncertain.

It was not deemed advisable to repeat the computations after the receipt of the Revised Multiplet Table. Many solar lines are due to a great number of minor contributors, among which are neutral atoms and ions, and it is impossible to predict the intensity of such a line in the spectrum of δ Cephei if the contributions from these different sources are not disentangled. Mereover we had at our disposal only two plates of the spectrum of δ Cephei, by far too few to be of real value for the determination of the variations in the spectrum. And then it was shown above that the difficulties in the determination of the transmission curve, with the ensuing uncertainties in the line profiles and the instrumental curve, already at the start deprived us from the possibility of getting accurate results. So at present we must be content, if we succeed in showing the applicability and the potential accuracy of a method, which then may be employed to a more extended material, which has been obtained with all necessary precautions.

The results of the computations are given in Table 26. The lines were taken from Table 21*a* and 21*b*, with omission of such lines where the corrections from the minor contributors were larger than 0.10 in the logarithm, or where, in a few cases, the excitation potential was not given in the tables which were at our disposal at that time.

Since for the determination of the curve of growth we intended, for the sake of simplicity, to use lines of one element only, the table includes only lines of *Fe I* and Fe^+. The inclusion of other elements, however, would not have been in conflict with the principles of our method.

The different columns in Table 26 have the following meanings : Col. 1. Wave length. Col. 2. Indication of spectrum. *Ia*, *Ib* = δ Cephei 10607, 10617; *IIa*, *IIb* = ϑ Cygni 10616, 10619; *IIIa*, *IIIb* = π Cephei 10610, 10618. Col. 3. log of equivalent width of chief component; Col. 4. Part of this line between the cutting distances; Col. 5. Calculated equivalent width for the entire blend. Col. 6, 7, 8, 9, 10, differential corrections with respect to log b, log a, log ε_0/k, log $x/(1-x)$, and Θ; Col. 11 differential correction with respect to the background, calculated by eq. 18; Col. 12 difference log B (measured, Table 21) — log B (calculated); Col. 13 adopted weight.

Table 26. Calculated equivalent widths.

Table 26*a*. Chief component = *Fe I*.

λ	Sp.	log A	log B *Fe*	log B blend	∂_b	∂_a	∂_s	∂_x	∂_Θ	∂_h	Δ log B $m-c$	w
4062.45	I*a*	2.40	2.47	2.55	0.97	0.02	0.32	+ 0.09	— 0.66	1.3	— 0.15	7
	II*a*	2.11	2.22	2.27	0.97	—	.22	+ .03	— 0.55	1.1	— .01	6
4065.39	I*a*	2.15	2.07	2.08	0.81	0.01	0.46	—	— 1.53	2.8	— 0.14?	2
	II*a*	1.91	2.02	2.05	1.02	—	.39	—	— 1.33	2.9	— .03	4
4070.78	II*a*	2.08	2.20	2.19	0.94	—	0.22	+ 0.01	— 0.66	1.4	— 0.04	5
4072.51	I*a*	2.13	2.21	2.24	0.94	0.04	0.48	—	— 1.57	2.1	— 0.03	6
	II*a*	1.90	1.96	2.00	1.00	—	.41	—	— 1.34	4.1	+ .05	4
4079.85	I*a*	2.28	2.36	2.36	1.58	0.01	0.41	+ 0.03	— 1.11	1.8	— 0.09	6
	II*a*	2.01	2.13	2.05	0.87	—	.28	+ .01	— 0.83	1.4	+ .07	5
4084.50	I*a*	2.40	2.45	2.42	1.11	—	0.28	—	— 0.92	2.2	— 0.08	7
	II*a*	2.10	2.22	2.24	0.93	—	.22	—	— 0.72	1.5	— .08	5
4089.23	I*a*	2.01	2.05	2.13	1.21	—	0.56	+ 0.04	— 1.28	3.4	+ 0.07	6
	II*a*	1.80	1.92	1.92	0.99	—	.45	—	— 1.31	3.5	+ .02	3
4091.56	I*a*	1.97	2.05	1.98	1.00	—	0.59	— 0.03	— 1.75	5.0	+ 0.03	4
	II*a*	1.78	1.83	1.79	0.90	—	.46	—	— 1.36	3.6	+ .41?	4
4109.06	I*a*	2.12	2.18	2.25	1.24	—	0.49	+ 0.06	— 1.40	1.8	— 0.06?	3
	II*a*	1.89	2.01	2.03	0.95	—	.42	— .04	— 1.47	3.2	— .08?	2
	II*b*	1.89	1.97	2.00	1.04	—	.43	— .05	— 1.53	2.6	+ .14?	3
4112.32	I*a*	1.97	2.05	2.00	0.62	—	0.61	—	— 2.09	3.2	— 0.10	3
	II*a*	1.76	1.85	1.76	0.98	—	.52	—	— 1.91	4.9	+ .15?	2
	II*b*	1.76	1.87	1.81	0.97	—	.50	—	— 1.78	4.1	+ .12?	2
4114.45	I*a*	2.31	2.37	2.36	1.11	—	0.33	—	— 0.94	2.1	— 0.06	7
	II*a*	2.04	2.08	2.03	1.03	—	.25	—	— 0.70	3.5	+ .14	5
	II*b*	2.04	2.09	2.05	1.04	—	.31	—	— 0.88	3.0	+ .14	5
4126.19	I*a*	2.31	2.38	2.38	0.87	—	0.30	—	— 0.98	1.7	— 0.23	5
	I*b*	2.26	2.36	2.37	0.95	—	.31	—	— 1.09	2.1	— .26	5
	II*a*	2.04	2.13	2.10	0.98	—	.25	—	— 0.85	3.0	— .08	4
	II*b*	2.04	2.15	2.09	0.90	—	.37	—	— 1.22	2.8	— .19	3
4130.05	II*a*	1.72	1.85	1.88	0.89	—	0.59	— 0.04	— 1.17	6.7	— 0.20	2
	II*b*	1.72	1.79	1.76	1.07	—	.67	— .10	— 1.26	6.7	+ .13	2
4132.91	II*a*	2.09	2.17	2.18	1.01	—	0.23	—	— 0.31	1.7	— 0.15	4
	II*b*	2.09	2.21	2.21	0.91	—	.22	—	— 0.31	2.0	— .16	4
4134.69	I*a*	2.47	2.43	2.39	0.89	—	0.19	— 0.01	— 0.58	1.5	— 0.17	6
	II*a*	2.17	2.27	2.28	0.98	—	.21	—	— 0.63	2.0	— .12	5
	II*b*	2.17	2.25	2.30	1.02	—	.22	—	— 0.68	2.3	— .10	6

Table 26*a*. (continued).

λ	Sp.	log A	log B Fe	log B blend	∂_b	∂_a	∂_s	∂_x	∂_Θ	∂_h	Δ log B $m-c$	w
4136.53	I*a*	2.10	2.18	2.10	1.09	—	0.33	—	— 1.83	4.0	— 0.08	4
	I*b*	2.06	2.16	2.10	1.02	—	.54	—	— 1.84	4.2	— .01	4
	II*a*	1.87	1.99	1.99	0.95	—	.38	—	— 1.28	3.9	— .13	2
	II*b*	1.87	1.97	1.87	1.00	—	.42	—	— 1.47	5.9	— .03	2
4139.94	I*a*	2.21	2.26	2.232	0.93	—	0.42	+ 0.09	— 0.24	4.4	— 0.20	5
	I*b*	2.16	2.22	2.29	0.95	—	.45	.09	— 0.25	3.8	— .12	5
	II*a*	1.95	2.03	2.03	0.96	—	.32	—	— 0.32	5.5	— .14	2
	II*b*	1.95	2.03	2.04	0.99	—	.35	+ .06	— 0.19	6.7	— .13	3
4140.41	II*a*	1.72	1.84	1.83	0.96	—	0.58	+ 0.04	— 1.69	4.3	0.00	2
	II*b*	1.72	1.82	1.82	0.95	—	.61	+ .06	— 1.65	4.3	— .04	2
4143.88	I*a*	2.64	2.67	2.68	1.03	—	0.18	— 0.02	— 0.41	1.1	— 0.18	7
	I*b*	2.59	2.63	2.65	0.82	—	.17	—	— 0.34	1.1	— .24?	5
	II*a*	2.36	2.36	2.39	0.87	0.04	.18	— .01	— 0.39	1.4	— .07?	5
	II*b*	2.36	2.38	2.38	0.89	.06	.18	— .01	— .36	2.0	— .01	7
4145.20	II*b*	1.36	1.32	1.26	1.00	—	0.72	— 0.11	— 2.22	7.7	+ 0.32	1
4147.68	I*b*	2.37	2.44	2.49	1.02	—	0.29	—	— 0.54	1.8	— 0.15	7
	II*b*	2.12	2.22	2.24	0.99	—	.22	—	— 0.38	2.7	— 0.13	5
4150.26	I*b*	2.16	2.20	2.29	0.96	—	0.47	—	— 1.18	2.8	— 0.18	5
4154.51	II*a*	2.14	2.15	2.19	0.98	—	0.27	+ 0.17	— 0.29	2.2	— 0.13	4
	II*b*	2.14	2.26	2.23	1.02	—	.20	+ .05	— 0.45	1.6	— .08	5
4154.82	I*a*	2.43	2.52	2.48	1.11	—	0.22	— 0.02	— 0.81	1.3	— 0.13	7
	I*b*	2.39	2.45	2.49	1.08	—	.27	+ .05	— 0.72	1.6	— .18	7
	II*a*	2.14	2.26	2.26	1.04	—	.18	— .01	— 0.62	1.9	— .15	5
	II*b*	2.14	2.24	2.18	0.96	—	.18	—	— 0.61	2.7	— .09	4
4157.79	I*a*	2.43	2.48	2.50	0.98	—	0.25	—	— 0.82	1.8	— 0.10	7
	I*b*	2.39	2.42	2.44	1.03	—	.26	—	— 0.85	2.7	— .09	7
	II*a*	2.14	2.22	2.23	1.00	—	.20	—	— 0.61	2.8	— .07	5
	II*b*	2.14	2.24	2.24	0.98	—	.18	—	— 0.63	2.3	— .08	5
4158.80	I*a*	2.31	2.34	2.30	0.84	—	0.30	—	— 1.04	1.7	— 0.06	6
	I*b*	2.26	2.35	2.31	0.86	—	.30	—	— 1.06	2.1	— .19	5
	II*a*	2.04	2.14	2.11	1.05	—	.27	—	— 0.91	3.4	— .05	4
	II*b*	2.04	2.12	2.07	1.06	—	.26	—	— 0.92	3.2	+ .04	5
4168.62	I*a*	1.81	1.89	1.83	0.91	—	0.66	—	— 2.38	3.0	+ 0.10	3
	I*b*	1.76	1.88	1.91	1.05	—	.65	—	— 2.06	2.7	+ .12	4
	II*a*	1.63	1.73	1.69	1.06	—	.57	—	— 1.98	5.9	+ .17	2
	II*b*	1.63	1.75	1.68	1.04	—	.56	—	— 2.04	6.6	+ .09	2
4174.92	I*a*	2.37	2.43	2.53	1.00	—	0.39	—	— 0.62	2.3	— 0.21	7

Table 26*a*. (continued).

λ	Sp.	log A	log B Fe	log B blend	∂_b	∂_a	∂_s	∂_x	∂_θ	∂_h	Δ log B $m - c$	w
4175.64	I*a*	2.42	2.45	2.49	1.04	—	0.30	—	— 0.96	2.1	— 0.04	7
	I*b*	2.37	2.41	2.45	1.04	—	.31	—	— 0.93	2.4	— .04	7
	II*a*	2.13	2.18	2.23	1.00	—	.24	—	— 0.74	2.9	— .05	5
	II*b*	2.13	2.20	2.26	1.00	—	.24	—	— 0.74	2.6	— .04	6
4182.39	I*a*	2.26	2.35	2.26	0.98	0.01	0.34	—	— 1.03	2.0	— 0.09	5
	I*b*	2.23	2.30	2.33	0.97	—	.39	—	— 1.11	2.5	— .11	6
	II*b*	2.00	2.13	2.05	0.95	—	.25	—	— 0.77	3.7	— .14	3
	III*a*	2.20	2.27	2.19	0.99	—	.23	—	— 0.69	2.1	— .01	5
4187.05	I*a*	2.57	2.63	2.62	0.93	—	0.17	+ 0.06	— 0.25	0.8	— 0.20	7
	I*b*	2.52	2.58	2.64	1.00	—	.18	+ .09	— 0.25	1.4	— .25	7
	II*a*	2.26	2.35	2.37	1.02	—	.13	+ .04	— 0.24	2.2	— .18	5
4202.04	II*a*	2.33	2.37	2.44	0.95	0.05	0.21	— 0.01	— 0.17	2.6	— 0.07	7
4205.55	I*b*	2.14	2.18	2.18	1.56	—	0.59	— 0.01	— 1.42	2.0	+ 0.25	7
	II*a*	1.93	2.04	2.06	0.99	—	.41	— .07	— 1.01	3.4	.00	4
	II*b*	1.93	2.04	2.05	0.99	—	.41	— .07	— 1.02	3.2	+ .04	4
	III*a*	2.14	2.38	2.45	1.00	—	.27	— .04	— 0.57	1.7	— .18	6
4206.70	II*a*	2.06	2.16	2.25	1.02	—	0.35	+ 0.06	— 0.12	3.8	— 0.19	4
	II*b*	2.06	2.18	2.26	1.01	—	.34	+ .04	— 0.12	3.5	— .21	4
	III*a*	2.25	2.35	2.40	0.89	—	.24	—	— 0.12	1.0	— .14	6
4207.14	I*a*	2.26	2.32	2.27	1.13	—	0.37	—	— 1.11	2.5	+ 0.03	7
	I*b*	2.22	2.27	2.20	0.92	—	.35	—	— 1.11	2.0	+ .16	7
	II*a*	2.00	2.08	2.02	0.95	—	.29	—	— 0.92	3.7	+ .08	5
	II*b*	2.00	2.09	2.01	0.98	—	.29	—	— 0.93	3.9	+ .07	4
4208.61	I*a*	2.28	2.27	2.24	0.89	—	0.42	— 0.03	— 1.41	2.6	+ 0.04	6
	I*b*	2.24	2.17	2.12	0.79	—	.37	— .04	— 1.30	2.8	+ .04	5
	II*a*	2.01	2.12	2.08	1.02	—	.29	— .04	— 1.04	3.4	— .03	4
	II*b*	2.01	2.10	2.07	0.97	—	.31	— .04	— 1.08	3.7	.00	4
	III*a*	2.21	2.24	2.25	0.87	—	.27	— .02	— 0.88	1.8	— .14	5
4216.19	I*a*	2.45	2.53	2.60	1.03	0.01	0.35	+ 0.01	— 0.44	1.5	— 0.17	7
	I*b*	2.41	2.48	2.53	0.99	—	.33	— .02	— 0.39	1.9	— .15	7
	II*a*	2.16	2.25	2.32	0.98	—	.24	—	— 0.29	3.2	— .22	5
	II*b*	2.16	2.24	2.30	1.01	—	.28	— .02	— 0.43	3.8	— .19	5
4222.22	I*a*	2.48	2.53	2.59	1.07	—	0.22	+ 0.05	— 0.42	1.5	— 0.09	7
	I*b*	2.44	2.49	2.59	1.02	—	.23	+ .08	— 0.46	1.5	— .10	7
	II*a*	2.18	2.29	2.28	0.96	—	.14	— .02	— 0.37	1.8	— .06	6
	II*b*	2.18	2.29	2.28	0.98	—	.14	— .01	— 0.37	2.1	— .08	6
	III*a*	2.36	2.45	2.46	0.88	—	.13	—	— 0.32	1.5	— .21	6
4224.18	II*a*	2.10	2.23	2.24	0.98	—	0.25	—	— 0.81	2.3	— 0.14	5
	II*b*	2.10	2.21	2.31	1.01	—	.29	—	— 0.92	2.3	— .10	6
	III*a*	2.29	2.38	2.38	0.91	—	.20	—	— 0.69	1.3	— .19	5

Table 26*a*. (continued).

λ	Sp.	log A	log B Fe	log B blend	∂_b	∂_a	∂_s	∂_x	∂_Θ	∂_h	$\triangle$ log B $m - c$	w
4233.61	I*a*	2.54	2.57	2.51	0.89	0.04	0.16	+ 0.02	— 0.37	1.3	— 0.27	6
	I*b*	2.50	2.57	2.53	1.23	.02	.16	+ .02	— 0.39	1.5	— .19	7
	II*a*	2.25	2.31	2.26	0.94	.01	.12	— .01	— 0.30	2.0	— .06	6
	II*b*	2.25	2.33	2.29	1.03	.02	.15	+ .01	— 0.36	2.1	— .05	6
	III*a*	2.42	2.52	2.48	0.81	.07	.16	— .01	— 0.39	1.3	— .18	7
4235.95	I*a*	2.61	2.65	2.74	1.07	0.01	0.23	0.09	— 0.34	1.2	— 0.13	7
4238.82	I*a*	2.42	2.50	2.54	1.14	—	0.29	+ 0.02	— 0.91	1.6	— 0.13	7
	I*b*	2.38	2.44	2.54	1.07	—	.29	+ .07	— 0.78	1.7	— .09	7
	II*a*	2.13	2.23	2.22	1.01	—	.22	— .02	— 0.82	2.1	+ .03	6
	II*b*	2.13	2.21	2.23	1.02	—	.23	+ .01	— 0.76	2.9	— .03	6
	III*a*	2.31	2.41	2.47	0.95	—	.26	— .02	— 0.90	1.4	— .14?	5
4250.13	I*a*	2.59	2.62	2.66	0.83	0.01	0.20	+ 0.10	— 0.26	1.8	— 0.18	7
	I*b*	2.55	2.61	2.63	1.13	—	.21	.10	— 0.28	1.6	— .19	7
	II*a*	2.30	2.38	2.39	0.93	0.04	.19	.05	— 0.33	1.5	— .07	7
	II*b*	2.30	2.40	2.42	0.90	.03	.19	.06	— 0.30	1.4	— .12	7
	III*a*	2.49	2.53	2.51	1.03	.09	.19	.05	— 0.42	1.3	— .07	7
4264.22	I*b*	2.12	2.21	2.27	0.99	—	0.53	+ 0.05	— 1.33	3.0	— 0.12	5
	II*a*	1.92	2.04	2.08	0.99	—	.40	— .02	— 0.96	4.5	— .10	3
	II*b*	1.92	2.05	2.09	0.99	—	.40	—	— 0.92	5.4	— .21	2
	III*a*	2.13	2.26	2.32	1.00	—	.34	— .01	— 0.84	2.3	— .20	5
4266.97	II*b*	1.98	2.09	2.17	0.99	—	0.48	+ 0.01	— 0.96	4.5	— 0.14	4
4271.17	I*a*	2.59	2.64	2.66	0.86	0.02	0.20	+ 0.04	— 0.41	1.3	— 0.17	7
	I*b*	2.54	2.62	2.62	1.07	.02	.21	+ .01	— 0.49	1.5	— .21	7
	II*a*	2.30	2.38	2.41	0.89	.05	.20	—	— 0.49	1.5	— .17	6
	II*b*	2.30	2.39	2.41	1.00	.08	.26	—	— 0.62	2.0	— .13	6
	III*a*	2.48	2.49	2.55	0.91	.07	.24	—	— 0.45	1.0	— .18	7
4271.78	I*a*	2.72	2.71	2.77	1.12	0.03	0.24	—	— 0.46	1.1	— 0.12	7
	I*b*	2.66	2.70	2.72	0.95	.02	.18	—	— 0.34	1.0	— .17	7
	II*a*	2.48	2.48	2.52	0.91	.13	.29	—	— 0.53	1.6	— .10	7
	II*b*	2.48	2.48	2.52	0.91	.14	.29	—	— 0.51	1.8	— .11	7
4282.41	I*a*	2.48	2.57	2.58	1.06	—	0.28	+ 0.03	— 0.55	1.1	— 0.04	7
	I*b*	2.44	2.50	2.51	1.14	—	.28	.03	— 0.53	1.8	— .06	7
	II*a*	2.19	2.29	2.30	0.96	—	.21	.01	— 0.41	2.3	— .10	6
	II*b*	2.19	2.28	2.28	0.99	—	.19	.02	— 0.35	2.8	— .10	5
	III*a*	2.36	2.47	2.47	0.96	0.02	.18	.01	— 0.36	1.5	— .11	7
4348.95	III*a*	2.00	2.10	2.12	0.98	—	0.43	— 0.05	— 1.31	3.7	— 0.07	3
4365.91	III*a*	1.86	1.99	2.06	0.94	—	0.54	— 0.03	— 1.63	6.5	— 0.28	2
4375.95	I*a*	2.47	2.55	2.56	0.96	—	0.25	— 0.01	— 0.22	1.9	— 0.09	5
	I*b*	2.44	2.52	2.55	1.00	—	.24	—	— 0.14	2.1	— .18	4
	II*a*	2.17	2.26	2.29	0.98	—	.23	—	— 0.23	3.6	— .06	4
	II*b*	2.17	2.26	2.28	0.96	—	.21	—	— 0.19	3.7	— .12	3

Table 26*a*. (continued).

λ	Sp.	log A	log B Fe	log B blend	∂_b	∂_a	∂_s	∂_x	∂_Θ	∂_h	Δ log B $m - c$	w
4383.56	I*a*	2.80	2.78	2.78	0.86	0.07	0.14	—	— 0.22	1.0	— 0.12	6
	I*b*	2.71	2.75	2.75	0.85	.04	.12	—	— 0.19	1.2	— .20	5
	II*a*	2.59	2.56	2.57	0.85	.20	.28	—	— 0.49	1.6	— .05	5
	II*b*	2.59	2.56	2.57	0.85	.21	.29	—	— 0.49	1.8	— .05	5
	III*a*	2.85	2.72	2.73	0.91	.16	.22	—	— 0.43	0.7	— .08	6
4388.42	I*a*	2.32	2.40	2.38	1.01	—	0.35	—	— 1.18	2.3	— 0.08	4
	I*b*	2.29	2.37	2.36	0.95	—	.36	—	— 1.21	2.5	— .06	4
	II*a*	2.05	2.18	2.18	1.01	—	.31	—	— 0.99	3.7	— .09	3
	II*b*	2.05	2.18	2.21	1.01	—	.33	—	— 1.02	3.5	— .07	3
4389.26	I*a*	2.12	2.22	2.15	1.01	—	0.61	—	— 0.33	4.6	— 0.01	3
	I*b*	2.08	2.20	2.18	0.91	—	.54	—	— 0.27	4.6	— .15	3
	II*a*	1.89	1.99	1.99	0.99	—	.50	—	— 0.56	8.2	— .13	2
	II*b*	1.89	2.01	2.02	0.98	—	.50	—	— 0.48	9.3	— .23	2
	III*a*	2.11	2.20	2.21	0.97	—	.39	—	— 0.48	3.3	— .15	3
4404.76	II*a*	2.48	2.49	2.58	0.89	0.12	0.29	—	— 0.45	1.6	— 0.12	5
4442.35	I*a*	2.52	2.62	2.55	1.08	—	0.17	— 0.02	— 0.40	1.6	— 0.15	5
	I*b*	2.47	2.58	2.51	0.89	—	.14	— .13	— 0.36	1.9	— .19	4
	II*a*	2.22	2.33	2.26	1.01	—	.15	.00	— 0.40	3.9	— .12	3
	II*b*	2.22	2.32	2.29	1.01	—	.17	— .02	— 0.41	4.7	— .15	3
	III*a*	2.39	2.48	2.54	1.03	0.03	.27	— .01	— 0.59	2.3	— .14	5
4447.73	I*a*	2.51	2.59	2.59	1.02	—	0.20	—	— 0.45	2.2	— 0.14	5
	I*b*	2.46	2.51	2.51	1.03	—	.22	—	— 0.52	3.4	— .03	5
	II*a*	2.20	2.30	2.30	1.01	—	.19	—	— 0.46	3.5	— .07	4
	II*b*	2.20	2.31	2.30	0.99	—	.18	—	— 0.43	4.3	— .16	3
	III*a*	2.38	2.47	2.52	1.01	0.03	.23	—	— 0.61	2.3	— .12	5
4484.23	III*a*	2.24	2.26	2.36	0.97	—	0.30	+ 0.02	— 0.80	3.9	— 0.24	3
4490.78	II*a*	2.07	2.00	2.00	1.01	—	0.61	— 0.04	— 1.95	7.8	— 0.11	2
	II*b*	2.07	2.02	2.00	0.98	—	.60	— .04	— 1.95	9.0	— .23	2
4492.69	II*a*	1.40	1.51	1.58	0.97	—	0.74	—	— 2.63	9.5	+ 0.03	1
	II*b*	1.40	1.49	1.46	0.97	—	.79	— 0.07	— 3.07	9.7	+ .17	1
4494.58	III*b*	2.40	2.46	2.56	0.95	0.03	0.26	+ 0.06	— 0.45	2.5	— 0.15	5
4602.01	II*a*	1.93	2.07	2.00	0.99	—	0.33	— 0.03	— 0.49	7.8	— 0.07	2
	II*b*	1.93	2.04	1.99	0.99	—	.36	+ .02	— 0.61	11.8	— .23	2
	III*a*	2.14	2.27	2.23	0.97	—	.32	— .02	— 0.57	6.3	— .19	3
	III*b*	2.14	2.26	2.21	1.00	—	.33	— .02	— 0.58	6.9	— .17	3
4602.95	I*a*	2.41	2.52	2.47	1.01	—	0.22	— 0.03	— 0.33	2.1	+ 0.04	5
	I*b*	2.36	2.44	2.48	1.00	—	.29	+ .06	— 0.28	3.3	— .03	5
	II*a*	2.12	2.22	2.20	1.00	—	.21	—	— 0.26	4.1	+ .08	4
	II*b*	2.12	2.22	2.20	1.01	—	.22	—	— 0.25	5.4	+ .03	4
	III*a*	2.30	2.39	2.38	0.99	—	.21	—	— 0.26	3.5	+ .01	4
	III*b*	2.30	2.37	2.42	0.98	—	.23	—	— 0.29	3.0	— .05	4

Table 26*a*. (continued).

λ	Sp.	log A	log B Fe	log B blend	∂_b	∂_a	∂_s	∂_x	∂_Θ	∂_h	Δ log B $m-c$	w
4625.05	II*a*	2.00	2.13	2.20	0.99	—	0.35	+ 0.12	— 0.77	3.9	+ 0.02	4
	II*b*	2.00	2.13	2.18	0.99	—	.36	+ .12	— 0.80	6.2	— .13	3
4630.13	II*a*	1.86	1.94	1.85	1.06	—	0.51	—	— 1.20	7.0	+ 0.32	3
	II*b*	1.86	1.98	1.89	1.00	—	.49	—	— 1.15	11.6	+ .05	2
	III*a*	2.09	2.15	2.20	0.97	—	.49	—	— 1.26	5.8	— .01	3
	III*b*	2.09	2.14	2.18	0.97	—	.44	—	— 1.10	4.5	— .02	3
4643.47	I*a*	2.17	2.28	2.29	0.99	—	0.46	— 0.02	— 1.57	3.3	+ 0.12	5
	I*b*	2.13	2.22	2.24	1.00	—	.46	—	— 1.54	4.4	+ .10	4
	II*a*	1.93	2.00	2.00	1.00	—	.33	—	— 1.20	6.4	+ .26	4
	II*b*	1.93	2.03	2.03	1.00	—	.33	—	— 1.19	8.4	+ .07	3
	III*a*	2.14	2.20	2.30	1.00	—	.40	— .02	— 1.20	3.6	+ .20	5
4647.44	I*a*	2.34	2.46	2.46	0.97	—	0.36	— 0.03	— 1.08	2.2	+ 0.04	5
	I*b*	2.30	2.42	2.43	0.99	—	.35	— .03	— 1.05	3.2	— .07	4
	II*b*	2.06	2.18	2.22	1.00	—	.36	—	— 1.05	5.8	+ .01	4
4683.57	I*a*	1.83	1.94	1.90	1.05	—	0.73	— 0.06	— 2.32	7.5	+ 0.22	3
	I*b*	1.80	1.83	1.85	0.96	—	.70	— .01	— 2.00	6.8	+ .36	4
	II*a*	1.66	1.79	1.74	1.00	—	.53	— .04	— 1.64	8.7	+ .27	3
	III*a*	1.92	2.04	2.10	0.99	—	.51	— .02	— 1.54	4.6	+ .19	4
	III*b*	1.92	2.01	2.07	1.00	—	.53	— .02	— 1.55	5.8	+ .12	3
4728.55	I*a*	2.24	2.32	2.24	0.99	—	0.40	—	— 1.33	3.1	+ 0.10	4
	I*b*	2.20	2.29	2.32	1.01	—	.46	—	— 1.19	5.6	— .01	4
	II*a*	1.99	2.05	2.10	1.01	—	.45	—	— 1.02	7.2	+ .18	4
	II*b*	1.99	2.10	2.15	0.99	—	.41	—	— 1.04	8.5	— .03	3
	III*a*	2.18	2.31	2.35	0.99	—	.36	—	— 0.87	6.6	— .04	4
4733.60	I*a*	2.26	2.39	2.43	0.97	—	0.37	+ 0.03	— 0.43	2.8	— 0.01	5
	I*b*	2.23	2.34	2.36	0.97	—	.38	— .02	— 0.54	4.4	— .12	4
	II*a*	2.00	2.06	2.16	1.00	—	.42	+ .04	— 0.46	9.4	+ .04	4
	II*b*	2.00	2.10	2.19	1.00	—	.37	+ .07	— 0.35	8.2	.00	3
4741.54	I*a*	2.13	2.24	2.30	1.00	—	0.51	— 0.02	— 1.52	5.6	0.00	4
	I*b*	2.09	2.18	2.22	1.01	—	.54	— .05	— 1.52	6.1	+ .10	4
	II*a*	1.90	2.04	2.07	0.98	—	.38	—	— 1.10	5.5	+ .07	3
	II*b*	1.90	1.93	1.93	1.00	—	.35	—	— 1.00	6.7	+ .07	3
	III*a*	2.11	2.25	2.31	0.99	—	.35	—	— 0.99	6.0	— .20	3
4772.82	I*a*	2.32	2.43	2.40	0.97	—	0.29	— 0.04	— 0.58	4.8	— 0.13	4
	I*b*	2.29	2.35	2.33	0.98	—	.32	— .04	— 0.66	5.7	— .15	3
	II*a*	2.05	2.18	2.17	0.99	—	.26	— .03	— 0.54	6.9	.00	3
	II*b*	2.05	2.16	2.16	1.00	—	.26	— .03	— 0.54	10.1	— .20	2
	III*a*	2.23	2.36	2.39	1.00	—	.29	— .02	— 0.62	4.8	— .08	4
	III*b*	2.23	2.33	2.38	1.00	—	.30	— .02	— 0.62	5.5	— .08	4

Table 26*a*. (continued).

λ	Sp.	log A	log B Fe	log B blend	∂_b	∂_a	∂_s	∂_x	∂_Θ	∂_h	Δ log B $m - c$	w
4903.32	I*a*	2.40	2.52	2.51	0.98	—	0.27	— 0.02	— 0.77	3.7	— 0.05	5
	I*b*	2.36	2.49	2.49	1.00	—	.28	— .01	— 0.79	4.7	— .11	4
	II*a*	2.12	2.24	2.27	0.99	—	.26	—	— 0.72	6.4	— .05	4
	II*b*	2.12	2.25	2.27	0.99	—	.26	—	— 0.70	6.1	— .05	4
4920.52	II*b*	2.39	2.47	2.56	0.98	0.07	0.27	+ 0.14	— 0.38	5.1	— 0.16	5
4930.31	I*a*	2.05	2.15	2.19	0.99	—	0.55	—	— 2.18	8.0	+ 0.05	4
	I*b*	2.01	2.12	2.16	0.98	—	.54	—	— 2.11	5.5	+ .04	4
	II*a*	1.83	1.80	1.83	0.99	—	.46	—	— 1.71	8.4	+ .20	3
	II*b*	1.83	1.94	1.97	1.00	—	.45	—	— 1.71	15.6	— .05	2
4946.40	I*a*	2.36	2.49	2.51	0.96	—	0.30	—	— 0.98	4.0	— 0.19	4
	I*b*	2.32	2.43	2.45	0.99	—	.30	—	— 0.99	3.6	— .08	4
4950.11	I*a*	2.24	2.28	2.28	0.98	—	0.37	—	— 1.25	5.3	— 0.01	4
	I*b*	2.20	2.33	2.33	0.98	—	.37	—	— 1.25	5.2	— .01	4
	III*a*	2.18	2.30	2.31	0.99	—	.26	—	— 0.76	5.1	.00	4
4966.10	I*b*	2.35	2.47	2.48	0.99	—	0.26	—	— 0.88	4.6	— 0.03	5
	III*a*	2.29	2.41	2.47	0.99	—	.25	—	— .0.77	5.0	— .22	4

Table 26*b*. Chief component = Fe^+.

4128.74	I*a*	2.42	2.50	2.47	1.00	—	0.21	0.24	— 0.56	1.8	— 0.17	7
	I*b*	2.38	2.47	2.46	0.96	—	.22	.22	— 0.54	2.2	— .26	6
	II*a*	1.97	2.10	2.07	0.92	—	.31	.34	— 0.79	3.9	— .22	2
4178.86	I*a*	2.58	2.59	2.54	0.69	—	.07	.11	— 0.22	1.1	+ 0.04	7
	I*b*	2.54	2.60	2.57	0.99	—	.10	.13	— 0.25	1.0	— .09	7
	II*a*	2.17	2.24	2.19	1.02	—	.12	.16	— 0.32	2.9	— .01	5
	II*b*	2.17	2.26	2.21	1.01	—	.12	.16	— 0.33	2.7	— .02	5
	III*a*	2.30	2.28	2.27	0.96	—	.22	.15	— 0.52	2.8	— .22	4
4233.17	II*a*	2.29	2.37	2.39	1.02	0.03	0.23	0.21	— 0.69	1.5	— 0.07	7
	II*b*	2.29	2.36	2.39	0.92	.02	.23	.19	— 0.62	1.9	— .16	6
	III*a*	2.41	2.47	2.47	0.82	.01	20	.20	— 0.64	1.5	— .31	5
4416.83	I*a*	2.58	2.64	2.66	1.01	0.02	0.27	0.13	— 0.57	1.9	— 0.10	5
	I*b*	2.54	2.60	2.65	0.96..	.04	.26	.14	— 0.49	2.1	— .16	5
	II*a*	2.17	2.23	2.31	0.99	—	.33	.12	— 0.73	4.8	— .05	4
	II*b*	2.17	2.24	2.31	0.97	—	.30	.10	— 0.66	5.2	— .13	3
	III*a*	2.30	2.41	2.45	0.94	—	.24	.15	— 0.66	2.8	— .30	3
4491.41	I*a*	2.59	2.67	2.69	1.02	0.01	0.18	0.13	— 0.50	1.8	— 0.12	5
	I*b*	2.55	2.64	2.65	1.00	—	.15	.12	— 0.40	1.7	— .15	5
	II*a*	2.18	2.31	2.31	0.98	—	.19	.16	— 0.50	4.0	— .21	3
	II*b*	2.18	2.29	2.30	1.01	—	.21	.15	— 0.56	4.5	— .12	3
	III*a*	2.31	2.39	2.43	1.00	—	.28	.14	— 0.75	3.7	— .13	4

Table 26*b*. (continued).

λ	Sp.	log A	log B Fe	log B blend	∂_b	∂_a	∂_s	∂_x	∂_Θ	∂_h	Δ log B $m - c$	w
4508.29	I*a*	2.61	2.66	2.67	1.02	0.02	0.17	0.12	— 0.45	1.7	— 0.01	6
	I*b*	2.57	2.62	2.64	0.99	—	.15	.09	— 0.36	1.8	— .03	6
	II*a*	2.22	2.31	2.33	0.99	—	.18	.13	— 0.45	3.0	— .06	4
	II*b*	2.22	2.27	2.32	1.00	—	.23	.12	— 0.57	5.1	— .07	4
4515.34	I*a*	2.66	2.70	2.76	1.01	0.03	0.21	0.20	— 0.35	1.9	— 0.12	6
	I*b*	2.60	2.65	2.72	1.00	.02	.21	.18	— 0.35	2.1	— .13	5
	II*a*	2.26	2.36	2.41	0.99	—	.22	.15	— 0.46	1.6	— .12	4
	II*b*	2.26	2.33	2.40	0.99	—	.23	.14	— 0.51	4.8	— .16	4
	III*a*	2.38	2.46	2.56	0.99	0.03	0.31	.16	— 0.66	3.5	— .21	4
	III*b*	2.38	2.45	2.55	0.99	.03	.30	.17	— 0.64	4.2	— .28	4
4576.34	I*a*	2.51	2.58	2.58	1.01	—	0.18	0.16	— 0.56	2.1	+ 0.01	5
	I*b*	2.47	2.54	2.55	1.02	—	.19	.17	— 0.53	2.4	— .03	5
	II*a*	2.08	2.18	2.19	0.97	—	.24	.21	— 0.67	4.4	+ .02	4
	II*b*	2.08	2.16	2.18	1.00	—	.26	.20	— 0.73	6.2	+ .01	3
	III*a*	2.20	2.32	2.37	0.98	—	.29	.19	— 0.86	4.9	— .23	3
	III*b*	2.20	2.28	2.34	0.98	—	.32	.19	— 0.92	4.6	— .15	3
4582.84	I*a*	2.47	2.54	2.45	0.95	0.01	0.22	0.22	— 0.64	2.1	+ 0.10	5
	I*b*	2.43	2.49	2.41	0.90	.01	.22	.19	— 0.66	2.4	+ .04	5
	II*a*	2.03	2.12	2.05	0.97	—	.36	.26	— 1.01	6.3	+ .15	4
	II*b*	2'03	2.17	2.16	1.00	—	.34	.27	— 0.86	7.1	— .13	3
	III*a*	2.15	2.26	2.34	1.01	—	.45	.22	— 1.16	4.4	— .04	4
	III*b*	2.15	2.23	2.23	1.04	.01	.52	.23	— 1.41	5.4	+ .08	4
4583.84	II*b*	2.26	2.34	2.43	1.00	—	0.24	0.17	— 0.51	3.5	— 0.05	4
4620.52	I*a*	2.48	2.54	2.52	0.98	—	0.20	0.18	— 0.35	2.3	— 0.01	5
	I*b*	2.44	2.53	2.51	1.01	—	.18	.18	— 0.48	3.1	— .07	5
	II*a*	2.04	2.13	2.13	1.00	—	.24	.24	— 0.68	6.5	+ .04	3
	II*b*	2.04	2.13	2.10	1.01	—	.28	.33	— 0.56	10.4	— .06	3
	III*a*	2.16	2.23	2.25	1.01	—	.34	.28	— 0.88	7.8	— .04	4
	III*b*	2.16	2.17	2.23	0.98	—	.32	.25	— 0.95	9.1	— .20	3
4731.48	I*a*	2.60	2.70	2.74	0.97	0.01	0.19	0.11	— 0.58	2.0	— 0.14	6
	II*a*	2.19	2.29	2.32	0.97	—	.19	.14	— 0.63	5.4	— .29	3
	II*b*	2.19	2.29	2.39	1.00	—	.26	.12	— 0.83	5.4	— .07	4
4923.93	II*a*	2.36	2.47	2.49	0.96	0.08	0.18	0.16	— 0.52	3.8	— 0.07	5
	II*b*	2.36	2.45	2.48	0.98	.09	.21	.17	— 0.56	5.9	— .07	5

In order to get some idea about the possible importance of systematic errors, due to errors in the instrumental curve and to insufficient information about the disturbing lines we calculate the average correction which has been applied to lines of different strength. It is shown in Table 27 for the different spectra separately. The four columns of this table indicate : 1) the intensity of the line before correction, 2) the average correction for cutting of the chief component, 3) the average correction for blend and 4) the number of lines used in determining these figures.

Table 27. Average of the corrections applied to equivalent width.

δ Cephei 10607.				δ Cephei 10617.			
log A	cutting	blend	n	log A	cutting	blend	n
< 2.20	+ 0.073	— 0.005	13	< 2.20	+ 0.081	+ 0.026	11
2.20 — 2.40	+ .074	— .008	16	2.20 — 2.40	+ .075	+ .010	21
2.40 — 2.50	+ .067	+ .002	16	2.40 — 2.50	+ .074	+ .004	8
> 2.50	+ .047	+ .011	17	> 2.50	+ .058	+ .015	13
	ϑ Cygni.				π Cephei.		
< 1.90	+ 0.092	— 0.022	24	< 2.10	+ 0.092	+ 0.050	6
1.90 — 2.10	+ .097	+ .001	52	2.10 — 2.30	+ .100	+ .033	23
2.10 — 2.20	+ .095	+ .019	37	2.30 — 2.40	+ .080	+ .041	12
> 2.20	+ .063	+ .023	29	> 2.40	+ .023	+ .018	6

It appears that the correction for cutting is positive, a consequence of the negative wings in the contracted instrumental profile. The cutting correction has a tendency to decrease with increasing line strength, somewhat differently for the different spectra. This different behaviour is partially caused by a different cutting of the lines and partially by differences in the curve of growth. The cutting distance increases with line strength sothat for stronger lines a greater part of the negative instrumental wing has been included and the cutting correction becomes less important. This increase will be accompanied by the inclusion of a greater number of disturbing lines, so that the blend correction may increase from a negative value for weak lines (disturbing lines at a relatively great distance outside the blend, so that only their negative instrumental wings are of importance) to a positive value for stronger lines. The somewhat unexpected result, that this relation is reversed in the spectrum of π Cephei is caused by the very slight inclination of the curve of growth for this star, which makes the influence of the many very weak solar lines important, and moreover by the circumstance that the violet part of this spectrum, where many relatively weak, but sharply cut lines are situated, is excluded from our measures. Indeed, from a somewhat closer inspection it is seen that negative blend corrections for moderate lines in the spectrum of ϑ Cygni occur chiefly in the violet region ; near the green end of the spectrum the blend corrections are positive for moderate lines too.

Correction of the curve of growth.

From the material contained in Table 26 we now calculate the corrections of the different curves of growth. The method used is the ordinary method of least squares, the formulae of which have been given in Chapter II. The unknown quantities are log b, log a, $\Delta \log s_0/k$, $\Delta \log x/(1-x)$, $\Delta\Theta$ and the background correction. The latter has been determined independently in three parts of the spectrum, i.e. in the violet region limited by $H\gamma$, in the region between $H\gamma$ and $\lambda = 4600$ and in the region between 4600 and the green end of the spectrum. So for each of the plates of δ Cephei, which are treated independently, we have 8 unknowns (the five spectral parameters and the three background corrections), for the two spectra of ϑ Cygni, there are $5 + 2 \times 3 = 11$ unknowns.

The results are given in Table 28. Here $\Delta \log s_0/k$ (from *Fe I* lines), $\Delta \log x/(1-x)$, and $\Delta\Theta$ are differences relative to the solar values; ε is the quadratic mean deviation of a measured from a computed equivalent width, for a line of weight 1; w is the mean weight of the lines used, so that ε/w is the mean error in the determination of an equivalent width.

Table 28. Parameters of corrected curves of growth.

	δ Cephei 10607	δ Cephei 10617	ϑ Cygni 10616/19	π Cephei 10610/18
log $2b$ (mA)	2.112 ± 0.032	2.093 ± 0.049	1.792 ± 0.025	1.873 ± 0.084
b (mA)	64.7 ± 4.7	61.9 ± 7.0	31.0 ± 1.8	37.3 ± 7.3
log a	$\overline{5}.8$ ± 0.8	$\overline{6}.3$ ± 1.7	$\overline{3}.39$ ± 0.20	$\overline{3}.43$ ± 0.43
log $\gamma(A)$	$\overline{6}.6$ ± 0.8	$\overline{7}.1$ ± 1.6	$\overline{5}.88$ ± 0.20	$\overline{4}.00$ ± 0.39
$\gamma/\gamma\, cl$	(0.07)	(0.002)	(1.3)	(1.7)
$\Delta \log s_0/k$	$\overline{1}.15$ ± 0.19	$\overline{1}.54$ ± 0.24	$\overline{1}.14$ ± 0.15	$\overline{1}.98$ ± 0.34
$\Delta \log x/(1-x)$	1.83 ± 0.17	1.71 ± 0.24	0.93 ± 0.10	0.55 ± 0.19
$\Delta\, \Theta$	−0.104 ± 0.040	−0.112 ± 0.055	−0.163 ± 0.033	−0.098 ± 0.086
h (violet)	−0.031 ± 0.021	−0.099 ± 0.030	+ 0.003 ± 0.012 −0.002 ± 0.010	−0.083 ± 0.033 —
h (central)	+ 0.006 ± 0.017	−0.046 ± 0.025	+ 0.004 ± 0.007 −0.008 ± 0.011	−0.051 ± 0.023 —
h (green)	−0.005 ± 0.011	−0.041 ± 0.021	+ 0.018 ± 0.009 + 0.001 ± 0.006	−0.013 ± 0.014 −0.025 ± 0.016
ε	0.44	0.54	0.34	0.40
w	5.5	5.3	3.9	4.3
ε/w	0.08	0.10	0.09	0.09

The errors given in the above table are quadratic mean errors. They are calculated taking into account all dependances between the different parameters.

A discussion of the correlations between the different quantities is very important. But we shall not enter into it, before we have treated some other aspects of our results.

The continuous background.

One of the obvious peculiarities of the figures of Table 28 is the very large correction for background which occurs in some cases. Since the correction in log A contains a factor 0.434, a value of h equal to 0.10 corresponds to an error in the continuous background of 23 %.

It is almost incredible, that such large errors should have been made. In addition, the circumstance, that no appreciable background error has been found in the spectrum of ϑ Cygni throws some doubt on the reality also of the other determinations. It seems much more probable that our "background corrections" are only artificial products, resulting from erroneous corrections for cutting and blend. If we compare the figures of Table 27 we see, that in the spectra of δ Cephei 10617 and of π Cephei the corrections which we applied to the calculated equivalent width decrease with increasing line strength. In δ Cephei 10607 no such decrease exists, except for the very strong lines and for ϑ Cygni it is even reversed. Now if the calculated equivalent widths of the very weak lines are too great, we will erroneously assume an error in the continuous background, which has made the measured width too small. This is just what occurred in our spectra. And so it becomes clear at once, why we found large background corrections in the spectra of δ Cephei 10617 and π Cephei and the smallest correction for ϑ Cygni.

Now of course, affairs are not simply such that the corrections applied to π Cephei would be erroneous and those for ϑ Cygni right. For both corrections are applied according to the same system, and the circumstance that they show different dependence on line strength is a result of the peculiarities of the spectrum and not of the method of correction. If then we assume the corrections applied to π Cephei to be erroneous, this must be true for ϑ Cygni as well. The capricious behaviour of the corrections is due chiefly to the strong negative wings of the instrumental curve. So if we suppose, that these negative wings have been overestimated in the calculation, it becomes possible that after a due correction the large differences between the spectra of π Cephei and of ϑ Cygni will diminish and that the suggested background correction for π Cephei will disappear. So it might seem to be necessary, if we want to eliminate the influence of these errors, to try a new determination of the instrumental profile. But it is clear that we can expect little result from such an attempt. Introducing in our calculations a parameter determining the shape of the instrumental curve and determining it by a least-square solution together with the others, cannot give a result as accurate as the direct determination of the line profiles.

On the other hand it might seem, that we would be justified in maintaining the background corrections just as they were calculated, regardless of their reality and to consider them as a kind of empirical counterbalance of the error committed when we assumed too large values for the negative instrumental wings. It can be shown, however, that this supposition is wrong.

In order to demonstrate this, we start again from the system of normal equations from which the spectral parameters are deduced. The system may be written :

$$b_{pq}\, x_p = u_q, \tag{51}$$

where the b_{pq} are the coefficients of the normal equations, x_q are the spectral parameters to be determined and u_q are the summed products of the differential line coefficients and the deviations from the provisional curves of growth.

We assume, that the b_{pq} and are u_q subject to systematic errors which we denote by δb_{pq} and δu_q. Then the calculated values of x_p will be in error also and the error committed is determined by :

$$b_{pq}\, \delta x_p = \delta u_q - x_p\, \delta b_{pq} = \triangle_q. \tag{52}$$

From this equation dx may be solved :

$$B\, \delta x_r = B_{qr} \triangle_q \tag{53}$$

in accordance with our previous notation.

Now we suppose, that one of the x_p may be determined by an independent method. This particular x_p, which we denote by x_1, may be the background correction, which we assume to be much smaller than the value calculated from the normal equations, or practically equal to zero.

If now we apply to x_l a forced variation y_l, so that $\delta x_1 + y_l = 0$, the solutions for the other x_p as determined from the normal equations will be changed by an amount y where

$$B_{11}\, y_p = B_{1p} y_1, \tag{54}$$

a relation, which was obtained already in Chapter II. (eq. 25).

If now in the further calculations we exclude the index 1 from the summation, we obtain from (53) :

$$B\, y_1 = - B_{q_1} \triangle_q - B_{11} \triangle_1, \tag{55}$$

hence

$$B\,y_r = -\frac{B_{q_1}\,B_{r_1}}{B_{11}}\,\Delta_q - B_{r_1}\Delta_1. \tag{56}$$

On the other hand we have:

$$B\,\delta x_r = B_{qr}\Delta_q + B_{1r}\Delta_1 \tag{57}$$

So after the correction y_p has been applied the remaining error in x_p is equal to:

$$B\,(\delta x_p + y_p) = B_{qp}\,\Delta_q - \frac{B_{1p}\,B_{q_1}}{B_{11}}\,\Delta_q. \tag{58}$$

Now by a simple rule of the algebra of determinants this equation can be transformed into:

$$C\,(x_p + y_p) = C_{qp}\,\Delta_q, \tag{59}$$

where $C = B_{11}$ and C_{pq} is the minor of b_{qp} in C. If we compare this equation with the original equation (53), it is seen, that the Δ_1 has disappeared altogether, whereas the coefficient of Δ_q has been changed from B_{pq}/B into C_{pq}/C. It can be easily shown, that in cases where the b_{pq} are the coefficients of a system of normal equations, the absolute value of C_{qp}/C will be smaller than that of B_{qp}/B. So after the correction y_p has been applied, all systematic errors enter into the calculation with reduced coefficients, whereas one of them has disappeared altogether.

Thus it appears, that we shall arrive at better values for the spectral parameters, if at the start we assume the background correction to be zero. Then we obtain a reduced system of normal equations, from which the spectral parameters may be determined in precisely the same way as has been done before, when the background correction was still included in the calculations, and starting from the same system of equations, from which only those which correspond to the background corrections have to be omitted. So instead of 11 equations with 11 unknowns as for the spectrum of ϑ Cygni, we now only have 5 equations with 5 unknowns.

The results of the calculations are given in Table 29, which has the same arrangement as Table 28.

Table 29. Parameters of corrected curves of growth (without background correction).

	δ Cephei 10607	δ Cephei 10617	ϑ Cygni 10616/19	π Cephei 10610/18
log $2b$ (mA)	2.109 ± 0.033	2.027 ± 0.070	1.778 ± 0.023	1.731 ± 0.058
b (mA)	64.3 ± 4.9	53.2 ± 8.6	30.0 ± 1.6	26.9 ± 3.4
log a (A)	$\bar{4}.1$ ± 0.8	$\bar{5}.4$ ± 1.7	$\bar{3}.33$ ± 0.18	$\bar{3}.82$ ± 0.39
log γ	$\bar{6}.9$ ± 0.8	$\bar{6}.2$ ± 1.7	$\bar{5}.81$ ± 0.18	$\bar{4}.25$ ± 0.37
$\gamma/\gamma\,cl$	(0.14)	(0.025)	(1.1)	(3.0)
$\Delta \log s_0/k$	$\bar{1}.01$ ± 0.15	$\bar{1}.16$ ± 0.38	$\bar{1}.26$ ± 0.12	0.17 ± 0.32
$\Delta \log x/(1-x)$	1.86 ± 0.16	1.69 ± 0.26	0.94 ± 0.10	0.38 ± 0.18
$\Delta\,\Theta$	−0.104 ± 0.041	−0.114 ± 0.086	−0.158 ± 0.034	−0.044 ± 0.089
ε	0.45	0.59	0.36	0.44
w	5.5	5.3	3.9	4.3
ε/w	0.08	0.11	0.09	0.10

When we compare Tables 28 and 29, we remark many interesting peculiarities. It is seen that the influence of an error in the adopted background is very different for different spectra. In the spectra of δ Cephei the value of $\Delta \log s_0/k$ decreases when the continuous background is raised; because then the weakest lines almost disappear, whereas the strongest lines are only little influenced, the curve of growth will become steeper so that the value of $\log s_0/k$ for the lines will be estimated smaller. In the spectrum of π Cephei the effect is precisely reversed. Here the estimated temperature decreases when the background is raised; the value of $\log s_0/k$ has increased with about 0.19, for lines with excitation potential zero, hence for lines with excitation potential E the increase will be 0.19—0.054 E. For lines with excitation potential above 3.5 $e.V.$ this will become negative; for lines with intermediate excitation potential, the shift will still be positive, but only about 0.10. This value corresponds still to a slight decrease in the slope of the curve of growth, instead of the expected increase; but it turns into a real increase when we take into account the increase of the calculated resonance constant by a factor 2.5. This example shows, how intricate the interrelations are between the determinations of the different spectral parameters.

In the spectrum of δ Cephei the calculated temperature is practically not affected by the correction for background and the resonance is of no significance. So in this case the interrelations are simpler. Nevertheless, we observe a singular difference in the behaviour of these spectra, as by δ Cephei 10607 the Doppler width is practically unaffected by the correction for background, whereas in δ Cephei 10617 it changes by an amount equal to about twice its probable error. In the spectrum of π Cephei this influence of the background on the calculated Doppler width is strong too. It is difficult to give a general explanation of these circumstances, but they may be considered as an indication that the systematic errors which result from a wrong determination of the background may be quite different in different spectra or in different treatments of the same spectrum, dependent on the selection of lines. We will enter into more details in the following section.

Correlations between the calculated spectral parameters.

In Table 29 we gave only the quadratic mean errors of the different spectral parameters. But equally important are the correlations between the different results. If *e.g.* the calculated Doppler width in one of the spectra is wrong, how will this error affect the other determinations? Questions of this kind should be answered if we want to make a critical use of the results obtained.

In Chapter II we already gave a theoretical answer to this question, as we obtained the result, that a change y_p in the parameter x_p, will induce a variation y_q in x_q, where $B_{pp}\, y_q = B_{qp}\, y_p$. The values of B_{qp}/B_{pp} are contained in Table 30. This table gives the values for δ Cephei 10607, δ Cephei 10617, ϑ Cygni and π Cephei in such a way, that the four values in the short divisions of a column apply to these four spectra in the order mentioned. The short indications b, a, s, x and Θ above and at the left hand side represent the expressions $\log b$, $\log a$, $\Delta \log s_0/k$, $\Delta \log x/(1—x)$ and $\Delta\Theta$.

As it is important to know also the absolute amount of the variations which can be expected from the influence of the correlations, the results are put into another form in Table 31. Here we have fixed the supposed change of the independent variable to an amount equal to its positive quadratic mean error, as given in Table 29. Now in a vertical column of this table we find the absolute changes in the dependent variables, which are due to possible errors of the amount upposed.

Table 30. Correlations between determinations of spectral parameters.

Independent variables	Dependent variables				
	b	a	s	x	Θ
b	1.000	— 5.46	— 3.06	— 2.13	— 0.121
	1.000	— 18.6	— 4.75	— 1.50	— 0.750
	1.000	— 0.707	— 3.28	— 1.28	— 0.041
	1.000	— 2.86	— 3.91	— 0.045	— 0.352
a	— 0.010	1.000	+ 0.002	— 0.017	— 0.005
	— 0.031	1.000	+ 0.183	+ 0.008	+ 0.036
	— 0.013	1.000	— 0.176	+ 0.017	— 0.060
	— 0.064	1.000	+ 0.074	+ 0.009	— 0.028
s	— 0.139	+ 0.051	1.000	+ 0.087	+ 0.206
	— 0.159	+ 3.70	1.000	+ 0.100	+ 0.206
	— 0.120	— 0.363	1.000	+ 0.041	+ 0.213
	— 0.129	+ 0.111	1.000	— 0.002	+ 0.229
x	— 0.086	— 0.358	+ 0.076	1.000	— 0.040
	— 0.111	+ 0.372	+ 0.220	1.000	— 0.010
	— 0.069	+ 0.051	+ 0.060	1.000	— 0.026
	— 0.005	+ 0.041	— 0.008	1.000	+ 0.044
Θ	— 0.079	— 1.62	+ 2.95	— 0.653	1.000
	— 0.487	+ 14.2	+ 3.99	— 0.090	1.000
	— 0.019	— 1.57	+ 2.70	— 0.221	1.000
	— 0.151	— 0.537	+ 2.97	+ 0.174	1.000

Table 31.

Independent variables	Dependent variables				
	b	a	s	x	Θ
b	+ 0.033	— 0.18	— 0.10	— 0.07	— 0.004
	+ 0.070	— 1.30	— 0.33	— 0.10	— 0.052
	+ 0.023	— 0.02	— 0.08	— 0.03	— 0.001
	+ 0.058	— 0.17	— 0.23	0.00	— 0.020
a	— 0.008	+ 0.76	0.00	— 0.01	— 0.004
	— 0.052	+ 1.71	+ 0.31	+ 0.01	+ 0.062
	— 0.002	+ 0.18	— 0.03	0.00	— 0.011
	— 0.025	+ 0.39	+ 0.03	0.00	— 0.011
s	— 0.022	+ 0.01	+ 0.15	+ 0.01	+ 0.032
	— 0.060	+ 1.41	+ 0.38	+ 0.04	+ 0.078
	— 0.015	— 0.04	+ 0.12	+ 0.01	+ 0.026
	— 0.041	+ 0.04	+ 0.32	0.00	+ 0.073
x	— 0.014	— 0.06	+ 0.01	+ 0.16	— 0.007
	— 0.028	+ 0.10	+ 0.06	+ 0.26	— 0.003
	— 0.007	+ 0.01	+ 0.01	+ 0.10	— 0.003
	— 0.001	+ 0.01	0.00	+ 0.18	+ 0.008
Θ	— 0.003	— 0.07	+ 0.12	— 0.03	+ 0.041
	— 0.042	+ 1.23	+ 0.34	— 0.01	+ 0.086
	— 0.001	— 0.05	+ 0.09	— 0.01	+ 0.034
	— 0.013	— 0.05	+ 0.26	+ 0.02	+ 0.089

The coefficients of correlation, which measure the degree of dependence between the different variables, may be computed directly from the figures in Table 30. They are obtained by multiplying the two coefficients B_{pq}/B_{pp} and B_{pq}/B_{qq}. So in the spectrum of δ Cephei 10607 the coefficient of correlation for the variables s and b is equal to (—3.06) (—0.139) = 0.43.

If we compare the different values of the correlation coefficients which may be computed from Table 30, we find cases where the correlation is always strong, but also other cases, where the different spectra behave very unequal. So the correlation between b and s is always strong. This is easily explained by the fact that an increase in the adopted value of b would augment the computed equivalent widths of the lines, so that it must be compensated by a corresponding decrease in s. The correlation between b and x can be explained in about the same way. For the mean intensity of the ion lines is larger than that of the lines originating from neutral atoms, from which follows, that the ion lines are situated on a more horizontal part of the curve of growth. So for the ion lines a greater decrease is necessary in order to balance the increase of b than for the atom lines and this results in an apparent decrease of the degree of ionization.

Very singular is the behaviour of the correlation (b, Θ). In the two spectra of δ Cephei this coefficient is resp. 0.01 and 0.37! From an inspection of the calculation of these coefficients it is seen, that in the first case the small value follows from the cancelling out of two terms of opposite signs. Indeed, an increase in b works on Θ in a very complicated way. The general increase in equivalent width which would follow from the larger value of b is counterbalanced by the decrease in s. But whereas this combined variation of b and s leaves the mean intensities of the lines unaltered, it at the same time results in an increase in the slope of the curve of growth. Now this slope may be reduced to its original value when we change b, s and Θ simultaneously. For in the mean the weaker lines will have a somewhat higher excitation potential than the strong lines in the spectrum. So a slight decrease of Θ, which corresponds to an increase in the temperature will make the weak lines a little stronger relatively to the strong lines in the spectrum and so it will reduce the slope of the curve of growth. At the same time, of course, it will contribute to a general increase in the strength of the lines and so it must be counteracted by a still graeter decrease in s. So as a general rule, we may expect that an increase in b will result in a decrease in Θ and in a much greater decrease in s. But in cases where the excitation potentials of lines of different strength does not differ systematically, the value of Θ may remain unaltered.

This example shows, that there is no general rule from which we might determine the influence of a wrong determination of a spectral parameter on the others; this influence depends to a very large extent on the special selection of lines. General tendencies may be traced, but their quantitative expressions must be determined for each case separately.

Coefficients of correlation may be derived also for the interdependence of the spectral parameters and the background correction. It is impossible to suppose a background correction as large as indicated in Table 28, but nevertheless it is possible, that the correction, which was supposed to be zero in Table 29, will have a small positive or negative value. In order to get an idea of the importance of such a change, we supposse the mean background to be lowered by 4.6 %, corresponding to a mean value of h equal to —0.020. This amount of error is probably about the largest to be expected. The variation in the computed spectral parameters, which would result from this change in the adopted background, has been given in Table 32.

In considering these values, it should be born in mind that they can give only a general impression about the dependence, since the influence of the background correction in one part of the spectrum may be contrary to that in the other part. So in the spectrum of π Cephei a background correction in the violet part of the spectrum only would give a change in s of —0.39 instead

Table 32. Change in spectral parameters when background is lowered by 4.6%.

Spectrum	Changing parameter				
	b	a	s	x	Θ
δ Cephei 10607	+ 0.006	— 0.06	+ 0.08	+ 0.03	— 0.001
δ Cephei 10617	+ 0.008	— 0.09	+ 0.07	+ 0.02	0.000
ϑ Cygni	+ 0.014	— 0.20	+ 0.17	+ 0.01	+ 0.012
π Cephei	+ 0.047	— 0.23	+ 0.02	+ 0.13	— 0.015

of the + 0.02 tabulated here, whereas it would be of no influence on the temperature. A background correction in the green part of the spectrum, however, would change s with + 0.24 for the spectrum 10610 and with + 0.59 for the spectrum 10618 and would have a serious effect on the calculated temperature. Since, however, the necessary background corrections are correlated also, it is impossible to get an adequate survey without very detailed calculations. Conditions as in the spectrum of π Cephei, however, are exceptional as they are the consequence of a somewhat particular selection of lines and, in general, the figures given here, together with an intercomparison of Tables 28 and 29 will give sufficient information about the possible consequences of an error in the determination of background.

If from the beginning we had worked in that direction, we in the same way could determine the influence of an error in the instrumental profile. But since the necessary basis for this calculation has not been made when we started our computations, we now cannot enter into this question any further.

Results for separate lines.

The differences remaining after the corrections for the changes in log b etc. to the calculated equivalent widths have been applied, are given in Table 33, for the same series of lines as in Table 26.

Table 33. Residuals for separate lines.

Table 33*a*. Lines of *Fe I*.

λ	Sp.	meas.	comp.	m—c	λ	Sp.	meas.	comp.	m—c
4062.45	Ia	2.40	2.46	— 0.06	4084.50	Ia	2.34	2.34	0.00
	IIa	2.26	2.21	+ 0.05		IIa	2.16	2.21	— 0.05
4065.39	Ia	1.94?	2.10	— 0.16?	4089.23	Ia	2.20	2.08	+ 0.12
	IIa	2.02	2.10	— 0.08		IIa	1.94	1.97	— 0.03
4070.78	IIa	2.15	2.15	0.00	4091.56	Ia	2.01	2.00	+ 0.01
4072.51	Ia	2.21	2.21	0.00		IIa	2.20?	1.86	+ 0.34?
	IIa	2.05	2.05	0.00	4109.06	Ia	2.19?	2.21	— 0.02?
4079.85	Ia	2.27	2.22	+ 0.05		IIa	1.95?	2.11	— 0.16?
	IIa	2.12	2.05	+ 0.07		IIb	2.14?	2.07	+ 0.07?

Table 33*a*. (continued).

λ	Sp.	meas.	comp.	*m*—*c*
4112.32	I*a*	1.90	2.12	— 0.22
	II*a*	1.91?	1.90	+ 0.01?
	II*b*	1.93?	1.92	+ 0.01?
4114.45	I*a*	2.30	2.28	+ 0.02
	II*a*	2.17	1.98	+ 0.19
	II*b*	2.19	2 02	+ 0.17
4126.19	I*a*	2.15	2.35	— 0.20
	I*b*	2.11	2.35	— 0.24
	II*a*	2.02	2.08	— 0.06
	II*b*	1.90	2.13	— 0.23
4130.05	II*a*	1.68	1.92	— 0.24
	II*b*	1.89	1.77	+ 0.12
4132.91	II*a*	2.03	2.08	— 0.05
	II*b*	2.05	2.12	— 0.07
4134.69	I*a*	2.22	2.31	— 0.09
	II*a*	2.16	2.23	— 0.07
	II*b*	2.20	2.25	— 0.05
4136.53	I*a*	2.02	2.12	— 0.10
	I*b*	2.09	2.19	— 0.10
	II*a*	1.86	2.04	— 0.18
	II*b*	1.84	1.94	— 0.10
4139.94	I*a*	2.12	2.21	— 0.09
	I*b*	2.17	2.20	— 0.03
	II*a*	1.89	1.93	— 0.04
	II*b*	1.91	1.91	0.00
4140.41	II*a*	1.83	1.93	— 0.10
	II*b*	1.78	1.90	— 0.12
4143.88	I*a*	2.50	2.56	— 0.06
	I*b*	2.41?	2.55	— 0.14?
	II*a*	2.32?	2.31	+ 0.01?
	II*b*	2.37	2.29	+ 0.08
4145.20	II*b*	1.58	1.44	+ 0.14
4147.68	I*b*	2.34	2.39	— 0.05
	II*b*	2.11	2.15	— 0.04
4150.26	I*b*	2.11	2.31	— 0.20
4154.51	II*a*	2.06	2.07	— 0.01
	II*b*	2.15	2.14	+ 0.01
4154.82	I*a*	2.35	2.39	— 0.04
	I*b*	2.31	2.40	— 0.09
	II*a*	2.11	2.20	— 0.09
	II*b*	2.09	2.13	— 0.04
4157.79	I*a*	2.40	2.43	— 0.03
	I*b*	2.35	2.37	— 0.02
	II*a*	2.16	2.18	— 0.02
	II*b*	2.16	2.19	— 0.06
4158.80	I*a*	2.24	2.28	— 0.04
	I*b*	2.12	2.30	— 0.18
	II*a*	2.06	2.09	— 0.03
	II*b*	2.11	2.05	+ 0.06
4168.62	I*a*	1.93	1.94	— 0.01
	I*b*	2.03	2.04	— 0.01
	II*a*	1.86	1.83	+ 0.03
	II*b*	1.77	1.82	— 0.05
4174.92	I*a*	2.32	2.46	— 0.14
4175.64	I*a*	2.45	2.43	+ 0.02
	I*b*	2.41	2.39	+ 0.02
	II*a*	2.18	2.19	— 0.01
	II*b*	2.22	2.20	+ 0.02
4182.39	I*a*	2.17	2.20	— 0.03
	I*b*	2.22	2.32	— 0.10
	II*b*	1.91	2.02	— 0.11
	III*a*	2.18	2.01	+ 0.17
4187.05	I*a*	2.42	2.51	— 0.09
	I*b*	2.39	2.51	— 0.12
	II*a*	2.19	2.26	— 0.07
4202.04	II*a*	2.37	2.32	+ 0.05
4205.55	I*b*	2.43	2.12	+ 0.31
	II*a*	2.06	2.07	— 0.01
	II*b*	2.09	2.05	+ 0.04
	III*a*	2.27	2.33	— 0.06
4206.70	II*a*	2.06	2.11	— 0.05
	II*b*	2.05	2.11	— 0.06
	III*a*	2.26	2.27	— 0.01
4207.14	I*a*	2.30	2.21	+ 0.09
	I*b*	2.36	2.20	+ 0.16
	II*a*	2.10	2.01	+ 0.09
	II*b*	2.08	2.00	+ 0.08

Table 33*a*. (continued).

λ	Sp.	meas.	comp.	*m*—*c*
4208.61	I*a*	2.28	2.24	+ 0.04
	I*b*	2.16	2.17	— 0.01
	II*a*	2.05	2.09	— 0.04
	II*b*	2.07	2.09	— 0.02
	III*a*	2.11	2.18	— 0.07
4216.19	I*a*	2.43	2.47	— 0.04
	I*b*	2.38	2.43	— 0.05
	II*a*	2.10	2.22	— 0.12
	II*b*	2.11	2.21	— 0.10
4222.22	I*a*	2.50	2.47	+ 0.03
	I*b*	2.49	2.47	+ 0.02
	II*a*	2.22	2.20	+ 0.02
	II*b*	2.20	2.19	+ 0.01
	III*a*	2.25	2.27	— 0.02
4224.18	II*a*	2.10	2.22	— 0.12
	II*b*	2.21	2.29	— 0.08
	III*a*	2.19	2.24	— 0.05
4233.61	I*a*	2.24	2.36	— 0.12
	I*b*	2.34	2.32	+ 0.02
	II*a*	2.20	2.17	+ 0.03
	II*b*	2.24	2.19	+ 0.05
	III*a*	2.30	2.36	— 0.06
4235.95	I*a*	2.61	2.61	0.00
4238.82	I*a*	2.41	2.46	— 0.05
	I*b*	2.45	2.46	— 0.01
	II*a*	2.25	2.20	+ 0.05
	II*b*	2.20	2.20	0.00
	III*a*	2.33?	2.37	— 0.04?
4250.13	I*a*	2.48	2.56	— 0.08
	I*b*	2.44	2.46	— 0.02
	II*a*	2.32	2.29	+ 0.03
	II*b*	2.30	2.32	— 0.02
	III*a*	2.44	2.33	+ 0.11
4264.22	I*b*	2.15	2.31	— 0.16
	II*a*	1.98	2.08	— 0.10
	II*b*	1.88	2.08	— 0.20
	III*a*	2.12	2.24	— 0.12
4266.97	II*b*	2.03	2.16	— 0.13
4271.17	I*a*	2.49	2.55	— 0.06
	I*b*	2.41	2.46	— 0.05
	II*a*	2.24	2.34	— 0.10
	II*b*	2.28	2.34	— 0.06
	III*a*	2.37	2.45	— 0.08
4271.78	I*a*	2.65	2.61	+ 0.04
	I*b*	2.55	2.56	— 0.01
	II*a*	2.42	2.44	— 0.02
	II*b*	2.41	2.43	— 0.02
4282.41	I*a*	2.54	2.47	+ 0.07
	I*b*	2.45	2.38	+ 0.07
	II*a*	2.20	2.22	— 0.02
	II*b*	2.18	2.19	— 0.01
	III*a*	2.36	2.30	+ 0.06
4348.95	III*a*	2.05	2.14	— 0.09
4365.91	III*a*	1.78	2.16	— 0.38
4375.95	I*a*	2.47	2.43	+ 0.04
	I*b*	2.37	2.40	— 0.03
	II*a*	2.23	2.18	+ 0.05
	II*b*	2.16	2.16	0.00
4383.56	I*a*	2.66	2.59	+ 0.07
	I*b*	2.55	2.56	— 0.01
	II*a*	2.52	2.48	+ 0.04
	II*b*	2.52	2.48	+ 0.04
	III*a*	2.65	2.64	+ 0.01
4388.42	I*a*	2.30	2.34	— 0.04
	I*b*	2.30	2.36	— 0.06
	II*a*	2.09	2.18	— 0.09
	II*b*	2.14	2.21	— 0.07
4389.26	I*a*	2.14	2.03	+ 0.11
	I*b*	2.03	2.11	— 0.08
	II*a*	1.86	1.92	— 0.06
	II*b*	1.79	1.93	— 0.14
	III*a*	2.06	2.15	— 0.09
4404.76	II*a*	2.46	2.49	— 0.03
4442.35	I*a*	2.40	2.42	— 0.02
	I*b*	2.32	2.39	— 0.07
	II*a*	2.14	2.17	— 0.03
	II*b*	2.14	2.20	— 0.06
	III*a*	2.40	2.42	— 0.02

Table 33*a*. (continued).

λ	Sp.	meas.	comp.	*m*—*c*
4447.73	I*a*	2.45	2.47	— 0.02
	I*b*	2.48	2.40	+ 0.08
	II*a*	2.23	2.22	+ 0.01
	II*b*	2.14	2.22	— 0.08
	III*a*	2.40	2.37	+ 0.03
4484.23	III*a*	2.12	2.26	— 0.14
4490.78	II*a*	1.89	2.14	— 0.25
	II*b*	1.77	2.15	— 0.38
4492.69	II*a*	1.61	1.83	— 0.22
	II*b*	1.63	1.78	— 0.15
4494.58	III*b*	2.41	2.42	— 0.01
4602.01	II*a*	1.93	1.92	+ 0.01
	II*b*	1.76	1.93	— 0.17
	III*a*	2.04	2.15	— 0.11
	III*b*	2.04	2.12	— 0.18
4602.95	I*a*	2.51	2.34	+ 0.17
	I*b*	2.45	2.35	+ 0.10
	II*a*	2.28	2.09	+ 0.19
	II*b*	2.23	2.09	+ 0.14
	III*a*	2.39	2.21	+ 0.18
	III*b*	2.37	2.26	+ 0.11
4625.05	II*a*	2.22	2.16	+ 0.06
	II*b*	2.05	2.14	— 0.09
4630.13	II*a*	2.17	1.87	+ 0.30
	II*b*	1.94	1.91	+ 0.03
	III*a*	2.19	2.23	— 0.04
	III*b*	2.16	2.18	— 0.02
4643.47	I*a*	2.41	2.29	+ 0.12
	I*b*	2.34	2.29	+ 0.05
	II*a*	2.26	2.03	+ 0.23
	II*b*	2.10	2.06	+ 0.04
	III*a*	2.50	2.28	+ 0.22
4647.44	I*a*	2.50	2.42	+ 0.08
	I*b*	2.36	2.41	— 0.05
	II*b*	2.23	2.23	0.00
4683.57	I*a*	2.12	1.97	+ 0.15
	I*b*	2.21	1.99	+ 0.22
	II*a*	2.01	1.83	+ 0.18
	III*a*	2.29	2.16	+ 0.13
	III*b*	2.19	2.13	+ 0.06
4728.55	I*a*	2.34	2.22	+ 0.12
	I*b*	2.31	2.33	— 0.02
	II*a*	2.28	2.10	+ 0.18
	II*b*	2.12	2.16	— 0.04
	III*a*	2.31	2.29	+ 0.02
4733.60	I*a*	2.42	2.33	+ 0.09
	I*b*	2.24	2.28	— 0.04
	II*a*	2.20	2.07	+ 0.13
	II*b*	2.19	2.08	+ 0.11
4741.54	I*a*	2.30	2.30	0.00
	I*b*	2.32	2.28	+ 0.04
	II*a*	2.14	2.09	+ 0.05
	II*b*	2.00	1.93	+ 0.07
	III*a*	2.11	2.25	— 0.14
4772.82	I*a*	2.27	2.30	— 0.03
	I*b*	2.18	2.25	— 0.07
	II*a*	2.17	2.11	+ 0.06
	II*b*	1.96	2.10	— 0.14
	III*a*	2.31	2.28	+ 0.03
	III*b*	2.30	2.28	+ 0.02
4903.32	I*a*	2.46	2.43	+ 0.03
	I*b*	2.38	2.42	— 0.04
	II*a*	2.22	2.24	— 0.02
	II*b*	2.22	2.23	— 0.01
4920.52	II*b*	2.40	2.45	— 0.05
4930.31	I*a*	2.24	2.26	— 0.02
	I*b*	2.20	2.29	— 0.09
	II*a*	2.03	1.94	+ 0.09
	II*b*	1.92	2.08	— 0.16
4946.40	I*a*	2.32	2.46	— 0.14
	I*b*	2.37	2.41	— 0.04
4950.11	I*a*	2.27	2.25	+ 0.02
	I*b*	2.32	2.33	— 0.01
	III*a*	2.31	2.18	+ 0.13
4966.10	I*b*	2.45	2.42	+ 0.03
	III*a*	2.25	2.34	— 0.09

Table 33*b*. Lines of Fe^+.

λ	Sp.	meas.	comp.	*m*—*c*	λ	Sp.	meas.	comp.	*m*—*c*
4128.74	I*a*	2.30	2.41	—0.11		II*a*	2.29	2.32	—0.03
	I*b*	2.20	2.36	—0.16		II*b*	2.24	2.32	—0.08
	II*a*	1.85	2.03	—0.18		III*a*	2.35	2.42	—0.07
						III*b*	2.27	2.40	—0.13
4178.86	I*a*	2.58	2.47	+ 0.11					
	I*b*	2.48	2.41	+ 0.07	4576.34	I*a*	2.59	2.50	+ 0.09
	II*a*	2.18	2.08	+ 0.10		I*b*	2.52	2.43	+ 0.09
	II*b*	2.19	2.10	+ 0.09		II*a*	2.21	2.13	+ 0.08
	III*a*	2.05	2.07	—0.02		II*b*	2.19	2.13	+ 0.06
						III*a*	2.14	2.21	—0.07
4233.17	II*a*	2.32	2.33	—0.01		III*b*	2.19	2.20	—0.01
	II*b*	2.23	2.33	—0.10					
	III*a*	2.16	2.30	—0.14	4582.84	I*a*	2.55	2.39	+ 0.16
						I*b*	2.45	2.32	+ 0.13
4416.83	I*a*	2.56	2.56	0.00		II*a*	2.20	2.04	+ 0.16
	I*b*	2.49	2.49	0.00		II*b*	2.03	2.12	—0.09
	II*a*	2.26	2.26	0.00		III*a*	2.30	2.26	+ 0.04
	II*b*	2.18	2.26	—0.08		III*b*	2.31	2.19	+ 0.12
	III*a*	2.15	2.28	—0.13					
					4583.84	II*b*	2.38	2.35	+ 0.03
4491.41	I*a*	2.57	2.59	—0.02					
	I*b*	2.50	2.52	—0.02	4620.52	I*a*	2.51	2.43	+ 0.08
	II*a*	2.10	2.23	—0.13		I*b*	2.44	2.38	+ 0.06
	II*b*	2.18	2.23	—0.05		II*a*	2.17	2.07	+ 0.10
	III*a*	2.30	2.27	+ 0.03		II*b*	2.04	2.01	+ 0.03
						III*a*	2.21	2.08	+ 0.13
4508.29	I*a*	2.66	2.55	+ 0.11		III*b*	2.03	2.07	—0.04
	I*b*	2.61	2.50	+ 0.11					
	II*a*	2.27	2.25	+ 0.02	4731.48	I*a*	2.60	2.65	—0.05
	II*b*	2.25	2.25	0.00		II*a*	2.03	2.27	—0.24
						II*b*	2.32	2.36	—0.04
4515.34	I*a*	2.64	2.64	0.00	4923.93	II*a*	2.42	2.40	+ 0.02
	I*b*	2.59	2.56	+ 0.03		II*b*	2.41	2.39	+ 0.02

Possible origin of the remaining errors.

The quadratic mean deviation of the computed from the observed equivalent width is about 0.36 in the spectrum of ϑ Cygni, for weight 1. For lines of average strength the deviation is about 0.09 in log B, corresponding to an uncertainty of about 20 %.

On the other hand, we found from a previous discussion that the quadratic mean accidental error of one measure of equivalent width is about 0.20 when the weight of the measure is 1. From this it would follow that a great part of the mean deviation 0.36 is not due to errors of measuring, but is a consequence of inaccuracies in the method of reduction or in the values of the solar equivalent width from which we started. In order to follow up this question a little further, because a knowledge of the sources of the remaining deviations may afford important indications for further improvements of the method, we use the deviations found for ϑ Cygni, where the two spectra have 61 lines (for π Cephei only 8) in common.

For each of these lines the deviation $c—m$ was multiplied by the appropriate weight factor, chosen equal for corresponding lines in the two spectra. If the deviation in the spectrum 10616 is called ε_1 and the corresponding deviation in the other spectrum ε_2, we may put $\varepsilon_1 = \eta_1 + \delta$ and $\varepsilon_2 = \eta_2 + \delta$, where η_1 and η_2 are accidental errors and δ is the systematic error. From this it follows, that $\Sigma\varepsilon_1^2 = \Sigma\eta_1^2 + 2\,\Sigma\eta_1\delta + \Sigma\delta^2$, $\Sigma\varepsilon_2^2 = \Sigma\eta_2^2 + 2\,\Sigma\eta_2\delta + \Sigma\delta^2$, and $\Sigma\varepsilon_1\varepsilon_2 = \Sigma\eta_1\eta_2 + \Sigma\eta_1\delta + \Sigma\eta_2\delta + \Sigma\delta^2$. Now we may suppose that η_1, η_2 and δ are mutually independent and the equations read : $\Sigma\varepsilon_1^2 = \Sigma\eta_1^2 + \Sigma\delta^2$, $\Sigma\varepsilon^2 = \Sigma\eta_2^2 + \Sigma\delta^2$ and $\Sigma\varepsilon_1\varepsilon_2 = \Sigma\delta^2$. From these three equations we immediately calculate the quadratic means of η_1, η_2 and δ.

In the case under consideration we have : $\Sigma\varepsilon_1^2 = 7.98$ $\Sigma\varepsilon_2^2 = 5.93$ and $\Sigma\varepsilon_1\varepsilon_2 = 3.66$, the number of lines used being 61. We then have : $\overline{\delta^2} = 0.060$, $\overline{\varepsilon_1^2} = 0.071$ and $\overline{\varepsilon_2^2} = 0.037$. So the quadratic mean systematic error is 0.24 and the accidental errors are 0.27 in the spectrum 10616 and 0.19 in the other spectrum. For the mean of the two spectra we have $\overline{\varepsilon^2} = 0.054$ and the quadratic mean accidental error is 0.23 for a line of weight 1, only little more than the value 0.20 which had been found by a direct comparison of the spectra. That the mean error in the spectrum 10619 is a larger than in the other spectrum is entirely due to the long wave-length region. If we treat separately the 33 pairs of lines to the violet side of $H\gamma$ and the 28 pairs at the other side, we find :

Violet region n = 33.			Green region n = 28.		
$\Sigma\varepsilon_1^2 = 3.74$	$\Sigma\varepsilon_2^2 = 3.72$	$\Sigma\varepsilon_1\varepsilon_2 = 2.45$	$\Sigma\varepsilon_1^2 = 4.24$	$\Sigma\varepsilon_2^2 = 2.21$	$\Sigma\varepsilon_1\varepsilon_2 = 1.21$
$\Sigma\eta_1^2 = 1.29$	$\Sigma\eta_2^2 = 1.27$	$\Sigma\delta^2 = 2.45$	$\Sigma\eta_1^2 = 3.03$	$\Sigma\eta_2^2 = 1.00$	$\Sigma\delta^2 = 1.21$
$\overline{\eta_1^2} = 0.0391$	$\overline{\eta_2^2} = 0.0385$	$\overline{\delta^2} = 0.0742$	$\overline{\eta_1^2} = 0.108$	$\overline{\eta_2^2} = 0.0357$	$\overline{\delta^2} = 0.0432$
$(\eta_1) = 0.20$	$(\eta_2) = 0.20$	$(\delta) = 0.27$	$(\eta_1) = 0.33$	$(\eta_2) = 0.19$	$(\delta) = 0.21$

From an inspection of the plates it is seen, that the plate 10616 is very black in the long wave-length region, the transmission of the plate in the points between the lines being about 7 %. On the plate 10619 the transmission at the corresponding points is 14 %. So it is easily understood, that the measures in the spectrum 10616 in this region cannot be as accurate as those in the other spectrum and we may even understand that in the spectrum 10616 systematic errors may occur, which cause the apparent "background error". It is to be expected, that in a heavily blackened region the slope of the transmission curve is abnormally low (in the stellar spectrum relative to that derived from the density marks), so that the line intensities will be overestimated. Indeed the deviations in this region of the spectrum 10616 show a very distinct tendency towards a positive value, which is expressed also in the positive value for h we have found for this region (Table 28). In the spectrum 10619 this tendency towards positive deviations is not present. In the case of the spectrum of ϑ Cygni the background correction which has been found initially, thus appears as a product of errors in the lower part of the adopted transmission curve. The same explanation, however, does not seem to apply to the other spectra, that are not so strongly blackened.

More important than the accidental error is the result about the systematic error, which is of the same order of magnitude.. The average weight of the 33 pairs of lines in the "violet" region is 4.45 and that of the 28 pairs in the "green" region is 3.18. So the quadratic mean systematic error of a line of average weight in these regions is resp. $0.27/4.45 = 0.061$ and $0.21/3.18 = 0.065$. We may adopt a mean value of about 0.063, corresponding to an error of 14 % in the equivalent width. This error may be due partly to errors in the adopted solar equivalent widths which have been taken from the tables of ALLEN. The quadratic mean error in the solar equivalent widths according to ALLEN is about 0.05. As the slope of the curve of growth for ϑ Cygni is about $^2/_3$ of that for the corresponding lines in the solar spectrum, the error in the

solar equivalent width will produce an error of about 0.03 in our results. Subtracting the squares of the errors, we find, that a systematic deviation of about 0.055 is still to be explained.

This error may be caused partly by errors in the instrumental curve and in the calculation of the cutting effect, partly by errors in the blend correction. We have tried to discriminate between both possibilities, by comparing with the results for δ Cephei.

In comparing the deviations m—c in the two spectra of δ Cephei we find for 48 common lines with a mean weight 5.33 $\Sigma\varepsilon_1\varepsilon_2 = 6.62$, from which we calculate a value of 0.37 for the quadratic mean systematic deviation for a line of weight 1 or 0.070 for an actual line. This is, notwithstanding the spectra are really different, only little more than the value 0.063 for ϑ Cygni. If most of the systematic errors had been due to an inaccurate correction for blend, we might expect a much wider deviation between the results for ϑ Cygni and δ Cephei. Because in the spectrum of δ Cephei the ion lines are relatively much stronger than in ϑ Cygni, there is a greater chance of wrong identifications of disturbing lines and of wrong corrections for blend. So at least a great part of the systematic error must be due to an incorrect calculation of the cutting effect, resulting from an inaccurate knowledge of the instrumental curve.

So we arrive at the same result which we obtained when the background correction was studied, *viz.* that a great part of the remaining discrepancies must be due to errors in the adopted instrumental curve. Since the great difficulties in the determination of this curve are chiefly due to the strong gradation of our plates and the correspondingly large deviations in the transmission curve, it does not pay to make attempts for a more accurate determination. It will be better to study spectra taken on plates with a softer gradation, where the photographic effects will be less disturbing. Further, a more accurate determination of the instrumental curve is possible when the comparison spectrum is photographed on a continuous background. As the necessary informations about the change in the transmission curve are lacking for the plates which are the subject of this investigation, efforts to improve the results by a more accurate determination of the instrumental curve will be in vain. Possibly the very notion "instrumental curve" is not strictly applicable to our plates, as the intensity scale will be distorted as a consequence of errors in the adopted transmission curve. If improvements are to be made, they must start at the very beginning, at the reduction of measured transmissions to intensities.

From the above considerations it follows, that under more favourable circumstances, when the difficulties with the transmission curve are avoided, the accuracy of the results obtained from the spectra will surpass that obtained in our case for ϑ Cygni. The fact, that the results for this spectrum are more accurate than those for δ Cephei and π Cephei, may well be related to the small intensities of the lines in ϑ Cygni, whence a distortion in the intensity scale will have less serious consequences.

Variations in the spectrum of δ Cephei.

The two spectra of δ Cephei which occur among our plates, need some special consideration. Originally, these plates were intended to represent the maximum and minimum phase of the spectrum and in the first part of this publication they were denoted as such. The precise calculation of the phase showed, however, that this designation was not accurate. The dates of the plates were *J.D.* 242 4032.774 and 33.764. By means of the formula [1]:

$$Max = J.D.\ 2393\ 659.873 + 5.366\ 396\ E - 0.84\ 10^{-8}\ E^2 \tag{60}$$

we find for the date of the maximum $E = 5\ 660$: *J.D.* 242 4033.405. So the plates have been taken

[1] Kleinere Veröffentlichugen der Universitätssternwarte zu Berlin-Babelsberg **25** (1941) p. 185.

$0^d.631$ before and $0^d.359$ after maximum. The first exposure, $0^d.789$ after minimum, corresponds within $1\frac{1}{2}$ hours with the moment where the star according to the radial-velocity curve had its smallest volume. The second exposure can be described approximately as corresponding with the phase of maximum. So for convenience we will denote the plates as δ Cephei v (minimum volume) and δ Cephei M (maximum brilliancy).

From Table 29 we cannot take any definite information about the variations in the spectrum between these two phases. But we may improve the comparison when we compare the plates directly instead of taking the sun as an intermediary.

As we have seen, the large errors in the determination of the spectral parameters are only partly due to accidental errors in the measured equivalent widths; a considerable part is caused by systematic errors in the reduction : cutting effect and inaccurate knowledge of the instrumental curve, uncertainties in blend correction. As such systematic errors will be nearly equal in both spectra of δ Cephei, we may expect more accurate results when we compare the spectra directly, the systematic errors than being canceled out almost completely.

The necessary calculations have been made in the same way as when the comparison with the solar spectrum was made. Of course, we could use only the 48 lines which were measured in both spectra of δ Cephei. For the constants for the differential correction the averages of the values from Table 26 for the two plates have been taken. No correction for wrong background was applied. The results are contained in Table 34.

Table 34. Variations in spectrum δ Cephei M — δ Cephei v.

$\Delta \log b = -0.089 \pm 0.034$ $\quad \Delta \log a = -0.45 \pm 0.83$ $\quad \Delta \log s_0/k = +0.08 \pm 0.15$
$\Delta \log x/(1\text{-}x) = -0.08 \pm 0.15$ $\quad \Delta\Theta = -0.018 \pm 0.037.$ $\quad \varepsilon = 0.35$ (difference between two measures).

It is very interesting that the only quantity showing conclusive evidence of variation is the Doppler width b! We shall return to this question in the concluding chapter.

The correlations between the calculated quantities are shown in Table 35 which has the same arrangement as Table 30. Table 36 is the equivalent of 31.

Table 35. Correlations between calculated parameters.

Independent variables	Dependent variables				
	b	a	s	x	Θ
b	1.000	— 11.0	— 3.00	— 2.37	— 0.082
a	— 0.015	1.000	+ 0.020	+ 0,011	— 0.005
s	— 0.162	+ 0.781	1.000	+ 0.203	+ 0.182
x	— 0.117	+ 0.401	+ 0.185	1,000	— 0.031
Θ	— 0·071	— 3.40	+ 2,92	— 0.549	1.000

Table 36.

Independent variables	Dependent variables				
	b	a	s	x	Θ
b	+ 0.034	— 0.37	— 0.10	— 0.08	— 0.003
a	— 0.013	+ 0.83	+ 0.02	+ 0.01	— 0.005
s	— 0,024	+ 0.11	+ 0.15	+ 0.03	+ 0.027
x	— 0.018	+ 0.06	+ 0.03	+ 0.15	— 0.005
Θ	— 0.003	— 0.13	+ 0.11	— 0.02	+ 0,037

Possible inferences from the other spectral lines.

Until now, we limited our discussion to the lines of iron. There are besides many lines belonging to other atoms, listed in Tables 21 *c* to 21 *l*. A preliminary discussion of these lines showed, however, that we cannot expect an appreciable improvement of our results from their study. About one half of the lines originating from neutral atoms must be omitted as a consequence of serious blending ; the remaing lines are too few in number to justify any definite conclusion. Even if we limit ourselves to the determination of the abundance of the element only, taking all spectral parameters as Doppler width, temperature and resonance from the discussion of the iron lines, the results are not sufficiently accurate to be of great use. So we shall postpone a further discussion of these lines to another time, when more and better material may be available.

General remarks about the method of reduction.

The method used in the preceding investigation may seem a little cumbersome. The rigorous mathematical methods used, the detailed computation of differential corrections and of correlations of the calculated parameters may seem a rather impracticable overestimate of the accuracy of the determinations and of the possibilities of spectral photometry. A short description of the manner in which we arrived at this method may contribute in destroying the doubt.

When we made, fully aware of the difficulties caused by the photographic effects, our first attempts for the analysis of the spectrum, we considered the measured equivalent widths not to be quantitatively trustworthy and we resigned from the use of a theoretical curve of growth. Assuming that the measured intensity would still be some function of the true line strength, an empirical curve was constructed, and for each individual line the deviation from the mean curve in a horizontal direction (i.e. in the direction of $\log s_0/k$ or $\log Nf$ computed from the solar equivalent width) was determined. This deviation was plotted as a function of the excitation potential and from the slope of the line obtained in this way, the temperature difference between the star and the sun was computed.

The results of the method employed, which is the usual one, were, however, unacceptable. For ϑ Cygni, the first star which was reduced in this way, an early F-type, we found a very small temperature difference with the sun only. Afterwards it was seen, that this descrepancy could have been expected. When we arrange the lines according to their excitation potential, the lines of low $E.P.$ contain a great percentage of strong lines, whereas in the lines originating from higher levels a greater percentage of weak lines is contained. If the temperature of the star is considerably higher than that of the sun, this will result in a relative increase of the intensity of the weak lines. But this increase in strength has already been incorporated in the empirical curve of growth. So it does not appear in the deviations from that curve from which our temperature was derived. Hence the temperature calculated in this way will differ only little from the temperature of the sun.

In order to avoid this difficulty, we then resigned from the use of even an empirical curve of growth. We collected the lines into separate groups, each containing lines of about equal strength and situated in the same wave-length region of the spectrum ; from each group the temperature was determined in the ordinary way. So the systematical effects were eliminated, but of course the determination of temperature within each separate group, containing only a very few lines, with often little spread in excitation potential, could only be very rough. By taking then the weighted mean of all these determinations of temperature we obtained a result of fair accuracy, which was greatly free from systematic errors.

In exactly the same way the degree of ionization of iron and some other elements was computed, also referred to the sun as a standard. For π Cephei the computation was not entirely completed. The results are collected in Table 37, where, for comparison, the results given in Table 29 are repeated (in parentheses).

Table 37. Temperature and ionization, calculated by the method of comparison of equal lines.

		δ Cephei 10607	δ Cephei 10617	ϑ Cygni	π Cephei
$\Delta\Theta$		-0.088 ± 0.033	-0.112 ± 0.047	-0.142 ± 0.022	-0.038
		(-0.104 ± 0.041)	(-0.114 ± 0.086)	(-0.158 ± 0.034)	(-0.044 ± 0.089)
$\Delta \log x/(1-x)$	(*Fe*)	$+1.58 \pm 0.10$	$+1.96$	$+0.78 \pm 0.06$	
		$(+1.86 \pm 0.16)$	$(+1.69 \pm 0.26)$	$(+0.94 \pm 0.10)$	$(+0.38 \pm 0.18)$
id.	(*Cr*)	$+1.49 \pm 0.17$	$+1.49$	$+0.49$	
id.	(*Ti*)	$+1.58 \pm 0.27$	$+2.13$	$+0.58$	
id.	(*V*)	$+1.44 \pm 0.33$		$+0.79$	

The results, obtained by the method described here, are certainly useful, but they lack completeness. Nothing results about the Doppler width, about resonance or about the coefficient of continuous absorption. If we want to determine also these quantities, we cannot resign from the use of a theoretical curve of growth.

Moreover, the method of comparing only lines of equal intensities is a little unsatisfactory. The reciprocal comparison of weak and strong lines, if it is made in the right way, must yield valuable results about temperature and ionization as well, and the accuracy of the determination should even be increased in this way, as the number of usable comparisons is increased.

Thus we came to the method outlined in this publication. After a careful study of the photographic effects, we arrived at the result that the measured equivalent widths could be trusted within a limit of some ten percents if we were able to correct for the instrumental curve in an exact way. The remaining error was due to the difference in slope between the transmission curve of the plate which was valid for the stellar spectrum and that derived from the density marks, a difference, which could have been allowed for, if due caution had been taken to make its determination possible. As matters stood, we met with many difficulties in the determination of the instrumental profile, which were due to photographic effects. But these difficulties may be considered as accidental, because they are not inherent to the method. They can be diminished greatly by using plates with a soft gradation and they can be avoided altogether if the necessary precautions are taken when photographing the comparison spectrum. Then the measured equivalent widths could be used in a curve of growth. After some trials to obtain a trustworthy method for the separation of blends, we choose the other way, computing theoretical strengths of blends from adopted atmospheric parameters. By means of differential corrections we then obtained the true values of these parameters.

The results obtained by the new method may show systematic errors, if the equivalent widths are influenced by photographic effects. Since theoretical discussion convinced us that these errors could be avoided, and that on our plates they should be expected to be relatively small, we felt justified in trying the new method on our spectra. The results are certainly satisfactory. As to the determination of temperature there is excellent agreement with the simpler method. In the determination of ionization the agreement is less convincing, but there is no contradiction, as was the

case when we used the original rough method of comparing all lines with an empirical curve of growth, without separating them into intensity groups.

It is to be asked, which method yields the better results regarding ionization. Both methods are expected to be rather free from systematic errors, and indeed the deviations are in different directions. The method of "equal lines" gives smaller average errors, but this circumstance can hardly be noted as a real difference. In the new method we had to determine five unknown parameters instead of only two and we had not the possibility of smoothing the curve of growth to the observations, so that the systematic errors, which were the results of the inaccurately known instrumental curve still have their influence on the accuracy of the result. These errors are automatically eliminated in the old method. But since they may be eliminated even more completely when the instrumental curve is determined accurately from the line profiles, large photographic errors being avoided by using a soft developer, we cannot speak here of a real advantage.

A real advantage of the new method, however, is, that the blend correction can be applied with more certainty. In the old method we had to apply this correction without knowing anything about the true intensity ratios of the lines. So it could be hardly more than a guess. This is very important if a blend contains lines of neutral atoms and of ions at the same time. Indeed, we made large errors in this correction, as was seen afterwards, when the curve of growth had been determined. In the comparison between atomic and ion lines, this has caused systematic differences. When some lines are excluded which, according to the new calculations have to be considered as serious blends, the agreement becomes much better. From this circumstance we conclude that the results obtained by the new method should be preferred. Indeed, the determinations by the old method will have less accuracy than is indicated by their mean errors. There are some more reasons why the old method cannot be entirely satisfactory, especially in the determination of the ionization, because a direct comparison of equally strong lines is scarcely possible. So in this case we cannot resign from the use of an empirical curve of growth. Another source of error is, that averages are taken of horizontal deviations from the curve of growth whereas the observational errors cause vertical deviations ; at the right hand side they are larger, at the left hand side they are smaller than corresponds to the observed vertical deviations. Still more systematic errors occur when the spread of the error or the number of lines varies with line strength, as is actually the case.

Nevertheless, the general agreement between the two methods is remarkable. This is the more true, as the methods are indeed entirely different. This will be shown clearly by the following schematic comparison :

First method	Second method
Comparison of equal lines only.	Comparison of lines of all strengths.
No theoretical or empirical curve of growth is used.	The use of a theoretical curve of growth is at the basis of the method.
The blends are analysed according to a very rough and approximate estimate.	The blends have not been analyzed, but theoretical strengths have been calculated from adopted spectral parameters.
No correction for instrumental curve.	The correction for instrumental curve has been applied.
Empirical corrections are used in order to reduce lines differing a very little in strength or wave-length to one scale.	Corrections for background are not applied or have been calculated theoretically.

When finally we consider that the material used was only partly identical, the agreement between the results of both methods is certainly convincing, and we may infer that both methods, when appropriate precautions are taken in the determination of the essential basic data (transmission curve and instrumental curve) are free from systematic errors of any importance. Whereas the first of the methods has the advantage of being the simpler one, the second method has more possibilities.

The time needed for the investigation of the spectrum according to the second method is not as large as it might seem. By far the greatest amount of time is spent in calculating the blend correction and its differential variations. But this work is greatly diminished if we dispose of spectra obtained with a great resolving power and if the instrumental curve is accurately known. Even under the present circumstances, we may estimate the total amount of labour for the calculation of the differential corrections for one blend at ten to twenty minutes. So for some 100 lines in one spectrum a few days will suffice. When one has the disposition of a number of spectra of the same (constant or variable) star or of different stars with similar spectra, one may use one and the same calculation for all plates, if necessary with differential corrections for small variations in the cutting of the lines. It then becomes possible to treat several spectra simultaneously. By far the greatest amount of labour is involved in the selection of the lines which have to be taken into account and in assigning appropriate intensities to them ; once this has been done, the other calculations, including the correction for instrumental profile, can be made in a relatively short time.

Indeed the most practical applications of the method will be found in the study of variable stars. One needs only to investigate exactly the spectrum belonging to an average phase and then one can easily refer the spectral variations to that phase, using the method of differential correction. If the variations are large, it will be necessary of course, to choose two standard spectra. But the principles of the method will remain the same.

V. THE PHYSICAL CONDITIONS IN THE STELLAR ATMOSPHERES.

Excitation temperature.

In the preceding we only determined the quantity $\Delta\Theta$, which represents the temperature difference between the star and the sun. In order to determine the absolute value of the temperature, we should know first the excitation temperature for the sun.

It is known that this temperature is much lower than the effective temperature. From the intensities of different titanium lines in the solar spectrum, MENZEL, BAKER and GOLDBERG [1]) derived a value of $4400° \pm 100$. If we accept this value, we have $\Theta = 1.145 \pm 0.026$ for the sun. Using the results of Table 37 we find the following values for the excitation temperatures of the stars under investigation :

δ Cephei v 10607	$\Theta = 1.041 \pm 0.049$	$T = 4840 \pm 230$
δ Cephei M 10617	„ $= 1.031 \pm 0.090$	„ $= 4890 \pm 430$
ϑ Cygni	„ $= 0.987 \pm 0.043$	„ $= 5110 \pm 220$
π Cephei	„ $= 1.101 \pm 0.093$	„ $= 4580 \pm 390$

The excitation temperature, of course, has not the significance of a real temperature. It is only a parameter, describing approximately the relative occupation of the different atomic levels. This relative occupation does not correspond to conditions of thermodynamical equilibrium. The occupation of *e.g.* one of the higher levels of the iron atom, will be lower than would be derived from the temperature of an atmosphere, since the radiative transition from below to the level considered will be hampered by the presence of a Fraunhofer line. So the occupation ofthe higher levels cannot correspond to a true photospheric temperature. If it is described approximately by an excitation temperature, this parameter has no simple relation to the effective temperature of the star. The problem of the relation between excitation temperature and effective temperature cannot be treated here incidentally. So we restrict ourselves to the above result.

Turbulence.

The Doppler widths, collected in Table 29 are much greater than would follow from the normal thermal motion. This phenomenon is a very common one and it is generally interpreted as a consequence of turbulence.

The values for the Doppler width derived in this investigation must be accepted with some caution. The transmission curve which was derived from the density markings cannot be valid for the stellar spectrum and from an analogy with the plates taken in 1929, for which this difference has been measured, we estimated that the slope of the true transmission curve should be about 1.06 times the slope of the adopted curve. From a theoretical consideration of the photographic effects it seemed probable, that for our plates the difference might even be greater than for the

plates taken in 1929. This means, that the measured intensities cannot be the true ones and that the true intensities should be derived from the measured ones by applying a formula $I_t = I_m^p$ where $p = 0.94$ or even smaller.

This circumstance, surely, does not influence the profiles of the stellar lines seriously. If the measured depth of the line profile is equal to R_m, the true depth $R_t = 1 - (1 - R_m)^p =$ is approximately $p\ R_m$, which *e.g.* for $R_m = 0.50$, $p = 0.80$ gives 0.40 in stead of $R_t = 0.426$. So to a fair degree of approximation the line depths will be changed in a fixed proportion p. But if the measured depths are too great in a fixed ratio $1/p$ the same will be true for the measured equivalent widths, and so we will find a too large value for the Doppler width too. Then the Doppler widths given in Table 29 have to be reduced by a factor p which will presumably be about 0.94 or perhaps 0.90. We should remember this, when the Doppler widths have to be interpreted.

To find the turbulence, we have to subtract the thermal motion of the atoms. Since the latter is much the smaller part, we do not need to know the temperature accurately. We shall estimate it by multiplying the excitation temperatures by a factor 5740/4400 which applies in the case of the sun. Then we find the following values for the stellar temperature and for the Doppler width at λ 4400 for an atom of iron :

δ Cephei 10607	$T = 6300$	$b = 20.0\ mA$
δ Cephei 10617	$T = 6360$	$b = 20.1\ mA$
ϑ Cygni	$T = 6650$	$b = 20.5\ mA$
π Cephei	$T = 5960$	$b = 19.4\ mA$

We multiply the Doppler widths from Table 29 by a factor 0.94, as an approximate correction for the error in the transmission curve. From the square of the corrected Doppler widths we subtract the square thermal width ; from the remaining value the turbulent velocity is computed, as is given below.

	Total width	Total width (corrected)	Thermal width	Quadratic Difference	Turbulent Velocity (*Km*/sec)
δ Cephei *v* 10607	64.3 ± 4.9	60.4 ± 4.6	20.0	57.0 ± 4.9	3.9 ± 0.3
δ Cephei *M* 10617	53.2 ± 6.0	50.0 ± 5.6	20.1	45.8 ± 6.1	3.1 ± 0.4
ϑ Cygni	30.0 ± 2.3	28.2 ± 2.2	20.5	17.5 ± 3.5	1.2 ± 0.2
π Cephei	26.9 ± 5.5	25.3 ± 5.2	19.4	16.2 ± 8.1	1.1 ± 0.6

Whereas in the giant π Cephei there is no indication of a larger turbulent motion than in the dwarf ϑ Cygni, the first thing to be remarked is the relatively large turbulence in δ Cephei. More interesting still is the difference in turbulence which is indicated between the two spectra of δ Cephei. We found it confirmed when we compared the two spectra directly, the difference between the two values of log $2b$ being — 0.089 ± 0.034. If this difference should be real it would have so important consequences for the dynamics of the atmosphere, that it needs special consideration.

As the Doppler width resulting from the turbulent motion exceeds the thermal width by a factor 2.85 in δ Cephei *v* and by a factor 2.28 in the other spectrum, the corresponding energies are resp. 8 times and 5 times the thermal energy. So if the change in turbulence should be real, the energy transmissions accompanying this change would exceed the total thermal energy three times!

If this should be the case, the consequences for the dynamics of the atmosphere would be very important. Our calculations indicate that the turbulence diminishes when the star expands

from its minimum volume and the outward motion is accelerated. About the other phases our plates give no indication. It seems to be plausible indeed, that the pulsation of the star has some influence on the turbulence too. A contraction of the star, accompanied by a compression of the turbulent elements might cause an increase of the turbulent velocity if the angular momentum is to be conserved. On the other hand, the mutual penetration of the turbulent elements might cause a slowing down of the motion.

It is not necessary, theoretically, that these are changes of turbulence in the same layers ; if in different phases the light emitted comes from different effective layers with different turbulence we will have the same effect. Practically, the coefficient of absorption is not very different in the two phases here considered. It is possible also that the turbulent motion is not Maxwellian ; the curve of growth will be the flatter the more abrupt is the velocity distribution. Then a change in the mean velocity b would not be necessary ; but in this case too a change in the slope of the curve of growth would indicate important changes in the atmospheric motions.

It is impossible, of course, to treat this question fully in the present context. The problem is much too complicated for such a summary treatment as would be possible here. Also there is an almost complete lack of observational information. But it may be observed that quite generally turbulent motion can be maintained only if it is continuously sustained by some energy source. In an ordinary star the loss of turbulent energy by diffusion of the elements may be in a constant equilibrium with the source of energy, but this can scarcely be true in a pulsating star. So we well may expect a change of turbulence with phase. And even if it would be much smaller than is calculated here it would be of great importance. Since the turbulent energy is from 5 to 8 times as large as the thermal energy a change of only one fourth in it would be equally important for the dynamics of the atmosphere as a temperature variation of 600 or 1000 degrees.

In view of the importance of the question, some further discussions as to reality of the difference found may be of interest. It might be caused by some photographic effect. If it is to be attributed to a wrongly determined slope in the transmission curve, this error should amount to 0.089 (difference between the two plates) in the logarithm or to a factor 1.23 which seems not very probable. The effect cannot be a consequence of a wrong correction for blend or cutting, since it appeared already in the original measures, before any correction had been made. If attributed to an error in the background, this error should be improbably large.

It may be asked what would be the consequences if we reject the reality of a variation in the turbulent motion. It then becomes necessary to calculate the variations of the spectral parameters for the two phases anew. If this is done, the new calculation indicates a very large difference in the resonance constant between the two spectra. This is quite logical. Since a smaller slope of the curve of growth in the spectrum δ Cephei M, if not due to a change in the Doppler width can be represented by a smaller resonance constant as well, for which neither there seems to be a physical reason, we must exclude in the new computation a change in this constant as well. Then we find the following solution for the differences δ Cephei M—δ Cephei v :

$$\Delta \log s_0/k = -0.23 \pm 0.11 ; \Delta \log x/(1-x) = -0.33 \pm 0.14 ; \Delta\Theta = -0.038 \pm 0.039.$$

These values might be found also from the correlation coefficients calculated before. The new correlations are given on the next page. Now the correlation between x and s becomes negative, since it is no longer possible to vary b ; if s_0/k is increased for the neutral atoms, this of course will result in an apparent decrease in the degree of ionization. The correlation between s and Θ is now almost 100 % since a change in s_0/k can only be matched now by a corresponding change in Θ.

Independent variables	Dependent variables					
	s	x	Θ	s	x	Θ
s	1.000	−0.437	+0.332	+0.11	−0.05	+0.037
x	−0.274	1.000	−0.068	−0.04	+0.14	−0.010
Θ	+2.68	−0.880	1.000	+0.10	−0.03	+0.039

We now derive the residuals for the two solutions, one with $\Delta \log 2b = -0.089$, the other with b = constant. For $\Sigma\varepsilon^2$ we find in both cases 5.33 resp. 6.48 so that (for 48 lines) the average deviation is determined by $\sqrt{5.33/(48-5)} = 0.352$ and $\sqrt{6.48/(48-3)} = 0.379$ resp. If we plot the residuals against the line strength (more accurately against the logarithm of the measured equivalent width of the blend in δ Cephei v) as has been done in Figs. 7a and 7b, we find that in the case of the second

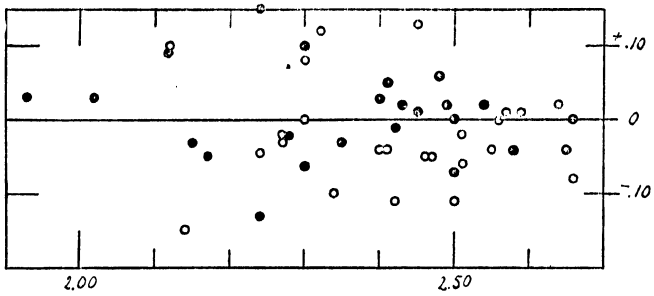

Fig. 7a.

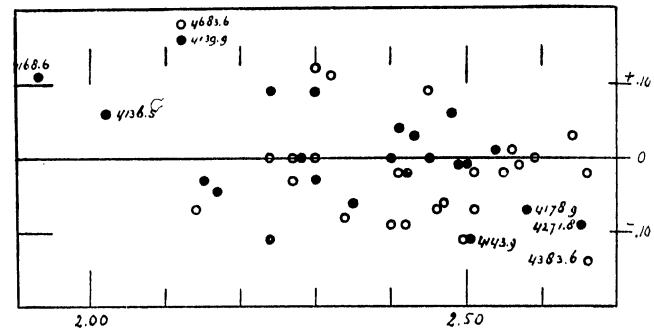

Fig. 7b.

solution with constant b (Fig. 7b) there remains a systematic trend which is eliminated in Fig. 7a. If it would be the result of photographic effects it should be expected to be largest in the green wave-length region, where the slope of the transmission curve is steepest and the blackening of the plate is greater than at the violet side of $H\gamma$. But this is not the case. The systematic trend is more clearly demonstrated by the lines at the violet side of $H\gamma$ (black dots) than by the lines in the green region of the spectrum (open circles). In Fig. 7a the systematic effect seems to be eliminated almost completely for both wave-length regions.

So the discussion of the spectra alone, ignoring the physical arguments, points into the direction of a real effect. But the evidence is by far too uncertain to draw any definite conclusion. To settle the question the study of a far more extensive material will be necessary.

Resonance.

In Table 29 we also gave values for the resonance constant. The values found are surprisingly low, especially in the case of δ Cephei where they are even smaller than the classical value. But we need not take these results very seriously. For the greater part of the resonance wings are cut off from the surface of the measured profile. Only the part which immediately adjoins the core of a line is included in the measures, and so the calculation of resonance width in any case depends on a strong extrapolation.

In the case of δ Cephei we cannot say any more than that the resonance must be relatively small. Trials, to determine it from the strongest lines in the spectrum, *i.e.* the line 4227 of *Ca* and 4078 of *Sr*+ failed completely. Effects of blend and of cutting exceed the total expected influence of resonance wings many times. If we calculate the equivalent width of the *Ca* line 4227 in the

spectrum of δ Cephei v 10607, using the provisional curve of growth (for which the resonance constant was supposed to be three times the classical value) we find for the equivalent width of the line when measured completely and free from blend 715 mA. Without resonance the width would have been 494 mA. The logarithmic difference, $2.85 - 2.69 = 0.16$ would be appreciable. But if we take into account the effect of cutting, the calculated equivalent width of the clipped line would be 601 mA including resonance wings and 543 mA when these wings are zero. (The latter value is larger than the Doppler profile because of the negative instrumental wings produced by the contraction process). The logarithmic difference is now reduced to $2.78 - 2.73 = 0.05$. If the secondary components of the blend are taken into account the theoretical width of the blend becomes 823 mA with and 765 mA without the resonance wings. The blend correction thus amounts to about 0.14 in the logarithm and is three times as large as the total expected correction for wings. The measured equivalent width of the blend is 519 mA, or 2.72 in the logarithm, exactly the value that would be calculated from the corrected curve of growth when there is no resonance at all. The total equivalent width of the blend would then be calculated at 528 mA.

So from the *Ca* line it is not possible to derive anything definite about the value of the resonance constant except that it should be probably small. For the Sr^+ lines things are equally difficult. One more difficulty is the lack of information about the concentration of the element. The difficulties in this respect are very great already since we must refer to the measures of ALLEN. If *e.g.* we compare the intensities of the lines 4078 and 4216 it is found, that the numbers. of active atoms producing these lines according to the measures of ALLEN stand in the ratio 1.3 : 1 whereas the theoretical ratio is 2 : 1. In our spectra λ 4216 is a blend, so that no direct comparison is possible.

So we cannot arrive at any definite conclusion about the value of the resonance constant. It only seems to be small. For ϑ Cygni and π Cephei there is an indication of a small value of the resonance constant, which should be of the same order of magnitude as the classical value. But also this result should be accepted with due caution. In the spectrum of δ Equulei our preliminary calculation gave indication of a large value for the resonance constant. But unfortunately the measures in this spectrum are very uncertain.

Ionization temperature and electron pressure.

Table 29 contains two more parameters, from which inferences may be drawn about the physical state of the atmosphere. These are $\Delta \log s_0/k$ and $\Delta \log x/(1\text{-}x)$ from which we may draw conclusions about ionization temperature and electron pressure.

The "ionization temperature" which, when put into the equation of Saha, determines the degree of ionization will be different from the excitation temperature. For the ionization of atoms is not hampered by the presence of Fraunhofer lines. So the ionization temperature may be appreciably higher than the excitation temperature. R. v. D. R. WOOLLEY [1]) gives a value of 5200° for the sun, which will here be adopted as a basis.

In our computations we will start from three suppositions, which are to a high degree of approximation fulfilled in the stars under consideration as well as in the sun. 1) Practically all atoms of hydrogen are in the neutral state, the number of positive as well as that of negative ions being relatively small. 2) Practically all atoms of iron are in the first stage of ionization. 3) The continuous absorption is chiefly due to the absorption by negative hydrogen ions.

[1]) M. N. **94**, 713 (1934).

The first two suppositions are easily verified by a rough calculation. The third supposition is true only, because in the observable region of the spectrum neutral H atoms can cause continuous absorption only if they occupy the third or a still higher level. The verification of the third supposition can only be made after the ionization temperature and the electron pressure have been determined. But it is found to be true in all cases under consideration.

The number of negative hydrogen ions is determined by a Saha equation :

(91) $n(H_-) = \text{Const.}\, n(H) T^{-5/2}\, 10^{-0.70\,\Theta}\, P_e$.

The coefficient of continuous absorption will be proportional to this expression. If then we compare the values for the star with those of the sun we have :

(92) $\Delta \log k = -{}^5/_2\, \Delta \log T + 0.70\, \Delta\Theta + \Delta \log P_e$,

the number of neutral hydrogen atoms per gram of matter being equal. (This will be true since hydrogen is by far the more abundant element.)

The number of neutral iron atoms is equally determined by an equation of Saha :

(93) $1 - x = \text{Const.}\, x\, T^{-5/2}\, 10^{7.83\,\Theta}\, P_e$

From this we derive for the relative number of neutral atoms in star and sun :

(94) $\Delta \log (1 - x) = -{}^5/_2\, \Delta \log T + 7.83\, \Delta\Theta + \Delta \log P_e$,

the number of ionized iron atoms being supposed to be equal. (This will be true only if the ratio hydrogen : iron is the same in both stars, which we will suppose to be the case).

The total number of neutral atoms, active in producing a line is not determined by s_0/k but by the integral of s/k over the entire profile of the line and so it is proportional to bs_0/k. So the s_0/k will be proportional to $(1-x)/kb$. We then have :

(95) $\Delta \log s_0/k = 7.13\, \Delta\Theta - \Delta \log b$. (neutral atoms).

From this equation the ionization temperature is readily derived. We find the following values for the stars under consideration :

Table 38. Ionization Temperatures.

Star	$\Delta\Theta$	Θ	T
δ Cephei v	-0.078 ± 0.019	0.884	5700
δ Cephei M	-0.068 ± 0.045	0.894	5640
ϑ Cygni	0.090 ± 0.015	0.872	5770
π Cephei	$+0.031 \pm 0.039$	0.993	5080

Direct comparison δ Cephei M — δ Cephei v :

b variable : $\Delta\Theta = -0.001 \pm 0.018$

b constant : $\Delta\Theta = -0.032 \pm 0.015$

For the sun we used the value $b = 22.3\, mA$, for the stars the observed value after correction by the factor 0.94. It is interesting, that the $-\Delta\Theta$ (*ioniz*) are systematically smaller than the $-\Delta\Theta$ (*exc*). Partly this is a consequence of the circumstance that Θ itself is smaller in the first case than in the second ; the same proportional variation then corresponds to a smaller absolute value of $\Delta\Theta$. But the excitation values multiplied by 4400/5200 (— 0.088, — 0.096, — 0.134 and — 0.037) still remain more negative than the ionization values.

So there is a systematic difference, which might be real. Ionization is chiefly caused by the radiation in the far ultraviolet. Now in the case of the sun for the relevant wavelengths the absorption by negative hydrogen predominates even over the Balmer continuum, as computation shows; In the stars considered the absorption by negative hydrogen is also present, but as these stars have higher temperatures or smaller densities, the Balmer absorption will now be relatively more important. Hence the intensity of the ultraviolet radiation undergoes an extra reduction as compared with the sun, which results in a relative lowering of the ionization temperature. As a control we will make a rough estimate of this effect, as soon as the electron pressure has been ascertained.

The electron pressure may be derived from the position of the curve of growth for the ion lines. For these lines eq. (94) is replaced by $\Delta \log x = 0$. So we find :

$$(96) \quad \Delta \log \frac{s_0}{k} + \Delta \log \frac{x}{1-x} = {}^5/_2 \Delta \log T - 0.70\, \Delta\Theta - \Delta \log b - \Delta \log P_e \text{ (ions)}$$

From this equation we derive :

Table 39. Electron pressure.

Star	$\Delta \log P_e$
δ Cephei v	-1.16 ± 0.24
δ Cephei M	-1.08 ± 0.50
ϑ Cygni	-0.13 ± 0.14
π Cephei	-0.66 ± 0.39

Direct comparison δ Cephei M — δ Cephei v :

b variable : $\Delta \log P_e = +0.09 \pm 0.23$
b constant : $\Delta \log P_e = +0.62 \pm 0.15$

The latter results clearly demonstrate the importance of a variation of b on the conclusions as to the variation of the other physically important parameters such as the electron pressure. It must be added that our observations indicate a greater strength of the hydrogen lines in the maximum phase than in the other spectrum, which, in so far not a higher temperature is responsible might be attributed to a higher value of the electron pressure (Stark effect) and then would afford an argument in favour of the hypothesis of constant b.

Table 40. Absorption by neutral and negative bydrogen.

	$\lambda = 4443$		$\lambda = 1642$	
Θ	Neutral H, log k	Neg. H, log k/P_e	Neutral H, log k	Neg. H, log k/P_e
0.8	$\bar{3}.75$	$\bar{2}.20$	$\bar{2}.41$	$\bar{3}.59$
0.9	$\bar{4}.54$	$\bar{2}.40$	$\bar{3}.39$	$\bar{3}.79$
1.0	$\bar{5}.34$	$\bar{2}.58$	$\bar{4}.38$	$\bar{3}.97$
1.1	$\bar{6}.14$	$\bar{2}.76$	$\bar{5}.36$	$\bar{2}.15$
1.2	$\bar{8}.93$	$\bar{2}.92$	$\bar{6}.35$	$\bar{2}.31$

We now are in a position to verify the supposition about the origin of the continuous absorption. We make use of the calculations of CHANDRASEKHAR for the absorption by negative

hydrogen[1]), which we compare with the calculations by UNSÖLD for neutral hydrogen[2]). The latter values are extrapolated to lower temperatures by applying a correction $10^{-12.04\,\Theta}$ for the Paschen continuum (the contributions from the higher continua may be neglected), and to other wave-lengths by the factor ν^3. (Table 40).

If we wish to apply these figures to the stars, we want the absolute value of the electron pressure. We take Θ (ioniz) for the sun 0.962 and we shall use the electron pressure at the same level, which is about $\tau = 0.25$ according to the calculations of STRÖMGREN [3]). The value of log P_e still depends on the relative abundance of the metals, which is expressed by the factor A = number of hydrogen atoms: number of (neutral or ionized) metal atoms. Using the values of log P_e of STRÖMGREN for different values of A we find the following values of log k for the sun, derived from negative hydrogen ions.

log A	3.0	3.4	3.8	4.2	Absorption by neutral H
log P_e	1.25	1.06	0.88	0.74	
log k ($\lambda = 4443$)	$\bar{1}.76$	$\bar{1}.57$	$\bar{1}.39$	$\bar{1}.25$	$\bar{5}.80$
log k ($\lambda = 1642$)	$\bar{1}.15$	$\bar{2}.96$	$\bar{2}.78$	$\bar{2}.64$	$\bar{4}.66$

So in both spectral regions the absorption by negative hydrogen predominates.

If we apply the same computation to the stars under consideration we arrive at the following results :

Table 41. Absorption by negative and neutral hydrogen.

log A		3.0	3.4	3.8	4.2	Absorption by neutral H
δ Cephei v	log k (4443)	$\bar{2}.46$	$\bar{2}.27$	$\bar{2}.09$	$\bar{3}.95$	$\bar{4}.73$
	log k (1642)	$\bar{3}.85$	$\bar{3}.66$	$\bar{3}.48$	$\bar{3}.34$	$\bar{3}.55$
ϑ Cygni	log k (4443)	$\bar{1}.46$	$\bar{1}.27$	$\bar{1}.09$	$\bar{2}.95$	$\bar{4}.88$
	log k (1642)	$\bar{2}.85$	$\bar{2}.66$	$\bar{2}.48$	$\bar{2}.34$	$\bar{3}.68$
π Cephei	log k (4443)	$\bar{1}.17$	$\bar{2}.98$	$\bar{2}.80$	$\bar{2}.66$	$\bar{5}.35$
	log k (1642)	$\bar{2}.56$	$\bar{2}.37$	$\bar{2}.19$	$\bar{2}.05$	$\bar{4}.39$

It is seen, that in all cases the absorption by negative hydrogen predominates in the visible region of the spectrum. So the basis of our calculations is confirmed. The hypothesis, however, that the reduction of the ionization temperature is caused by an increase of the absorption in the Balmer continuum is not generally confirmed. Even if we adopt the largest value for A, we find for the ratio k (neutral H): k (negative H) 0.01 for the sun and 1.6, 0.22 and 0.02 for δ Cephei, ϑ Cygni and π Chephei. So with the exception of δ Cephei the absorption by neutral H seems to be relatively unimportant even in the Balmer continuum. And it was precisely δ Cephei where the difference between $\Delta\Theta$ (ioniz.) and $\Delta\Theta$ (exc.) was smallest. Another explanation seems to be necessary, which probably has to start from a more accurate interpretation of the excitation temperature.

[1]) Ap. J. **102**, 395 (1945).
[2]) Physik der Sternatmosphären p. 121.
[3]) Publikationer og mindre Meddelelser fra Kobenhavns Observatorium **138** (1944).

Gravity.

The physical state of the atmosphere of a star in equilibrium is determined by the effect of two external forces : the flow of heat passing through one square centimetre of the surface, and gravitation. The first quantity is described by the effective temperature of the atmosphere. Gravity determines the pressure gradient ; hence it may be derived if we know the pressure at a certain optical depth in the atmosphere.

The measurements in the spectrum give no direct evidence about the total atmospheric pressure, but only of a certain part of it, *viz.* the electron pressure. From this quantity the total pressure may be derived, but only if we make certain assumptions about the chemical composition of the atmosphere, especially about the relative abundance of hydrogen and metal atoms.

We denote with B. STRÖMGREN the ratio of the numbers of hydrogen and of metal atoms by A, a large number of the order of $\log A = 3.8$. The continuous absorption at the relevant temperatures is entirely due to the small fraction of hydrogen atoms with negative charge. We assume the metal atoms to be singly ionized, *i.e.* the number of electrons from metal atoms to be equal to the number of these atoms themselves, whereas hydrogen is only ionized to a small degree. Denoting the ionized fraction of hydrogen by x, the electron pressure by P, the total pressure by p, and the temperature function in SAHA's equation for hydrogen by y, we have (neglecting terms of the order $1/A$)

$$dp = \frac{g}{k}\,d\tau\,; \quad \frac{x}{1-x} = \frac{y}{P},\ \text{or}\ x = \frac{y}{y+P},\ 1-x = \frac{P}{y+P}$$

$$\frac{p}{P} = \frac{A(1+x)}{Ax+1} = A\,\frac{2y+P}{Ay+P} \qquad k = k_T(1-x)\,P = k_T\,\frac{P^2}{y+P}.$$

Introducing

$$P = Ayu,\ \text{or}\ u = \frac{1-x}{Ax}\ \text{we find}$$

$$(97)\qquad dp = A^2y\,\frac{u^2+2u+2/A}{(1+u)^2}\,du \qquad dp = \frac{g}{k_T}\,\frac{u+1/A}{Ayu^2}\,d\tau.$$

For $u \gg {}^1/A$ (hydrogen only slightly ionized) the terms with ${}^1/A$ may be omitted, so that

$$(98)\qquad \frac{g}{k_TA^3y^2}\,d\tau = \frac{u^2(u+2)}{(u+1)^2},\ \text{or}\ \frac{g\tau}{k_TA^3y^2} = \tfrac{1}{2}\,u^2 + \frac{u}{1+u} - \ln(1+u) = \psi(u).$$

The function $\psi(u)$ is given in Table 42.

Table 42. Auxiliary Table for Gravity.

log u	log ψ (u)	log u	log ψ (u)
— 10	— 30.18	0.0	— 0.51
— 5	— 15.18	0.1	— 0.27
— 2	— 6.18	0.2	— 0.04
— 1	— 3.22	0.5	+ 0.64
— 0.5	— 1.81	1.0	+ 1.69
— 0.2	— 1.01	2	+ 3.70
— 0.1	— 0.76	5	+ 9.70
0.0	— 0.51	10	+ 19.70

In the integration the variation of the temperature function y with optical depth has been neglected. A comparison with the tables computed by means of numerical integration by B. STRÖMGREN for the sun (log $A = 3.8$; log $g = 4.44$) is made for some values of the temperature :

τ	Θ	log y	log k_T	log ψ (u)	log u	log P	log P_e (B.S.)
0.01	1.037	$\bar{6}.70$	$\bar{2}.59$	+ 3.05	+ 1.68	0.18	0.15
0.10	1.005	$\bar{5}.17$	$\bar{2}.53$	+ 3.17	+ 1.74	0.71	0.64
0.50	0.905	$\bar{4}.65$	$\bar{2}.35$	+ 1.09	+ 0.71	1.16	1.15

So equation (97) gives reliable results if the true temperature fitting to the optical depth is used.

In order to derive g we have to compute $y = f(T)$ as well as k_T, the absorption coefficient for negatively charged hydrogen, and to assume a value of A. First for the sun, with log $g = 4.4$ and $\Theta = 1.037$ ($\tau = 0.01$) $\psi(u)$ was computed ; from u the electron pressure P was found, and then the differences ΔP for the stars relative to the sun (Table 39) afforded P for the stars. By going now the way back the quantities u, $\psi(u)$ and log g, were found.

The mean error of log g may be computed by means of

$$\frac{\partial \log g}{\partial \Theta} = -\left(\frac{d \log \psi}{d \log u} - 2\right)\frac{d \log y}{d\Theta} + \frac{d \log k_T}{d\Theta}$$

$$\frac{\partial \log g}{\partial \log P} = \frac{d \log \psi}{d \log u}$$

For u large (all free electrons coming from metal atoms) $d \log \psi / d \log u$ approaches 2, so that g is nearly independent of Θ. For δ Cephei this condition is not fulfilled.

The values of the effective gravitation found in this way, are

Table 43. Effective gravity.

δ Cephei v	log g = 1.40	± 0.37
δ Cephei M	1.23	0.89
ϑ Cygni	3.76	0.47
π Cephei	3.05	0.82

The real accuracy of the results is, however, less than might be presumed from the mean error in the first case. When the ionization ratio of hydrogen is not very small, which through the low electron pressure probably is the case for δ Cephei, the auxiliary quantity u is extremely small, and even in an isothermal atmosphere the omission of the terms $1/A$ in the equations 97 is not allowed.

The tables of exact values of log P_e given by B. STRÖMGREN for different optical depth in different atmospheres [1]) do not extend to such low values of g and P_e as are needed here. Hence we have extended them by computing in the same way, by numerical integration, some additional values, for log $A = 3.8$ only and the optical depth $\tau = 0.25$. In Table 42 the values taken from STRÖMGREN are marked by an asterisk. Our computation in these cases shows differences of only one unit of the last decimal. Radiation pressure is neglected in these computations and probably is unimportant.

[1]) Publikationer og mindre Medd. fra Kobenhavns Obs. **138** (1944).

Table 44. Electron pressure P_e at $\tau = 0.25$ for different values of temperature and gravity.

$\log g$ / Θ_0	1.0	1.5	2.0	2.5	3.0	3.5	4.0	4.5	5.0
1.05			$\bar{1}.80$	0.01	0.23	0.45	0.68	0.90	
1.00		$\bar{1}.79$	$\bar{1}.98$	0.17	0.37*	0.56*	0.78*	0.99*	
0.95	$\bar{1}.84$	0.02	0.19	0.38	0.55	0.74	0.94	1.14	1.34
0.90				0.60	0.77	0.95*	1.12*	1.31*	1.50
0.85								1.54	1.71
0.80						1.39*	1.58*	1.76*	

With $\log g = 4.4$, $\Theta_0 = 1.037$ the table gives $\log P_e = 0.88$ for the sun; then with the differences $\Delta\Theta$ and $\Delta \log P_e$ from Tables 38 and 39 we find Θ and $\log P_e$ for the stars, whereupon Table 44, with slight extrapolation, gives $\log g$.

Table 45. Results for effective gravity.

	$\Delta\Theta$	$\Delta \log P_e$	Θ_0	$\log P_e$	$\log g$
δ Cephei v	— 0.078	— 1.16	0.959	$\bar{1}.72$	0.6
δ Cephei M	— 0.068	— 1.08	0.969	$\bar{1}.80$	0.7
ϑ Cygni	— 0.090	— 0.13	0.947	0.75	3.4
π Cephei	+ 0.031	— 0.66	1.068	0.22	3.1

In view of the uncertainties mentioned we may get a better survey of the problem by making use of a simplified atmospheric model. In the case of the sun, of ϑ Cygni and π Cephei the contribution of hydrogen to the number of free electrons is entirely negligible, whereas the same holds for the contribution of the metals in the case of δ Cephei. In the first case the ratio of the electron pressure to the total pressure is $1/A$. Putting the coefficient of absorption $k = k(T)P_e$, where $k(T)$ is a slowly varying function of the temperature, we have

$$\frac{dP_e}{d\tau} = \frac{1}{A}\frac{g}{k(T)P_e} \quad \text{or} \quad {}^1\!/_2\, P_e{}^2 = \frac{g}{A}\int \frac{d\tau}{k(T)}$$

In the second case the ratio of the electron to the total pressure is simply the rate of ionisation of hydrogen $x = y/P_e$, where y is a temperature function. Then from

$$\frac{dp}{d\tau} = \frac{g}{k(T)P_e} \quad \text{and} \quad p = P_e{}^2/y$$

we find

$$P_e{}^3 = {}^3\!/_2\, g\, y^{3/2} \int \frac{d\tau}{k(T)\sqrt{y}}.$$

For stars of the same temperature gravity in the first case is proportional to the square, in the second case to the third power of the electron pressure, whereas the abundance factor A is eliminated. Comparing δ Cephei v with the sun reduced to the temperature $\Theta = 0.95$, for which $\log P_e = 1.12$ instead of 0.88, the difference $\Delta \log P_e$ must be taken — 1.40 instead of — 1.16 Then for the two cases, taken as extreme limiting cases we have $\Delta \log g = -2.80$ and -4.20; hence $\log g$ is comprised between the limits 1.6 and 0.2.

It must be remarked, however, that in comparing two stars belonging to different cases — as is the case with δ Cephei and the sun — the abundance factor and the structure of the atmosphere are not eliminated. Bringing, approximately, a mean value of $\sqrt{y}$ outside the second integral, we find

$$\frac{g_*}{g_\odot} = \frac{4}{3A}\frac{P_*{}^3}{y\,P_\odot{}^2},$$

so that an error in the adopted value of A appears to its full amount in the resulting value of the gravitation.

In comparing the two spectra of δ Cephei the second equation may safely be used. Writing it

$$\Delta \log g = 3\,\Delta \log P_e - \Delta \log y = 3\,\Delta \log P_e + {}^5/_2\,\Delta \log \Theta - 13.54\,\Delta\Theta$$

we find

$$\Delta \log g\,(M\text{—}v) = +\,0.28 \pm 0.86\ (b \text{ variable})$$
$$\Delta \log g\,(M\text{—}v) = +\,1.92 \pm 0.70\ (b \text{ constant}).$$

The large m.e. are due to the fact that the errors in $\Delta \log P_e$ and in $\Delta\Theta$ are correlated and have the same sign.

SUMMARY.

In this investigation, a method has been developed for the accurate analysis of a stellar spectrum. The basic principle of the method consists in the comparison of the observed spectrum with a calculated theoretical spectrum. By a method of differential corrections, we obtained a least square solution for the physical parameters of the stellar atmosphere.

Due attention was paid to the internal correlations between the different parameters, and it was shown that their mutual influence is so strong that an error in one of them has important consequences for the determination of all the other ones. Systematic errors of all kinds and of great amount may occur if not very great care is taken in avoiding them.

In the course of the investigation it became necessary to make a special study of photographic effects. It is shown, that their influence may be much reduced if the necessary precautions are taken. In the present investigation, they remain the main disturbing factor, and they are responsible for many inaccuracies or even doubtfulness in the results. Some progress was made in the explanation of irregular behaviour of the transmission curves.

As to the determination of the physical parameters, an accurate determination of temperature and — if photographic errors have been avoided — of turbulence is possible. More difficult is the determination of electron pressure, whereas it is possible only to make a rather rough estimate of the surface gravity.

The two spectra of δ Cephei which were at our disposal showed no very distinct differences. This is due chiefly to the fact that they are situated almost symmetrically at both sides of the maximum. A difference in turbulence is indicated, which, if it should be real, would have very important astronomical consequences ; but it cannot be decided whether it possibly is due to photographic errors. Investigation of a much more extended material would be necessary to settle the question. Other changes in the spectrum have been discussed in the final chapter.

Resuming the results of the investigation it appears that the new method, however laborious, is not impracticable and that it yields accurate results, which are substantially free from systematic errors. The method is most adapted to the study of variable spectra or to a comparison of different stars belonging to the same spectral type.